

Doctoral Dissertation

博士論文

Adiabatic Charge Pumping in

Quantum Dot Systems

(量子ドット系における断熱電荷ポンピングの理論)

A Dissertation Submitted for the Degree of Doctor of
Philosophy

December 2019

令和元年12月博士（理学）申請

Department of Physics, Graduate School of Science,
The University of Tokyo

東京大学大学院理学系研究科

物理学専攻

Hasegawa Masahiro

長谷川 雅大

Acknowledgements

The author acknowledges the financial support of the Advanced Leading Graduate Course for Photon Science, Grant-in-Aid for JSPS Fellows No. JP19J11360, and Japan Society for the Promotion of Science KAKENHI Grants No. JP24540316 and No. JP26220711. The author also acknowledges T. Kato, R. S Whitney, and É. Jussiau as the collaborators. The author thanks R. Sakano for helping the numerical calculation of the Bethe ansatz. The author also thanks T. Yokoyama, T. Tamaya, and H. Shinaoka for greatful comments.

Abstract

Adiabatic charge pumping in quantum dot systems has been studied for long time as one of fundamental dynamical phenomena using time-dependent parameter driving. We study adiabatic charge pumping in the context of a possible probe clarifying detailed processes of electron transport via a quantum dot. We focus on two effects on the adiabatic charge pumping; (i) effect of the band structure of electron reservoirs, and (ii) quantum many-body effect due to strong Coulomb interaction.

First, we study the relation between the adiabatic pumping and the band structure of the reservoirs. We consider the adiabatic charge pumping via a non-interacting quantum dot coupled to electron reservoirs with an arbitrary band structure when the dot-reservoir couplings are driven. We show that, when the area enclosed by the contour in the driving parameter space is sufficiently large, the pumped charge in one cycle can be quantized to a fractional value depending on the ratio of the Lamb shift to the level-broadening which reflects the band structure of reservoirs. We call this pumping as *almost topological pumping*, because the pumped charge is quantized up to small corrections when the Berry curvature of adiabatic pumping is entirely enclosed by the driving contour in the driving parameter space.

Second, we study the effect of the Coulomb interaction on the adiabatic charge pumping. We consider a single-level quantum dot with the Coulomb interaction connected to electron reservoirs with time-dependent temperatures and electrochemical potentials. We introduce the thermomechanical field to describe the time-dependent temperature modulation in the quasi-static limit. Using the perturbation expansion with respect to the Coulomb interaction, we derive a general formula of the Berry connection which describes the pumped charge. Our formula is written in terms of one- and two-particle Keldysh Green's functions, so it is applicable to arbitrary strength of the Coulomb interaction and the dot-reservoir coupling. We show that the present pumping is induced by a rectification effect due to the delayed response of the quantum state of the quantum dot, such as the occupation number, and that one can probe the energy differential of the spectrum function of the quantum dot by measuring the pumped charge. We also show that the delay time can be estimated as a relaxation time of the quantum dot by considering the equivalent RC -circuit of the quantum dot. To see the interaction dependence on the pumped charge, we employ the renormalized perturbation

theory and consider the first-order perturbation with respect to the renormalized Coulomb interaction. As a result, we point out that the pumped charge reflects the renormalization effects due to the Coulomb interaction and that the Coulomb blockage effect is most strongly observed.

Table of contents

1	Introduction	1
1.1	Adiabatic pumping in a quantum dot	1
1.2	Almost topological aspects of adiabatic pumping	3
1.3	Kondo problem	4
1.4	Purpose of this thesis	5
1.4.1	General formalism for the adiabatic pumping	5
1.4.2	Quantization of adiabatic pumping in non-interacting quantum dot	5
1.4.3	Coulomb interaction effect on adiabatic pumping	6
1.5	Construction of thesis	6
2	Review of theoretical methods	7
2.1	Model for a single-level quantum dot	7
2.2	Scattering theory for a quantum dot system	8
2.2.1	Steady state transport	9
2.2.2	Brouwer's formula	11
2.3	Keldysh formalism for quantum dot system	13
2.3.1	Keldysh time contour	13
2.3.2	Green's function	15
2.3.3	Keldysh component	16
2.3.4	Langreth rules	17
2.3.5	Charge current through a single-level quantum dot	18
2.4	Kondo effect	20
2.4.1	Overview of the Kondo effect	21
2.4.2	Perturbation with respect to U	22
2.4.3	Renormalized perturbation theory (RPT)	26
3	Adiabatic approximation in the Keldysh formalism	29
3.1	Outline	29

3.2	Derivation of the dynamic conductance and the Berry connection	30
4	Almost topological pumping in non-interacting quantum dot system	35
4.1	Model Hamiltonian	35
4.2	Adiabatic almost-topological pumping of a fraction of an electron per cycle	38
4.2.1	Half an electron per cycle	40
4.2.2	Seeing the topology	41
4.2.3	Different fractions of an electron per cycle	43
4.2.4	Requirements for experimental observation	44
4.3	Detailed results	45
4.3.1	Low temperature pumping	46
4.4	Comparison with dot occupation	48
4.5	Short summary	49
5	Charge pumping in interacting quantum dot system	51
5.1	Model	51
5.2	Thermomechanical field method	53
5.3	Berry connection for the interacting quantum dot	54
5.4	Pumping Mechanism	57
5.4.1	$U = 0$ case	58
5.4.2	Delayed response	59
5.4.3	AC response: the single-reservoir case	60
5.4.4	AC response: the two-reservoir case	61
5.5	Evaluation of the Pumped Charge	63
5.5.1	Renormalized parameters	63
5.5.2	Electrochemical-potential-driven pumping	65
5.5.3	Temperature-driven pumping	67
5.6	Short summary	69
6	Summary and Perspectives	71
6.1	Summary and Future problems	71
6.2	Perspective: Towards steady state thermodynamics	72
	References	75
	Appendix A Keldysh Green's functions	79
	Appendix B Bethe anzats	81

Table of contents	ix
-------------------	----

Appendix C	Overcounting problem and counter term	85
-------------------	--	-----------

Appendix D	Derivation of Eq. (3.8)	87
-------------------	--------------------------------	-----------

Appendix E	Brief review of excess heat and extended Clausius relation	89
-------------------	---	-----------

Chapter 1

Introduction

1.1 Adiabatic pumping in a quantum dot

When a quasi-static and time-periodic operation is applied to a system, electron and heat are pumped from one reservoir to other reservoirs. This transport phenomenon is known as adiabatic pumping. Since adiabatic pumping was proposed by Thouless in his pioneering work [1], adiabatic pumping has been gathering attention in condensed matter physics for several decades. Adiabatic pumping has been also discussed intensively in mesoscopic physics in the context of single electron pumping [2, 3], dynamic conductance of mesoscopic capacitors [4], and adiabatic charge pumping via a quantum dot [5]. Brouwer's formula [6] is a milestone in the research of adiabatic pumping. This formula, which is derived from the scattering theory, describes the pumped charge in one cycle in terms of an integral of the Berry curvature on an area enclosed by a driving contour.

Adiabatic charge pumping can be considered as a process which observes a electronic signal induced by a quasi-static driving. From this viewpoint, adiabatic charge pumping can be regarded as a probe of electron transport. In addition, adiabatic pumping can be considered as a quasi-static and cyclic operation in thermodynamics. Therefore, studying adiabatic pumping is helpful for understanding of thermodynamic property in nanoscale quantum engines.

A number of theories have been developed so far to clarify pumping phenomena in general situations. Here we briefly summarize three developments, i.e., (i) non-adiabatic effect, (ii) heat transport, and (iii) Coulomb interaction effect.

Non-adiabatic effect

In order to discuss a non-adiabatic effect, the Floquet theory is a useful theoretical framework, which can describe time-dependent transport under a periodic driving. In the Floquet theory, one can estimate the driving frequency dependence of physical quantities and can discuss adiabatic pumping and its non-adiabatic correction by considering the zero-frequency limit. In mesoscopic physics, the Floquet theory was used in combination with other analytical methods such as the scattering matrix theory [4, 7–9] and the Keldysh formalism [10, 11].

Heat transport

Most of the early studies on adiabatic pumping have focused on only charge transport because it is easier to measure charge transport than heat flow. However, after heat transport via a nanoscale system was experimentally observed recently [12], adiabatic heat pumping has been attracting a lot of attention. In the case of a weak system-reservoir coupling where the system is sufficiently separated from the reservoirs, heat transfer is well-defined so that it is not difficult to generalize the theory of charge pumping to that of heat pumping. Actually, heat pumping has been discussed in several theoretical works such as heat pumping in molecular junctions [13], thermoelectric performance in quantum dots [14], and entropy production in quantum dots [15, 16] (see also Appendix E). On the other hand, heat pumping in the system strongly coupled to reservoirs has not been discussed so far because the standard definition of heat transfer is not well-defined. A proper definition of heat transfer is necessary to discuss heat pumping with the strong coupling.

Coulomb interaction effect

In theoretical treatment of nanoscale devices such as quantum dots, we need to consider the Coulomb interaction between electrons more or less. When the reservoir temperature is much larger than the dot-reservoir coupling, electron transport is well described by the master equation derived from the second-order perturbation with respect to the system-reservoir coupling. Transport in this weak dot-reservoir coupling region is referred to as the incoherent transport. In the incoherent region, the energy levels of the isolated quantum dot is affected by the Coulomb repulsion. When the Coulomb interaction is strong, the additional energy, which is an energy needed to add one more electron into the system, becomes large, and therefore charge transport via a quantum dot is suppressed except for specific values of gate voltages. This is called the Coulomb blockade. To analyse the Coulomb blockade, the generalized master equation approach is a better option [17, 18]. Based on the generalized

master equation approach, adiabatic charge pumping via a quantum dot with strong Coulomb interaction was discussed [14, 19, 20].

When the temperature is comparable to or smaller than the dot-reservoir coupling, hybridization between a quantum dot and reservoirs becomes important. Electron transport in this strong dot-reservoir coupling region is referred to as coherent transport. In the presence of strong Coulomb interaction, the Kondo effect emerges in the coherent transport. At low temperatures, electrons in a quantum dot forms the Kondo state, which is a spin-singlet state with reservoir electrons due to many-body effect. Understanding of adiabatic pumping via the Kondo state is important to clarify the quantum many-body effect on SST and establishing the new framework. In section 1.3, we give a brief introduction of the Kondo effect, and summarize unsolved problems in adiabatic pumping via the Kondo state.

1.2 Almost topological aspects of adiabatic pumping

Brouwer's formula provides a basis of a geometrical aspect of the adiabatic pumping: As already explained, the pumped charge in one cycle is calculated by a surface integral of the Berry curvature on an area enclosed by a driving contour. The amount of the pumped charge normally depends on the driving contour. However, when the Berry curvature is a delta function of driving parameters, the pumped charge depends only on topology of the contour, i.e., on whether the contour encloses the singular point or not. This is called quantized pumping or topological pumping. Topological pumping is favorable in experiments because it is robust against small changes of the contours. However, "exact" topological pumping is difficult to be realized in mesoscopic devices.

Instead of "exact" topological pumping, one can consider the "almost" topological pumping: When the Berry curvature has a sharp peak structure in the parameter space, the pumped charge on different contours become almost the same as long as the contours do not impinge on the peak. This pumping referred to as "almost" topological pumping and has been studied in a single-level quantum dot without Coulomb interaction [21, 22]. The number of the pumped electrons, however, depends on the model; the number of the pumped electrons is almost one half for a flat density of states of the reservoir [22], while it is almost one for the tight-binding model [21]. These two results indicate that the number of pumped electrons strongly depends on the density of states of the reservoirs. In the quantum dot system, the energy level of the quantum dot is shifted and broadened by the hybridization effect due to the tunnel coupling between the quantum dot and the reservoirs. The density of states of the reservoirs affects this energy shift and broadening. Therefore, it is expected that the number of pumped charge can be characterized by the energy shift and broadening.

However, there was no research on classification of the number of pumped charge in terms of the energy shift and broadening.

1.3 Kondo problem

Brief introduction of the Kondo effect

The Kondo effect was first considered to explain the local minimum of resistance in low temperature using a model of a magnetic impurity coupled to conduction electrons via exchange coupling, which was later called the Kondo model [23]. While the magnetic impurity keeps its magnetic moments at high temperatures, it disappears at low temperatures with the formation of a spin-singlet state with conduction electrons. The characteristic temperature of the screening of the magnetic moment at the impurity is known as the Kondo temperature. The Kondo temperature was first recognized through logarithmic divergence in the original perturbation theory. The entire picture of the Kondo physics, i.e., the crossover from the high-temperature paramagnetic behavior following the Curie law to the Pauli paramagnetism at low temperatures was clarified by the numerical renormalization group [24]. The low-temperature properties of the Kondo model is understood by the local Fermi liquid theory [25, 26]. Based on the concept of the Fermi liquid theory, a useful framework named the renormalized perturbation theory (RPT) has been developed [27, 28].

The Kondo effect has also been studied in the research field of mesoscopic physics. Electron transport through a single-level quantum dot is described by the impurity Anderson model, which can be mapped into the Kondo model for large Coulomb interaction. Actually, the Kondo effect in quantum dots was observed by measuring the temperature and gate-voltage dependence of the conductance [29–31]. There are a number of theoretical studies on the Kondo effect in quantum dots [32]. For electron transport via the Kondo state at low temperatures, it is useful to employ the local Fermi liquid theory [33, 34] and its variants such as the renormalized perturbation theory [27, 28, 35]. In particular, experimental measurement of the effective charge in the Kondo state [36–38] stimulated theoretical works [39–41].

Adiabatic pumping in the Kondo regime

Although adiabatic pumping in the Kondo regime is still a challenging problem, it provides a good first step to construct SST for interacting electron systems. Adiabatic charge pumping in the Kondo quantum dot was already investigated by the second-order perturbation theory [42] and the slave boson mean field approximation [43]. These theoretical works are, however, applicable only to the limited range of strength of Coulomb interaction. A framework of

the adiabatic charge pumping applicable to an arbitrary strength of Coulomb interaction was proposed in the Keldysh formalism [44]. However, the theory was still not satisfactory because it is applicable only when the dot-reservoir coupling and the energy level of the quantum dot are driven. For construction of SST, the theoretical framework for adiabatic pumping of heat and particles by driving the reservoir parameters such as the electro-chemical potentials and temperatures are preferable.

1.4 Purpose of this thesis

1.4.1 General formalism for the adiabatic pumping

In this thesis, we consider two problems related to adiabatic pumping via a quantum dot: (i) quantization of adiabatic pumping in non-interacting quantum dot and (ii) Coulomb interaction effect on adiabatic pumping. In order to discuss these problems, it is necessary to construct a general formalism which can treat the energy shift and broadening affected by the density of states of the reservoirs and time-dependent temperature of the reservoirs. To overcome such difficulties, we construct the perturbation theory in the infinite-order with respect to Coulomb interaction and formulate the adiabatic pumping in terms of one- and two-particle Green's function in the Keldysh formalism. This formalism is utilized to discuss two problems mentioned above.

1.4.2 Quantization of adiabatic pumping in non-interacting quantum dot

To clarify the nature of the almost topological adiabatic pumping, we consider charge pumping in a single-level non-interacting quantum dot when the dot-reservoir couplings are driven [22]. In this model, the Berry curvature is sharply peaked in the parameter space, and therefore so long as the pumping contour does not touch the peak, the pumped charge depends only on how many times the contour winds around the peak (up to exponentially small corrections). We show that the pumped charge averaged over many cycles is quantized at a fraction of an electron per cycle, determined by the ratio of the Lamb shift to level broadening; this ratio is imposed by the reservoir band structure. Finally, we formulate the adiabatic charge pumping for general types of reservoirs and discuss its almost topological feature and the relation between the number of pumped electron and the reservoir band structure.

1.4.3 Coulomb interaction effect on adiabatic pumping

We consider adiabatic charge pumping via a single-level quantum dot induced by the reservoir parameters, i.e., temperature and electrochemical potential driving [45]. We construct a general framework for the arbitrary strength of dot-reservoir coupling and Coulomb interaction, which is applicable also to the Kondo regime. We also calculate the pumped charge by the renormalized perturbation theory and discuss how the Coulomb interaction affects the charge pumping.

1.5 Construction of thesis

This thesis is composed as follows: In Chapter 2, we give a brief review of theoretical methods related to this thesis. The main results of this thesis are given in Chapter 3, 4 and 5. In Chapter 3, we give a common framework for the adiabatic charge pumping, which are utilized in subsequent two chapters. In Chapter 4, we discuss the almost topological pumping in the non-interacting quantum dot system. In Chapter 5, we discuss adiabatic charge pumping induced by reservoir parameter driving via the interacting quantum dot. In Chapter 6, we give a summary, future problems, and perspectives.

Chapter 2

Review of theoretical methods

In this chapter, we give a brief review of theoretical methods related to adiabatic pumping. First, we introduce the model of quantum dots in Sec. 2.1. We review the scattering matrix theory and derive the Brouwer's formula in Sec. 2.2. We introduce the Keldysh formalism in Sec. 2.3. We present theoretical treatment of quantum dots with Coulomb interaction, and briefly explain the Kondo problem in Sec. 2.4. Throughout this thesis we set $k_B = 1$ and $\hbar = 1$.

2.1 Model for a single-level quantum dot

We consider the Hamiltonian of a single-level quantum dot (Fig. 2.1), which is known as the Anderson impurity model:

$$H = H_d + \sum_{r=L,R} (H_r + H_{T,r}), \quad (2.1)$$

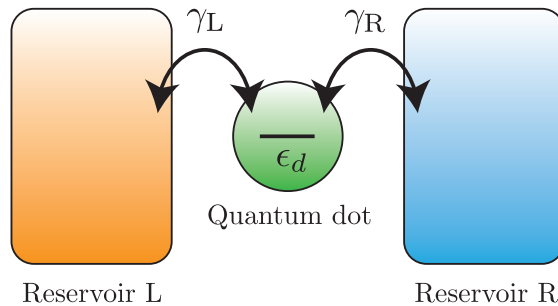


Fig. 2.1 A schematic of the model defined in Eq. (2.1).

where,

$$H_d = \sum_s \varepsilon_d d_s^\dagger d_s + U d_\uparrow^\dagger d_\uparrow d_\downarrow^\dagger d_\downarrow, \quad (2.2)$$

$$H_r = \sum_{k,s} \varepsilon_k c_{rks}^\dagger c_{rks}, \quad (2.3)$$

$$H_{T,r} = \sum_{k,s} \gamma_r (d_s^\dagger c_{rks} + c_{rks}^\dagger d_s). \quad (2.4)$$

Here d_s^\dagger and d_s denote creation and annihilation operators of electrons in the quantum dot with a spin $s \in \{\uparrow, \downarrow\}$ and an energy ε_d , respectively. c_{rks}^\dagger and c_{rks} denote creation and annihilation operators of electrons in the electron reservoir $r \in \{L, R\}$ with an energy ε_k , a wavenumber k , and a spin s , respectively. γ_r denotes a tunnel coupling constant between the quantum dot and the reservoir r and U denotes a strength of Coulomb interacting inside the dot.

In Chap. 4, we consider the noninteracting electron model ($U = 0$). There, we will consider the spinless model by dropping the spin index s because electrons with different spins are independent of each other in the absence of the Coulomb interaction.

The coupling between the reservoir r and the quantum dot is represented by a linewidth function defined as

$$\Gamma_r(\omega) = 2\pi |\gamma_r|^2 \rho(\omega), \quad (2.5)$$

where $\rho(\omega)$ is the density of states of the reservoirs at an energy ω . In the wide-band limit, for which the density of states is assumed to be constant near the Fermi energy, the linewidth function becomes

$$\Gamma_r = 2\pi |\gamma_r|^2 \rho. \quad (2.6)$$

We note that referring to the function $\Gamma_r(\omega)$ as the ‘‘linewidth’’ function is a slight abuse of terminology; the constant quantity in the wide-band limit, Γ_r , should be called as the linewidth in the exact sense. However, generalization to the frequency-dependent linewidth function is reasonable and useful for the present study, so we use this terminology hereafter.

2.2 Scattering theory for a quantum dot system

Although the central calculation of this thesis is done by the Keldysh formalism, the scattering theory is worth introducing because it is a powerful tool in the study of electron transport

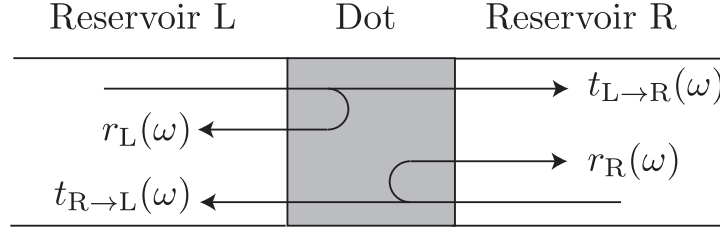


Fig. 2.2 Relation of transmission and reflection coefficients.

via a quantum dot without Coulomb interaction. We first review the scattering theory for time-independent transport in Sec. 2.2.1, and subsequently introduce the Brouwer's formula for adiabatic pumping in Sec. 2.2.2.

2.2.1 Steady state transport

In the scattering theory, a charge current is expressed by a difference between the amounts of incoming and outgoing electrons. We denote an annihilation operator of incoming electrons from the reservoir r with $a_r(\omega)$, and that for outgoing electrons into the reservoir r with $b_r(\omega)$, respectively, where ω denotes the energy of electrons. Then, the steady-state charge current from the reservoir r to a scatter, which is a quantum dot in the present study, is described as

$$I_r = e \int \frac{d\omega}{2\pi} \left[\langle a_r^\dagger(\omega) a_r(\omega) \rangle - \langle b_r^\dagger(\omega) b_r(\omega) \rangle \right]. \quad (2.7)$$

In the scattering theory, incoming and outgoing electrons are related with each other by the scattering matrix $S_{rr'}(\omega)$ as

$$b_r(\omega) = \sum_{r'} S_{rr'}(\omega) a_{r'}(\omega), \quad (2.8)$$

where

$$S_{LL}(\omega) = r_L(\omega), \quad S_{LR}(\omega) = t_{R \rightarrow L}(\omega), \quad S_{RL}(\omega) = t_{L \rightarrow R}(\omega), \quad S_{RR}(\omega) = r_R(\omega). \quad (2.9)$$

Here $r_L(\omega)$ ($r_R(\omega)$) denotes a reflection coefficient between a scatterer (a quantum dot) and the reservoir L (R), and $t_{L \rightarrow R}(\omega)$ ($t_{R \rightarrow L}(\omega)$) denote transmission coefficients from the reservoir L (R) to the reservoir R (L), respectively (see Fig. 2.2). Because of the conservation of probability, the scattering matrix is a unitary matrix. From this unitarity condition, we

obtain

$$|r_L(\omega)|^2 + |t_{L \rightarrow R}(\omega)|^2 = |r_R(\omega)|^2 + |t_{R \rightarrow L}(\omega)|^2 = 1. \quad (2.10)$$

Substituting Eq. (2.8) into Eq. (2.7), the steady-state charge current is expressed only by the operators of the incoming electrons as

$$I_r = e \int \frac{d\omega}{2\pi} \sum_{r_1, r_2} \left[(\delta_{r_1 r} \delta_{r r_2} - S_{r_1 r}^*(\omega) S_{r r_2}(\omega)) \langle a_{r_1}^\dagger(\omega) a_{r_2}(\omega) \rangle \right], \quad (2.11)$$

where δ_{r_1, r_2} is the Kronecker delta. Assuming that the reservoir $r(=L, R)$ is in equilibrium with temperature T_r and chemical potential μ_r , the ensemble average with respect to the incoming electrons is given as

$$\langle a_{r_1}^\dagger(\omega) a_{r_2}(\omega) \rangle = \delta_{r_1, r_2} f_r(\omega), \quad (2.12)$$

where $f_r(\omega) = \{1 + \exp[(\omega - \mu_r)/T_r]\}^{-1}$ is the Fermi distribution function of the reservoir r . Substituting Eqs. (2.9), (2.10), and (2.12) into (2.11), one obtains

$$I_r = e \int \frac{d\omega}{2\pi} [|t_{r \rightarrow \bar{r}}(\omega)|^2 f_r(\omega) - |t_{\bar{r} \rightarrow r}(\omega)|^2 f_{\bar{r}}(\omega)], \quad (2.13)$$

where $\bar{L} = R$ and $\bar{R} = L$. In the wide-band limit, the transmission coefficients for a single level quantum dot is calculated in a simple form [46]:

$$|t_{L \rightarrow R}|^2 = |t_{R \rightarrow L}|^2 = \frac{\Gamma_L \Gamma_R}{\Gamma} A(\omega), \quad (2.14)$$

$$A(\omega) = \text{Im} G^A(\omega) = \frac{\Gamma}{(\omega - \varepsilon_d)^2 + \Gamma^2/4}. \quad (2.15)$$

Here $\Gamma = \Gamma_L + \Gamma_R$, $A(\omega)$ is a spectrum function, and $G^A(\omega)$ is the advanced Green's function of electrons in the quantum dot. Using Eq. (2.14), the steady state charge current is summarized into the well-known Meir-Wingreen formula [46] for the quantum dot with Coulomb interaction:

$$I_r = e \int \frac{d\omega}{2\pi} \frac{\Gamma_L \Gamma_R}{\Gamma} A(\omega) [f_r(\omega) - f_{\bar{r}}(\omega)]. \quad (2.16)$$

In the later discussion (Sec. 2.3.5), we will derive Eq. (2.16) again in the Keldysh formalism.

2.2.2 Brouwer's formula

We consider charge transport induced by time-dependent slow modulation of parameters such as dot-reservoir couplings, a quantum level in a dot, and a shape of a dot. In the presence of the source-drain bias, a steady-state current may flow via a quantum dot during parameter modulation. In addition to this steady current, there exists an extra charge current due to the quasi-static parameter driving. The latter transport phenomenon is called adiabatic charge pumping. Brouwer's formula [6] describes the amount of pumped charge in one cycle of parameter driving.

First, we consider adiabatic charge pumping induced by driving of two parameters, $X_1(t)$ and $X_2(t)$,¹ with infinitesimal small amplitudes:

$$X_1(t) = X_{1,0} + \delta X_1 e^{-i\Omega t}, \quad X_2(t) = X_{2,0} + \delta X_2 e^{-i\Omega t}, \quad (2.17)$$

where $X_{n,0}$ ($n = 1, 2$) is a central value of the driving, δX_n is a driving amplitude, and Ω is a pumping frequency. In the quantum dot system, the driving parameters are typically supposed to be the coupling strength γ_r and the dot energy level ε_d . The amount of charge carried during one cycle from the reservoir r is defined as

$$\delta Q_r = \int_0^T dt I_r(t), \quad (2.18)$$

where $T = 2\pi\Omega^{-1}$ is the period of the parameter driving. As the driving amplitude is infinitesimally small, the time-dependent charge current is approximately written up to the linear order of amplitude as

$$I_r(t) \simeq I_r^{\text{st.}} + \mathcal{G}_{r,1}(\Omega)\delta X_1 e^{-i\Omega t} + \mathcal{G}_{r,2}(\Omega)\delta X_2 e^{-i\Omega t}. \quad (2.19)$$

Here $I_r^{\text{st.}}$ is the steady-state charge current, and $\mathcal{G}_{r,n}(\Omega)$ is a dynamic conductance obtained from the linear response theory with respect to δX_n , [4, 47]. For simplicity, we consider the case of $T_L = T_R = 0$ and $\mu_L = \mu_R = \mu$. In this case, the steady-state current $I_r^{\text{st.}}$ vanishes. Because $\mathcal{G}_{r,n}(\Omega)$ approaches zero in the static limit ($\Omega \rightarrow 0$), the leading contribution at low frequencies is written as

$$\mathcal{G}_{r,n}(\Omega) = -i\Omega A_{r,n} + O(\Omega^2). \quad (2.20)$$

¹ $X_1(t)$ and $X_2(t)$ should be chosen as the parameters defined in the Hamiltonian because the Brouwer's formula is derived by the scattering theory.

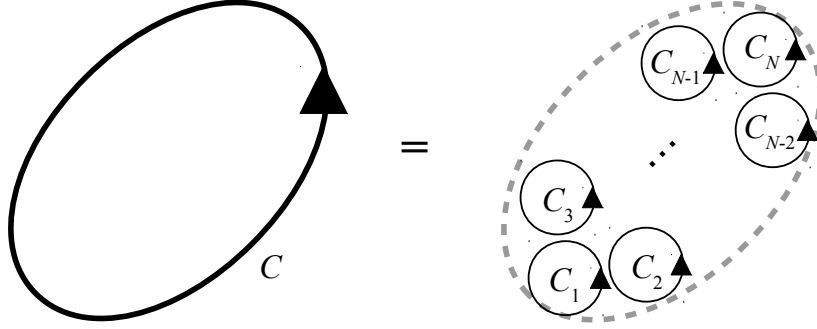


Fig. 2.3 A schematic of contour division. Any finite contour can be divided into a summation of infinitesimally small contours.

The coefficient $A_{r,n}$ is referred to as the Berry connection and is calculated from the scattering matrix as [48]

$$A_{r,n} = \frac{e}{2\pi} \sum_{r'} \text{Im} \left[S_{rr'}^*(\mu) \frac{\partial S_{r'r}(\mu)}{\partial X_n} \right]. \quad (2.21)$$

Using the Berry connection $A_{r,n}$, one obtains the adiabatic charge current as

$$I_r(t) \simeq \sum_n A_{r,n} \frac{dX_n}{dt} + O(\Omega^2). \quad (2.22)$$

The charge pumped in one cycle of adiabatic parameter driving is given as

$$\begin{aligned} \delta Q_r &= \sum_n \int_0^T dt A_{r,n} \frac{dX_n}{dt} \\ &= \sum_n \int_C dX_n A_{r,n}. \end{aligned} \quad (2.23)$$

Here $C = \{(X_1(t), X_2(t)) | t \in [0, T]\}$ is a closed contour with infinitesimally small amplitude in the parameter space.

It is straightforward to extend the present discussion for infinitesimally small contours into an arbitrary contour with a finite amplitude. Using the additivity property of the line integral

$$\sum_n \int_{C_1} dX_n(\dots) + \sum_n \int_{C_2} dX_n(\dots) = \sum_n \int_{C_1+C_2} dX_n(\dots), \quad (2.24)$$

any contour can be divided into a sum of infinitesimal small driving contours (see Fig. 2.3). Using the Stokes' theorem, the line integral can be rewritten into a surface integral on an area \mathcal{A} enclosed by C as

$$\delta Q_r = \int_{\mathcal{A}} dX_1 dX_2 \Pi_r, \quad (2.25)$$

$$\begin{aligned} \Pi_r &= \frac{\partial A_{r,2}}{\partial X_1} - \frac{\partial A_{r,1}}{\partial X_2} \\ &= \frac{e}{\pi} \sum_{r'} \text{Im} \left[\frac{\partial S_{rr'}^*(\mu)}{\partial X_2} \frac{\partial S_{rr'}(\mu)}{\partial X_1} \right], \end{aligned} \quad (2.26)$$

where Π_r is referred to as the Berry curvature. Eqs. (2.25) and (2.26) are known as Brouwer's formula.

It is straightforward to derive Brouwer's formula for driving of more than two parameters:

$$\delta Q_r = \sum_{n,m} \int_{\mathcal{A}} dX_n \wedge dX_m \Pi_r^{nm}, \quad (2.27)$$

$$\Pi_r^{nm} = \frac{\partial A_{r,m}}{\partial X_n}, \quad (2.28)$$

where \wedge is the wedge product.

2.3 Keldysh formalism for quantum dot system

Although the scattering theory is powerful in studying transport in quantum dot systems, it is not applicable to systems with Coulomb interaction. In this section, we give a brief introduction on the Keldysh formalism, which can treat time-dependent transport in interacting electron systems.

2.3.1 Keldysh time contour

The Keldysh formalism is a generalized quantum field theory for studying nonequilibrium states. In the Keldysh formalism, one can use the same procedure as the "ordinary" quantum field theory, that is, the quantum field theory for zero-temperature systems. The main difference between the Keldysh formalism and the ordinary quantum field theory appears in the definition of time contour: In the ordinary quantum field theory, the time contour is a one-way path which runs from $-\infty$ to $+\infty$ (see Fig. 2.4 (a)). On the other hand, in the Keldysh formalism, the time contour is composed of three contours, the forward contour C_+ , the backward contour C_- , and the Matsubara contour C_M (see Fig. 2.4 (b)).

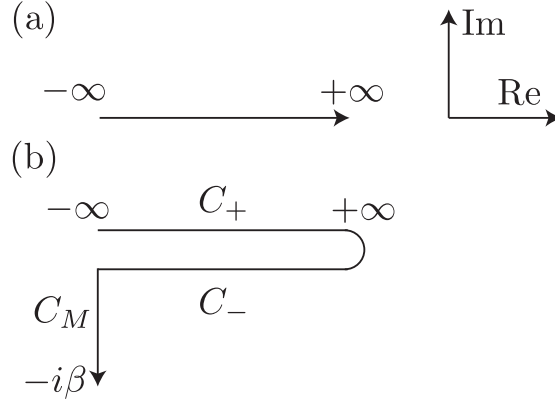


Fig. 2.4 Time contours for (a) zero temperature quantum field theory, (b) Keldysh formalism.

The reason to employ this complex time contour is explained as follows. The ensemble average of an observable O at time t is calculated as

$$\langle O(t) \rangle = \text{Tr}[O(t)\rho(t)], \quad (2.29)$$

$$\begin{aligned} \rho(t) &= U(t, -\infty)\rho(-\infty)U(-\infty, t) \\ &= \mathcal{T} \left\{ \exp \left[-i \int_{-\infty}^t d\tau H \right] \right\} \rho(-\infty) \tilde{\mathcal{T}} \left\{ \exp \left[-i \int_t^{-\infty} d\tau H \right] \right\}, \end{aligned} \quad (2.30)$$

where $\rho(t)$ is a density matrix at time t , $U(t, t')$ is an unitary time-evolution operator, and \mathcal{T} and $\tilde{\mathcal{T}}$ are a time-ordering operator and an anti-time-ordering operator, respectively. Assuming that the initial state at $t = -\infty$ is a thermal equilibrium state with inverse temperature β , $\rho(-\infty)$ is written by the imaginary-time evolution operator as

$$\rho(-\infty) = \frac{e^{-\beta H}}{\text{Tr}[e^{-\beta H}]} = \frac{\exp \left[-i \int_0^{-i\beta} d\tau H \right]}{\text{Tr} \left\{ \exp \left[-i \int_0^{-i\beta} d\tau H \right] \right\}}. \quad (2.31)$$

Substituting Eqs. (2.30) and (2.31) into Eq. (2.29), the ensemble average is evaluated by the time integral on the three contours,

$$\begin{aligned} \langle O(t) \rangle &= \frac{\text{Tr} \left[\exp \left[-i \int_{C_M} d\tau H \right] \tilde{\mathcal{T}} \left\{ \exp \left[-i \int_{C_-} d\tau H \right] \right\} \mathcal{T} \left\{ O(t) \exp \left[-i \int_{C_+} d\tau H \right] \right\} \right]}{\text{Tr} \left[\exp \left[-i \int_{C_M} d\tau H \right] \tilde{\mathcal{T}} \left\{ \exp \left[-i \int_{C_-} d\tau H \right] \right\} \mathcal{T} \left\{ \exp \left[-i \int_{C_+} d\tau H \right] \right\} \right]} \\ &=: \frac{\text{Tr} \left[\mathcal{T}_K \left\{ O(t) \exp \left[-i \int_{C_K} d\tau H \right] \right\} \right]}{\text{Tr} \left[\mathcal{T}_K \left\{ \exp \left[-i \int_{C_K} d\tau H \right] \right\} \right]}, \end{aligned} \quad (2.32)$$

where $C_+ = [-\infty, \infty]$, $C_- = [\infty, -\infty]$, $C_M = [0, -i\beta]$, and $C_K = C_+ \oplus C_- \oplus C_M$. \mathcal{T}_K is a time-ordering operator on the Keldysh contour C_K .

Here we give two comments: (i) For zero temperature systems, the time contour is simplified to the one-way time contour. This is because only the ground state is considered in zero-temperature systems. For the ground state, one can apply the Gell-Mann and Low theorem and cancel out the time evolution operators each other. (ii) As mentioned above, the ordinary quantum field theory and the Keldysh formalism are different only in terms of the time contour. This indicates that all the techniques in ordinary quantum field theory are still available in the Keldysh formalism, such as the method of the Feynman diagram.

2.3.2 Green's function

In the quantum field theory, physical objects are described in terms of Green's function (GF). A brief summary of the definitions and results for GFs is given in Appendix A.

One-particle full GF of electrons in the quantum dot is defined as a two-point correlation function

$$G_s(\tau_1, \tau_2) = (-i) \left\langle \mathcal{T}_K \left\{ d_s(\tau_1) d_s^\dagger(\tau_2) \right\} \right\rangle. \quad (2.33)$$

Here τ_1 and τ_2 indicate a ‘‘Keldysh time’’ defined on the time contour C_K . Hereafter, we use the Greek alphabet τ for Keldysh time and the Roman alphabet t for real time. The one-particle full GF can be calculated by Dyson's equation as follows:

$$G_s(\tau_1, \tau_2) = G_{0,s}(\tau_1, \tau_2) + \int_{C_K} d\tau_3 d\tau_4 G_{0,s}(\tau_1, \tau_3) \Sigma_{U,s}(\tau_3, \tau_4) G_s(\tau_4, \tau_2), \quad (2.34)$$

where $\Sigma_{U,s}(\tau_3, \tau_4)$ is a one-particle-irreducible(1PI) self-energy induced by the Coulomb interaction U and $G_{0,s}(\tau_1, \tau_2)$ is a non-interacting one-particle GF defined as

$$G_{0,s}(\tau_1, \tau_2) = (-i) \left\langle \mathcal{T}_K \left\{ d_s(\tau_1) d_s^\dagger(\tau_2) \right\} \right\rangle_{U=0}. \quad (2.35)$$

The non-interacting one-particle GF can be also calculated by Dyson's equation,

$$G_{0,s}(\tau_1, \tau_2) = g_s(\tau_1, \tau_2) + \int_{C_K} d\tau_3 d\tau_4 g_s(\tau_1, \tau_3) \Sigma_{\gamma,s}(\tau_3, \tau_4) G_{0,s}(\tau_4, \tau_2), \quad (2.36)$$

where $\Sigma_{\gamma,s}(\tau_1, \tau_2)$ is a 1PI self-energy induced by the dot-reservoir tunnel coupling γ_r (see Eq. (2.4)), and is defined as

$$\Sigma_{\gamma,s}(\tau_1, \tau_2) = \sum_r \Sigma_{r,s}(\tau_1, \tau_2), \quad (2.37)$$

$$\Sigma_{r,s}(\tau_1, \tau_2) = \sum_k |\gamma_r|^2 g_{rks}(\tau_1, \tau_2). \quad (2.38)$$

$g_{s_1}(\tau_1, \tau_2)$ and $g_{rks_1}(\tau_1, \tau_2)$ are isolated one-particle GFs of electrons in the quantum dot and the reservoir r , respectively, and are defined as

$$g_{rks}(\tau_1, \tau_2) = (-i) \left\langle \mathcal{T}_K \left\{ c_{rks}(\tau_1) c_{rks}^\dagger(\tau_2) \right\} \right\rangle_{U=\gamma_r=0}, \quad (2.39)$$

$$g_s(\tau_1, \tau_2) = (-i) \left\langle \mathcal{T}_K \left\{ d_s(\tau_1), d_s^\dagger(\tau_2) \right\} \right\rangle_{U=\gamma_r=0}. \quad (2.40)$$

We note that these definitions and formulas are the same as those in the ordinary quantum field theory except that all the time variables are defined on the Keldysh time contour.

2.3.3 Keldysh component

As shown in the previous section, all the time variables are defined on the Keldysh time contour in the Keldysh formalism. Here one might have a question: Which of time contours, C_+ and C_- , is proper to calculate an ensemble average of physical quantities at a ‘‘real’’ time t ? When one considers an average of an observable, $\langle O(t) \rangle$, such question is not serious, because the ensemble averages on C_+ and C_- are coincident with each other, that is, $\langle O^+(t) \rangle = \langle O^-(t) \rangle$. Here the superscript \pm indicates that the time variable t is located on the contour C_\pm .

On the other hand, the two-point correlation function $G_{s_1 s_2}(\tau_1, \tau_2)$ has four different components depending on which time contours τ_1 and τ_2 are located on:

$$G_s^{++}(t_1, t_2) = (-i) \left\langle T \left\{ d_s(t_1) d_s^\dagger(t_2) \right\} \right\rangle, \quad (2.41)$$

$$G_s^{+-}(t_1, t_2) = i \left\langle d_s^\dagger(t_2) d_s(t_1) \right\rangle, \quad (2.42)$$

$$G_s^{-+}(t_1, t_2) = (-i) \left\langle d_s(t_1) d_s^\dagger(t_2) \right\rangle, \quad (2.43)$$

$$G_s^{--}(t_1, t_2) = (-i) \left\langle \bar{T} \left\{ d_s(t_1) d_s^\dagger(t_2) \right\} \right\rangle. \quad (2.44)$$

Here the first and second superscripts indicate the contour of t_1 and t_2 , respectively. The components G^{++} and G^{--} are called time-ordering and anti-time-ordering components,

respectively. The components G^{+-} and G^{-+} , which are denoted also with $G^<$ and $G^>$, are called lesser and greater components. When one expresses physical quantities with Keldysh GFs, one should choose appropriate components of GFs.

Although these four components of GFs include sufficient information, it is useful to use other two components, a retarded component G^R and an advanced component G^A defined as follows:

$$\begin{aligned} G_s^R(t_1, t_2) &= G_s^{++}(t_1, t_2) - G_s^{+-}(t_1, t_2) = G_s^{-+}(t_1, t_2) - G_s^{--}(t_1, t_2) \\ &= (-i)\Theta(t_1 - t_2) \left\langle [d_s(t_1), d_s^\dagger(t_2)]_+ \right\rangle, \end{aligned} \quad (2.45)$$

$$\begin{aligned} G_s^A(t_1, t_2) &= G_s^{++}(t_1, t_2) - G_s^{-+}(t_1, t_2) = G_s^{+-}(t_1, t_2) - G_s^{--}(t_1, t_2) \\ &= i\Theta(t_2 - t_1) \left\langle [d_s(t_1), d_s^\dagger(t_2)]_+ \right\rangle. \end{aligned} \quad (2.46)$$

Here $\Theta(t)$ is the Heaviside step function and $[\cdot, \cdot]_+$ is an anti-commutator. These retarded and advanced components often make the calculation more transparent.

One might be curious about contour C_M . For the problems of steady states, one can assume that the initial time is infinitely far from the observation time and the information of the initial state should be completely erased. Under such assumption, the correlation between the initial state and the steady state realized near the origin ($t \simeq 0$) should be infinitely small. Therefore, a contribution from the contour C_M should be neglected as

$$G^{+M}(t_1, t_2) = G^{-M}(t_1, t_2) = G^{M+}(t_1, t_2) = G^{M-}(t_1, t_2) = 0. \quad (2.47)$$

As a result, it is sufficient to focus on C_\pm in calculation of the steady states.

2.3.4 Langreth rules

In the Keldysh formalism, it is necessary to perform convolution integral on the Keldysh time contour, which is composed of two real-time integrals: ²

$$\int_{C_K} d\tau = \int_{C_+} dt + \int_{C_-} dt. \quad (2.48)$$

²One might feel strange that the time integral on Keldysh time contour is composed of two time integrals on C_+ and C_- . Strictly speaking, the time integral on the Keldysh time contour should be composed of three time integrals. However, the time integral on C_M does not make any contribution because of Eq. (2.47), so the time integral on C_M can be dropped in the most cases.

Then, the time integral of a product of two quantities is written as

$$\int_{C_K} d\tau A(\tau)B(\tau) = \int_{-\infty}^{\infty} dt [A^+(t)B^+(t) - A^-(t)B^-(t)]. \quad (2.49)$$

A product of two-point correlation functions

$$A(\tau_1, \tau_2) = \int_{C_K} d\tau B(\tau_1, \tau)C(\tau, \tau_2). \quad (2.50)$$

is rewritten with real-time integrals by the so-called Langreth rules: Each Keldysh component of $A(\tau_1, \tau_2)$ is rewritten as follows:

$$A^{++}(t_1, t_2) = \int_{-\infty}^{\infty} dt [B^{++}(t_1, t)C^{++}(t, t_2) - B^{<}(t_1, t)C^{>}(t, t_2)], \quad (2.51)$$

$$A^{<}(t_1, t_2) = \int_{-\infty}^{\infty} dt [B^R(t_1, t)C^{<}(t, t_2) + B^{<}(t_1, t)C^A(t, t_2)], \quad (2.52)$$

$$A^{>}(t_1, t_2) = \int_{-\infty}^{\infty} dt [B^R(t_1, t)C^{>}(t, t_2) + B^{>}(t_1, t)C^A(t, t_2)], \quad (2.53)$$

$$A^{--}(t_1, t_2) = \int_{-\infty}^{\infty} dt [B^{>}(t_1, t)C^{<}(t, t_2) - B^{--}(t_1, t)C^{--}(t, t_2)], \quad (2.54)$$

$$A^R(t_1, t_2) = \int_{-\infty}^{\infty} dt B^R(t_1, t)C^R(t, t_2), \quad (2.55)$$

$$A^A(t_1, t_2) = \int_{-\infty}^{\infty} dt B^A(t_1, t)C^A(t, t_2). \quad (2.56)$$

We note that simple relations hold for the retarded and the advanced components. This indicates that it is easier to calculate the retarded and the advanced components of two-point correlation functions than other components.

2.3.5 Charge current through a single-level quantum dot

For a demonstration, we derive steady-state charge current through a quantum dot in the Keldysh formalism. The charge current flowing from the reservoir r into the quantum dot is

defined as

$$\begin{aligned}
\langle I_r(t) \rangle &= (-e) \frac{d}{dt} \left[\sum_{k,s} \langle c_{rks}^\dagger(t) c_{rks}(t) \rangle \right] \\
&= ie \sum_{k,s} \langle [c_{rks}^\dagger(t) c_{rks}(t), H(t)]_- \rangle \\
&= ie \sum_{k,s} \left[\langle \gamma_r^* c_{rks}^\dagger(t) d_s(t) \rangle - \langle \gamma_r d_s^\dagger(t) c_{rks}(t) \rangle \right] \\
&= 2e \text{Re} \left[\gamma_r^* \sum_{k,s} G_{d_s, c_{rks}^\dagger}^<(t, t) \right], \tag{2.57}
\end{aligned}$$

where $G_{d_s, c_{rks}^\dagger}^<$ is a GF defined as

$$G_{d_s, c_{rks}^\dagger}(\tau_1, \tau_2) = (-i) \langle \mathcal{T}_K d_s(\tau_1) c_{rks}^\dagger(\tau_2) \rangle. \tag{2.58}$$

Using the equation-of-motion technique [49], this GF is evaluated as

$$G_{d_s, c_{rks}^\dagger}(\tau_1, \tau_2) = \gamma_r \int d\tau G_{ss}(\tau_1, \tau) g_{rks}(\tau, \tau_2). \tag{2.59}$$

Substituting Eqs. (2.52) and (2.59) into Eq. (2.57), the charge current is calculated as

$$\langle I_r(t) \rangle = 2e \sum_s \int dt_1 \text{Re} \left[G_s^R(t, t_1) \Sigma_{r,s}^<(t_1, t) + G_s^<(t, t_1) \Sigma_{r,s}^A(t_1, t) \right]. \tag{2.60}$$

This equation holds for arbitrary strengths of U and γ_r and for arbitrary time-dependent parameter driving.

In order to compare with the result obtained by the scattering theory (Eq. (2.16)), we consider the steady-state current for non-interacting systems ($U = 0$), in which the one-particle full GFs, G_s , are replaced with the non-interacting ones, $G_{0,s}$. For time-independent Hamiltonians, the GF acquires the time-translation invariance, that is,

$$G_s^{\mu\nu}(t_1, t_2) = \int \frac{d\omega}{2\pi} G_s^{\mu\nu}(\omega) e^{-i\omega(t_1-t_2)}, \tag{2.61}$$

where $\mu, \nu \in \{+, -\}$ are Keldysh indices. Then the charge current for a non-interacting and time-independent system becomes

$$\langle I_r(t) \rangle = 2e \sum_s \int \frac{d\omega}{2\pi} \text{Re} \left[G_{0,s}^R(\omega) \Sigma_{r,s}^<(\omega) + G_{0,s}^<(\omega) \Sigma_{r,s}^A(\omega) \right]. \tag{2.62}$$

The 1PI self-energy is calculated as follows:

$$\begin{aligned}\Sigma_{r,s}^A(\omega) &= |\gamma_r|^2 \sum_k \frac{1}{\omega - \varepsilon_k + i0_+} \\ &= |\gamma_r|^2 \int d\varepsilon \rho(\varepsilon) \frac{1}{\omega - \varepsilon + i0_+} = \Lambda_r(\omega) + \frac{i}{2}\Gamma_r(\omega),\end{aligned}\quad (2.63)$$

$$\Sigma_{r,s}^R(\omega) = |\gamma|^2 \sum_k \frac{1}{\omega - \varepsilon_k - i0_+} = \Lambda_r(\omega) - \frac{i}{2}\Gamma_r(\omega),\quad (2.64)$$

$$\Sigma_{r,s}^<(\omega) = |\gamma|^2 \sum_k i f_r(\varepsilon_k) 2\pi \delta(\omega - \varepsilon_k) = \Gamma_r(\omega) f_r(\omega).\quad (2.65)$$

The non-interacting GF G_0 can be calculated by Dyson's equation,

$$G_{0,s}^A(\omega) = \left[g_s^A(\omega) - \Sigma_{\gamma,s}^A(\omega) \right]^{-1} = \frac{1}{\omega - \varepsilon_d - \Lambda_r(\omega) - i\Gamma(\omega)/2},\quad (2.66)$$

$$G_{0,s}^R(\omega) = \left[g_s^R(\omega) - \Sigma_{\gamma,s}^R(\omega) \right]^{-1} = \frac{1}{\omega - \varepsilon_d - \Lambda_r(\omega) + i\Gamma(\omega)/2},\quad (2.67)$$

$$G_{0,s}^<(\omega) = G_{0,s}^R(\omega) \Sigma_{\gamma,s}^<(\omega) G_{0,s}^A(\omega) = A(\omega) \sum_r \frac{\Gamma_r(\omega)}{\Gamma(\omega)} f_r(\omega).\quad (2.68)$$

Substituting Eqs. (2.63)-(2.68) into Eq. (2.62) and taking the wide-band limit, one obtains the formula for the charge current in Eq. (2.16).

2.4 Kondo effect

In Chapter. 5, we study adiabatic pumping via a quantum dot, which exhibits the Kondo effect due to strong Coulomb interaction. First we overview what changes in electron transport in the Kondo region, especially at the Kondo resonance. We next describe the perturbation theory with respect to U , which is effective to describe the Kondo effect. In order to include higher-order perturbations, we introduce the renormalized perturbation theory (RPT), in which the renormalized parameters are used instead of the bare parameters. Throughout this section, we consider only the wide-band limit.

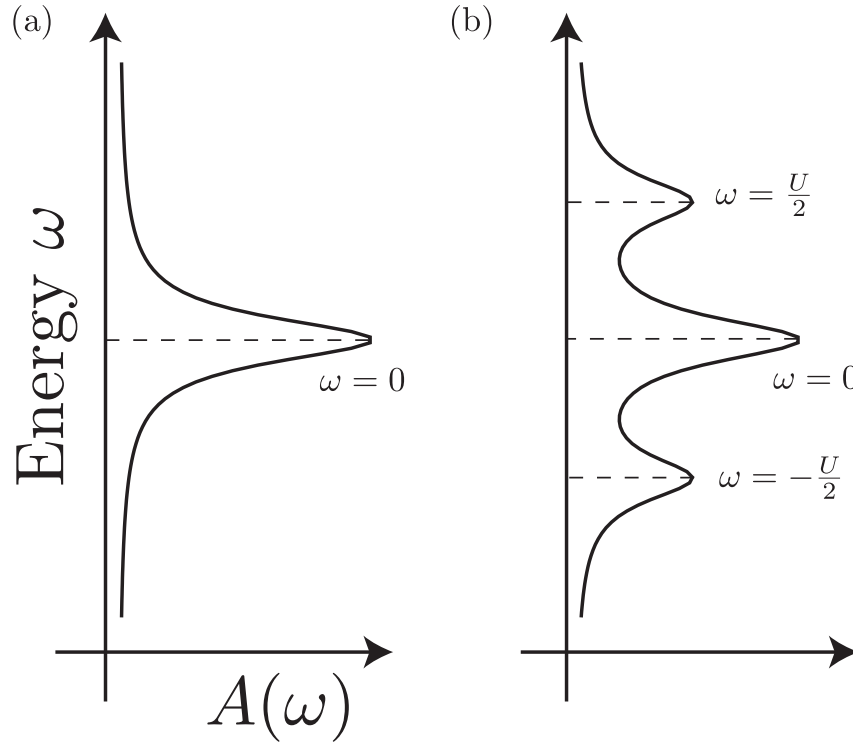


Fig. 2.5 A schematic of the spectrum function of a quantum dot for (a) a non-interacting case and (b) an interacting case. In this figure, we consider the particle-hole symmetric case, $\varepsilon_d = -U/2$, for simplicity.

2.4.1 Overview of the Kondo effect

To see what changes in electron transport by the Kondo effect, we consider a single-level quantum dot with strong Coulomb interaction. In the single-level quantum dot system, electrons are transported from a reservoir to the other through the density of states of the quantum dot, which is called the spectrum function $A(\omega)$. Without the Coulomb interaction, an electron with energy ε_d , that denotes the height of the energy level of a quantum dot, can enter the quantum dot by the tunneling effect and its tunneling probability does not depend on whether another electron with opposite spin already occupies the quantum dot. In this case, the spectrum function has a Lorentzian shaped peak at the quantum dot energy level, $\omega = \varepsilon_d$, with a finite broadening width (Fig. 2.5 (a)). However, for a finite strength of Coulomb interaction, $U \neq 0$, an electron with the energy ε_d can enter the dot when the energy level of the dot is vacant, while an electron with energy $\varepsilon_d + U$ can enter the dot due to the Coulomb repulsion when the energy level of the dot is already occupied by another electron with opposite spin. Then, one might guess that the spectrum function in this case would be two Lorentzian peaks, one peak at $\omega = \varepsilon_d$ and the other at $\omega = \varepsilon_d + U$. This is true

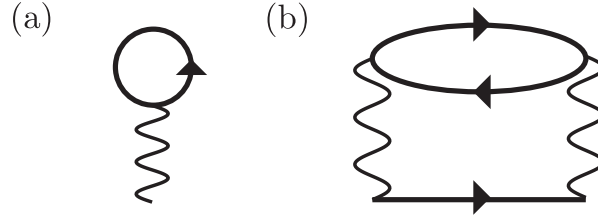


Fig. 2.6 Feynman diagrams representing (a) $\Sigma_{U,s}^{(1)}$ and (b) $\Sigma_{U,s}^{(2)}$. Solid and wavy lines indicate the one-particle GF and the Coulomb interaction U .

at high temperatures. However, when the temperature is lower than the typical energy scale called the Kondo temperature, the third strong peak appears at the Fermi energy between the two peaks. This new peak reflects electron transport through the Kondo state and called as the Kondo resonance peak (Fig. 2.5 (b)).

2.4.2 Perturbation with respect to U

We first discuss the perturbation expansion for the one-particle GFs, and subsequently discuss that for the two-particle GFs.

One-particle Green's function

The one-particle full GF is calculated by Dyson's equation (see Eq. (2.34)). In the perturbation theory, the 1PI self-energy is expanded into a series as

$$\Sigma_{U,s}(\tau_1, \tau_2) = \sum_{n=1}^{\infty} U^n \Sigma_{U,s}^{(n)}(\tau_1, \tau_2). \quad (2.69)$$

The first-order term is known as the Hartree term described as

$$\Sigma_{U,s}^{(1)}(\tau_1, \tau_2) = (-i)\delta(\tau_1 - \tau_2)G_{\bar{s}\bar{s}}(\tau_1, \tau_1 + \varepsilon), \quad (2.70)$$

where $\bar{\cdot}$ denotes the opposite direction of the spin, i.e., $\bar{\uparrow} = \downarrow$ and $\bar{\downarrow} = \uparrow$, and ε is an infinitesimal time on the Keldysh time contour introduced to maintain the order of operators in the Keldysh time ordering. The second-order term is described as

$$\Sigma_{U,s}^{(2)}(\tau_1, \tau_2) = G_s(\tau_1, \tau_2)G_{\bar{s}\bar{s}}(\tau_1, \tau_2)G_{\bar{s}\bar{s}}(\tau_2, \tau_1). \quad (2.71)$$

Feynman diagrams of $\Sigma_{U,s}^{(1)}(\tau_1, \tau_2)$ and $\Sigma_{U,s}^{(2)}(\tau_1, \tau_2)$ are shown in Fig. 2.6 (a) and (b), respectively.

We define the spectrum function as

$$A_s(\omega) = 2\text{Im} \left[G_s^A(\omega) \right] = -2\text{Im} \left[G_s^R(\omega) \right]. \quad (2.72)$$

Since the advanced GF for $U = 0$ is described in Eq. (2.66), the spectrum function takes a Lorentzian form:

$$A_s(\omega) = \frac{\Gamma}{(\omega - \varepsilon_d)^2 + \Gamma^2/4}. \quad (2.73)$$

For the interacting case, the spectrum function is modified by the 1PI self-energy as

$$A_s(\omega) = \frac{\tilde{\Gamma}_s(\omega)}{(\omega - \tilde{\varepsilon}_{d,s}(\omega))^2 + \tilde{\Gamma}_s^2(\omega)/4} \quad (2.74)$$

where $\tilde{\varepsilon}_{d,s}(\omega)$ and $\tilde{\Gamma}_s(\omega)$ is defined as

$$\tilde{\varepsilon}_{d,s} = \varepsilon_d + U\Sigma_{U,s}^{(1),A}(\omega) + U^2\text{Re} \left[\Sigma_{U,s}^{(2),A}(\omega) \right] + O(U^3), \quad (2.75)$$

$$\tilde{\Gamma}_s = \Gamma + 2U^2\text{Im} \left[\Sigma_{U,s}^{(2),A}(\omega) \right] + O(U^3). \quad (2.76)$$

In these equations, we have dropped $\text{Im} \left[\Sigma_{U,s}^{(1),A}(\omega) \right]$ because $\Sigma_{U,s}^{(1),A}(\omega)$ is a purely real function

$$\begin{aligned} \Sigma_{U,s}^{(1),A}(\omega) &= (-i) \int \frac{d\omega}{2\pi} G_s^<(\omega) = \int \frac{d\omega}{2\pi} \left\langle d_s^\dagger(\omega) d_s(\omega) \right\rangle \\ &=: \langle n_s \rangle. \end{aligned} \quad (2.77)$$

Here $\langle n_s \rangle$ denotes the occupation number of electrons in the dot with spin s . This indicates that the first-order self-energy $\Sigma_{U,s}^{(1)}$ describes only a shift of the energy-level, known as the Hartree potential. The Kondo resonance effect is described mainly by the second-order self-energy $\Sigma_{U,s}^{(2)}$.

Two-particle Green's function

Next we consider the perturbation theory for two-particle GFs, whose formulation is used in Chapter 5. The two-particle GF is a four-point correlation function defined as

$$\begin{aligned} &D_{s_1 s_2 s_3 s_4}(\tau_1, \tau_2, \tau_3, \tau_4) \\ &= (-i)^2 \left\langle \mathcal{T}_K \left\{ d_{s_1}(\tau_1) d_{s_2}^\dagger(\tau_2) d_{s_3}^\dagger(\tau_3) d_{s_4}(\tau_4) \right\} \right\rangle - \delta_{s_1, s_2} \delta_{s_3, s_4} G_{s_1}(\tau_1, \tau_2) G_{s_3}(\tau_4, \tau_3). \end{aligned} \quad (2.78)$$

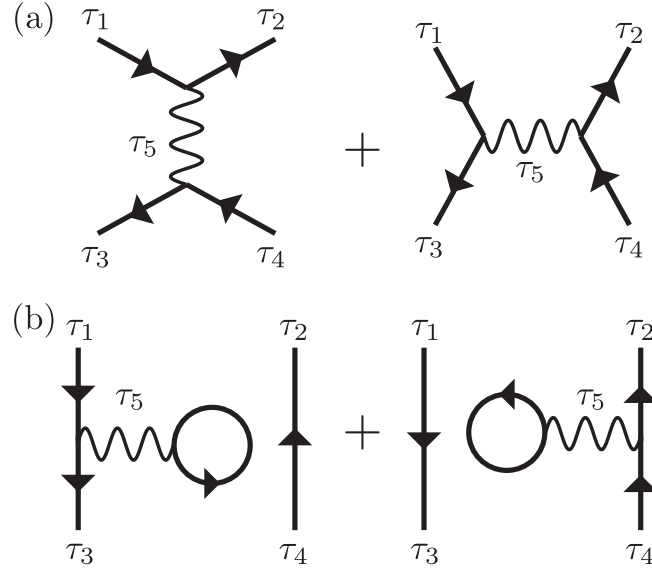


Fig. 2.7 Feynman diagrams representing (a) $D_{s_1 s_2 s_3 s_4}^{(1),a}(\tau_1, \tau_2, \tau_3, \tau_4)$ and (b) $D_{s_1 s_2 s_3 s_4}^{(1),b}(\tau_1, \tau_2, \tau_3, \tau_4)$. Solid and wavy lines indicate the one-particle GF and the Coulomb interaction U .

The two-particle GF can be expanded into a series with respect to U as

$$D_{s_1 s_2 s_3 s_4}(\tau_1, \tau_2, \tau_3, \tau_4) = \sum_n U^n D_{s_1 s_2 s_3 s_4}^{(n)}(\tau_1, \tau_2, \tau_3, \tau_4). \quad (2.79)$$

The first-order term is calculated as

$$D_{s_1 s_2 s_3 s_4}^{(1)}(\tau_1, \tau_2, \tau_3, \tau_4) = D_{s_1 s_2 s_3 s_4}^{(1),a}(\tau_1, \tau_2, \tau_3, \tau_4) + D_{s_1 s_2 s_3 s_4}^{(1),b}(\tau_1, \tau_2, \tau_3, \tau_4), \quad (2.80)$$

where,

$$\begin{aligned} & D_{s_1 s_2 s_3 s_4}^{(1),a}(\tau_1, \tau_2, \tau_3, \tau_4) \\ &= (-i)\delta_{s_2, s_1} \delta_{s_3, \bar{s}_1} \delta_{s_4, \bar{s}_1} \int d\tau_5 G_{0, s_1}(\tau_1, \tau_5) G_{0, s_1}(\tau_5, \tau_2) G_{0, \bar{s}_1}(\tau_5, \tau_3) G_{0, \bar{s}_1}(\tau_4, \tau_5) \\ &+ (-i)\delta_{s_2, \bar{s}_1} \delta_{s_3, s_1} \delta_{s_4, \bar{s}_1} \int d\tau_5 G_{0, s_1}(\tau_1, \tau_5) G_{0, \bar{s}_1}(\tau_5, \tau_2) G_{0, s_1}(\tau_5, \tau_3) G_{0, \bar{s}_1}(\tau_4, \tau_5), \end{aligned} \quad (2.81)$$

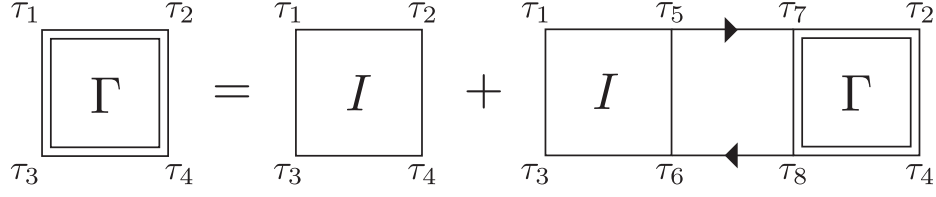


Fig. 2.8 Feynman diagrams representing the Bethe-Salpeter equation. Squares with single lines and doubled lines represent the 2PI vertex function and the full vertex function, respectively. Solid lines indicate the one-particle GFs.

and,

$$\begin{aligned}
& D_{s_1 s_2 s_3 s_4}^{(1),b}(\tau_1, \tau_2, \tau_3, \tau_4) \\
&= (-i) \delta_{s_3, s_1} \delta_{s_4, s_2} \int d\tau_5 G_{0, s_1}(\tau_1, \tau_5) G_{0, s_1}(\tau_3, \tau_5) G_{0, \bar{s}_1}(\tau_5, \tau_5 + \varepsilon) G_{0, s_2}(\tau_4, \tau_2) \\
&+ (-i) \delta_{s_3, s_1} \delta_{s_4, s_2} \int d\tau_5 G_{0, s_1}(\tau_1, \tau_3) G_{0, s_2}(\tau_5, \tau_2) G_{0, \bar{s}_2}(\tau_5, \tau_5) G_{0, s_2}(\tau_4, \tau_5). \quad (2.82)
\end{aligned}$$

Feynman diagrams of $D_{s_1 s_2 s_3 s_4}^{(1),a}(\tau_1, \tau_2, \tau_3, \tau_4)$ and $D_{s_1 s_2 s_3 s_4}^{(1),b}(\tau_1, \tau_2, \tau_3, \tau_4)$ are presented in Fig. 2.7 (a) and (b), respectively. The higher-order contributions of the two-particle GF can be constructed in a similar way.

We have seen that for the one-particle GF, the iterative structure in the perturbation series can be summarized using the self-energy and Dyson's equation. In a similar way, the iterative structure in the perturbation expansion for the two-particle GFs can be summarized using the irreducible vertex functions. We first define the full vertex function for the two-particle GF, $\Gamma_{s_1 s_2 s_3 s_4}(\tau_1, \tau_2, \tau_3, \tau_4)$, as

$$\begin{aligned}
& D_{s_1 s_2 s_3 s_4}(\tau_1, \tau_2, \tau_3, \tau_4) \\
&= \delta_{s_1, s_3} \delta_{s_2, s_4} G_{s_1}(\tau_1, \tau_3) G_{s_2}(\tau_4, \tau_2) \\
&+ \sum_{s_5 \cdots s_8} \int d\tau_5 \cdots d\tau_8 G_{s_1}(\tau_1, \tau_5) G_{s_3}(\tau_7, \tau_3) \Gamma_{s_1 s_2 s_3 s_4}(\tau_5, \tau_6, \tau_7, \tau_8) G_{s_2}(\tau_6, \tau_2) G_{s_4}(\tau_4, \tau_8). \quad (2.83)
\end{aligned}$$

The vertex function $\Gamma_{s_1 s_2 s_3 s_4}(\tau_1, \tau_2, \tau_3, \tau_4)$ is related to the two-partible-irreducible (2PI) vertex function $I_{s_1 s_2 s_3 s_4}(\tau_1, \tau_2, \tau_3, \tau_4)$ via the Bethe-Salpeter equation (Fig. 2.8) as

$$\begin{aligned} & \Gamma_{s_1 s_2 s_3 s_4}(\tau_1, \tau_2, \tau_3, \tau_4) \\ &= I_{s_1 s_2 s_3 s_4}(\tau_1, \tau_2, \tau_3, \tau_4) \\ &+ \sum_{s_5, s_6} \int d\tau_5 \cdots d\tau_8 I_{s_1 s_5 s_3 s_6}(\tau_1, \tau_5, \tau_3, \tau_6) G_{s_5}(\tau_5, \tau_7) G_{s_6}(\tau_8, \tau_6) \Gamma_{s_5 s_2 s_6 s_4}(\tau_7, \tau_2, \tau_8, \tau_4). \end{aligned} \quad (2.84)$$

Solving the Bethe-Salpeter equation iteratively with a given 2PI vertex function, one obtains the two-particle full vertex function and the two-particle GF.

Although one can calculate the one- and two-particle GFs for an arbitrary strength of U in principle, solving the Dyson's equation and the Bethe-Salpeter equation is a hard task and its calculation cost increases explosively for higher-order perturbation. In order to calculate the one-particle and the two-particle GFs with smaller calculation cost, one should employ approximate methods.

2.4.3 Renormalized perturbation theory (RPT)

The renormalized perturbation theory (RPT) [27, 28] is one of the successful method which describe the electron transport via the strongly correlated system, such as a quantum dot in the Kondo region. In the Kondo region, the Kondo resonance peak appears at the Fermi level in the spectrum function (see Fig. 2.5). When the temperature of the reservoirs and the chemical potential difference between the reservoirs are sufficiently smaller than the Kondo temperature, only the Kondo resonance peak contributes to the electron transport. In this picture, the quasi-particles with renormalized parameters, such as a renormalized quantum-dot level, a renormalized linewidth, and a renormalized Coulomb interaction, are transported through the Kondo resonance peak. This concept is known as the phenomenological local Fermi liquid theory [26]. RPT is a perturbation theory which replaces the parameters of the Anderson impurity model to the renormalized ones. This method effectively describes the electron transport via the Kondo impurities at low energies.

In this method, we focus on the low-energy part of the 1PI self-energy as follows:

$$\Sigma_{U,s}^A(\omega) = \Sigma_{U,s}^A(0) + \omega \Sigma'_{U,s}{}^A(0) + \Sigma_{U,s}^{\text{rem},A}(\omega). \quad (2.85)$$

The first and the second term describe the lower energy part of the 1PI self-energy, while the third term describes high energy part, $\Sigma_s^{\text{rem},A}(\omega) \sim O(\omega^2)$. Once one substitutes Eq.

(2.85) back into the advanced GF, one finds that $\Sigma_s^A(0)$ and $\omega\Sigma_s'^A(0)$ can be renormalized into parameters such as³

$$G_s^A(\omega) = \frac{z}{\omega - \tilde{\epsilon}_d - i\tilde{\Gamma}/2 - \tilde{\Sigma}_{U,s}^A(\omega)}, \quad (2.86)$$

$$z = (1 - \Sigma_s'^A(0))^{-1} \quad (2.87)$$

$$\tilde{\epsilon}_d = z(\epsilon_d + \Sigma_s^A(0)) \quad (2.88)$$

$$\tilde{\Gamma} = z\Gamma \quad (2.89)$$

$$\tilde{\Sigma}_{U,s}^A(\omega) = z\Sigma_{U,s}^{\text{rem},A}(\omega), \quad (2.90)$$

where z , $\tilde{\epsilon}_d$, $\tilde{\Gamma}$ and $\tilde{\Sigma}_{U,s}^A$ are referred to as a wavefunction renormalization factor, a renormalized quantum-dot level, a renormalized linewidth, and a renormalized 1PI self-energy, respectively.⁴ The renormalized 1PI self-energy $\tilde{\Sigma}_{U,s}^A$ can be regarded as the one induced by a renormalized Coulomb interaction \tilde{U} defined from the 2PI vertex function as

$$\tilde{U} = z^2 I_{ss\bar{s}\bar{s}}^{++++}(0, 0, 0, 0). \quad (2.91)$$

Using the renormalized parameters, z , $\tilde{\epsilon}_d$, $\tilde{\Gamma}$, and \tilde{U} , one can construct the perturbation theory called the renormalized perturbation theory (RPT) [27, 28]. In the RPT, the renormalized parameters are evaluated by an alternative method such as the numerical renormalization group [24] and the Bethe Ansatz [50]. The physics of the Kondo effect such as strong reduction of the hybridization energy and suppression of the quasi-particle weight is reflected in the renormalized parameters.

Here, we should note that simple replacement from the bare parameters to the renormalized ones causes an overcounting problems. This problem can be avoided by introducing counter terms (see Appendix C).

³Here we explicitly exhibit the overall z factor in Eq. (2.86). This overall factor can be cancelled by rescaling the creation and the annihilation operators, $d_s, d_s^\dagger \rightarrow \sqrt{z}d_s, \sqrt{z}d_s^\dagger$.

⁴We note that the renormalized parameters are independent of the spin in the absence of a magnetic field.

Chapter 3

Adiabatic approximation in the Keldysh formalism

In this chapter, we introduce the adiabatic approximation and derive a general formula for the Berry connection in the Keldysh formalism. Our new formulation is applicable to the interacting quantum dot systems with drivings of arbitrary parameters, including the temperatures of the reservoirs. Adiabatic pumping via the interacting quantum dot was formulated in the slave-boson mean field theory [43] and in the perturbation expansion up to infinite order [44]. Compared with these previous works, our formulation has an advantage that the effect of the Coulomb interaction is integrated in terms of the one- and two-particle GFs. The formula derived in this chapter (Eq. (3.21)) is one of the fundamental results of this thesis and will be utilized to discuss the topological nature of adiabatic pumping in Chapter 4 and the effect of the Coulomb interaction in Chapter 5.

3.1 Outline

In order to estimate the amount of adiabatically pumped charge in one cycle, one should formulate the adiabatic approximation. In this section, we show an outline of the derivation. A detailed derivation is given in the next section.

In Sec. 2.2.2, we have derived Brouwer's formula using the adiabatic approximation. The present derivation is almost the same as discussed in Sec. 2.2.2. We consider parameter driving with an infinitesimally small amplitude:

$$X_n(t) = X_{n,0} + \delta X_n e^{-i\Omega t}, \quad (3.1)$$

where $X_n(t)$ is the n -th driving parameter. The amount of pumped charge in one cycle is defined as

$$\langle \delta Q_r \rangle = \int_0^T dt \langle I_r(t) \rangle. \quad (3.2)$$

Assuming that the driving amplitude is infinitesimally small, the time-dependent charge current can be approximated up to the linear order as

$$I_r(t) \simeq I_r^{\text{st.}} + \sum_n \mathcal{G}_{r,n}(\Omega) \delta X_n e^{i\Omega t}. \quad (3.3)$$

Considering the Ω -linear term of the dynamical conductance, one can define the Berry connection $A_{r,n}$,

$$\mathcal{G}_{r,n}(\Omega) = -i\Omega A_{r,n} + O(\Omega^2), \quad (3.4)$$

and obtain the Brouwer's formula,

$$\begin{aligned} \langle \delta Q_r \rangle &= \sum_n \int_C dX_n A_{r,n} \\ &= \sum_{n,m} \int_A dX_n \wedge dX_m \Pi_{r,nm}, \end{aligned} \quad (3.5)$$

$$\Pi_{r,nm} = \frac{\partial A_{r,m}}{\partial X_n}. \quad (3.6)$$

3.2 Derivation of the dynamic conductance and the Berry connection

In the scattering theory, we evaluate the Berry connection $A_{r,n}$ simply by the scattering matrix without solving specific models. Here, we calculate the dynamical conductance using the Keldysh formalism. By the Fourier transformation, one can define the dynamical conductance with time arguments

$$\mathcal{G}_{r,n}(t_1, t_2) = \int \frac{d\Omega}{2\pi} \mathcal{G}_{r,n}(\Omega) e^{-i\Omega(t_1 - t_2)}. \quad (3.7)$$

This dynamical conductance equals to a functional derivative with respect to the driving parameters (for detail derivation, see Appendix D),

$$\mathcal{G}_{r,n}(t_1, t_2) = \left. \frac{\delta \langle I_r(t_1) \rangle}{\delta X_n(t_2)} \right|_{\delta X_n=0}. \quad (3.8)$$

For example, let us regard the dot-reservoir coupling driving as a driving parameter:

$$\gamma_r(t) = \gamma_{r,0} + \delta\gamma_r e^{-i\Omega t}. \quad (3.9)$$

Substituting Eq. (2.57) into Eq. (3.8),

$$\mathcal{G}_{r,r_2}(t_1, t_2) = 2e\text{Re} \left[\sum_{k,s} \frac{\delta\gamma_r^*(t_1)}{\delta\gamma_{r_2}(t_2)} G_{d_s, c_{rks}^\dagger}^<(t_1, t_1) + \sum_{k,s} \gamma_r^*(t_1) \frac{\delta}{\delta\gamma_{r_2}(t_2)} G_{d_s, c_{rks}^\dagger}^<(t_1, t_1) \right]. \quad (3.10)$$

The former term of Eq. (3.10) contains a delta function $\delta(t_1 - t_2)$, which comes from $\frac{\delta\gamma_r^*(t_1)}{\delta\gamma_{r_2}(t_2)}$. This indicates that its Fourier component is Ω -independent and does not contribute to the Berry connection. Therefore, the former term can be neglected. The functional derivative of the Keldysh GF in the latter term can be calculated as

$$\frac{\delta}{\delta\gamma_{r_2}(t_2)} G_{d_s, c_{rks}^\dagger}^<(t_1, t_1) = T_{r,r_2}^{+--+}(t_1, t_1, t_2) - T_{r,r_2}^{+---}(t_1, t_1, t_2), \quad (3.11)$$

where T_{r,r_2} is a three-point diagram defined as

$$T_{r,r_2}(\tau_1, \tau_2, \tau_3) = (-i)^2 \left\langle \mathcal{T}_K \left\{ d_s(\tau_1) c_{rks}^\dagger(\tau_2) \frac{\partial H}{\partial \gamma_{r_2}}(\tau_3) \right\} \right\rangle, \quad (3.12)$$

$$\frac{\partial H}{\partial \gamma_{r_2}} = \sum_{k,s} (d_s^\dagger c_{r_2ks} + c_{r_2ks}^\dagger d_s), \quad (3.13)$$

and the superscripts indicates the Keldysh contour which τ_1 , τ_2 , and τ_3 belong to. Using the equation-of-motion technique, the triangle diagram can be described by a two-particle GF and the 1PI self-energy as follows:

$$\begin{aligned} & (-i)^2 \left\langle \mathcal{T}_K \left\{ d_s(\tau_1) c_{rks}^\dagger(\tau_2) \frac{\partial H}{\partial \gamma_{r_2}}(\tau_3) \right\} \right\rangle \\ &= \sum_{k_3, s_3} (-i)^2 \left\langle \mathcal{T}_K \left\{ d_s(\tau_1) c_{rks}^\dagger(\tau_2) d_{s_3}^\dagger(\tau_3) c_{r_2k_3s_3}(\tau_3) \right\} \right\rangle \\ & \quad + (-i)^2 \left\langle \mathcal{T}_K \left\{ d_s(\tau_1) c_{rks}^\dagger(\tau_2) c_{r_2k_3s_3}^\dagger(\tau_3) d_{s_3}(\tau_3) \right\} \right\rangle, \end{aligned} \quad (3.14)$$

and

$$\begin{aligned}
& \sum_{k_3, s_3} (-i)^2 \left\langle \mathcal{T}_K \left\{ d_s(\tau_1) c_{rks}^\dagger(\tau_2) d_{s_3}^\dagger(\tau_3) c_{r_2 k_3 s_3}(\tau_3) \right\} \right\rangle \\
&= \sum_{k_3, s_3} (-i)^2 \left\langle \mathcal{T}_K \left\{ d_s(\tau_1) d_{s_3}^\dagger(\tau_3) \right\} \right\rangle \left\langle \mathcal{T}_K \left\{ c_{r_2 k_3 s_3}(\tau_3) c_{rks}^\dagger(\tau_2) \right\} \right\rangle \\
&\quad + \sum_{r_4, r_5, k_3, k_4, k_5, s_3, s_4, s_5} \int_{C_K} d\tau_4 d\tau_5 \left[(-i)^4 \gamma_r \gamma_{r_5}^* \left\langle \mathcal{T}_K \left\{ d_s(\tau_1) d_{s_3}^\dagger(\tau_3) d_{s_4}^\dagger(\tau_4) d_{s_5}(\tau_5) \right\} \right\rangle_c \right. \\
&\quad \quad \quad \left. \times \left\langle \mathcal{T}_K \left\{ c_{r_4 k_4 s_4}(\tau_4) c_{rks}^\dagger(\tau_2) \right\} \right\rangle \left\langle \mathcal{T}_K \left\{ c_{r_2 k_3 s_3}(\tau_3) c_{r_5 k_5 s_5}^\dagger(\tau_5) \right\} \right\rangle \right] \\
&= \delta_{r, r_2} |\gamma_r|^{-2} G_{ss}(\tau_1, \tau_3) \Sigma_{r,s}(\tau_3, \tau_2) \\
&\quad + \sum_{s_2} \int d\tau_4 d\tau_5 (\gamma_r^* \gamma_{r_2})^{-1} D_{ss s_2 s_2}(\tau_1, \tau_4, \tau_5, \tau_3) \Sigma_{r,s}(\tau_4, \tau_2) \Sigma_{r_2, s_2}(\tau_3, \tau_5), \tag{3.15}
\end{aligned}$$

$$\begin{aligned}
& \sum_{k_3, s_3} (-i)^2 \left\langle \mathcal{T}_K \left\{ d_s(\tau_1) c_{rks}^\dagger(\tau_2) c_{r_2 k_3 s_3}^\dagger(\tau_3) d_{s_3}(\tau_3) \right\} \right\rangle \\
&= \sum_{s_2} \int d\tau_4 d\tau_5 (\gamma_r^* \gamma_{r_2}^*)^{-1} D_{ss s_2 s_2}(\tau_1, \tau_4, \tau_3, \tau_5) \Sigma_{r,s}(\tau_4, \tau_2) \Sigma_{r_2, s_2}(\tau_5, \tau_3). \tag{3.16}
\end{aligned}$$

Here $D_{ss s_2 s_2}(\tau_1, \tau_4, \tau_3, \tau_5)$ is the two-particle GF defined in Eq. (2.78). As a result, we obtain

$$\begin{aligned}
\mathcal{G}_{r, r_2}(t_1, t_2) &= 2e \sum_s \text{Re} \left[\sum_{\mu} \gamma_r^{-1} G_s^{+\mu}(t_1, t_2) \Sigma_{r,s}^{\mu-}(t_2, t_1) \delta_{r, r_2} \right. \\
&\quad + \sum_{\mu_2, \mu_3, \mu_4} \sum_{s_2} \int dt_3 dt_4 \gamma_{r_2}^{-1} D_{ss s_2 s_2}^{+\mu_3 \mu_4 \mu_2}(t_1, t_3, t_4, t_2) \Sigma_{r,s}^{\mu_3-}(t_3, t_1) \Sigma_{r_2 s_2}^{\mu_2 \mu_4}(t_2, t_4) \\
&\quad \left. + \sum_{\mu_2, \mu_3, \mu_4} \sum_{s_2} \int dt_3 dt_4 (\gamma_{r_2}^*)^{-1} D_{ss s_2 s_2}^{+\mu_3 \mu_2 \mu_4}(t_1, t_3, t_2, t_4) \Sigma_{r,s}^{\mu_3-}(t_3, t_1) \Sigma_{r_2 s_2}^{\mu_4 \mu_2}(t_4, t_2) \right]. \tag{3.17}
\end{aligned}$$

Here the summation of Keldysh indices denotes

$$\sum_{\mu} A^{\mu} = A^{+} - A^{-}. \tag{3.18}$$

The Fourier component of the dynamic conductance becomes

$$\begin{aligned}
\mathcal{G}_{r,r_2}(\Omega) = & 2e \sum_s \text{Re} \left[\sum_{\mu} \int \frac{d\omega}{2\pi} \gamma_r^{-1} G_s^{+\mu}(\omega) \Sigma_{r,s}^{\mu-}(\omega - \Omega) \delta_{r,r_2} \right. \\
& + \sum_{\mu_2, \mu_3, \mu_4} \sum_{s_2} \int \frac{d\omega_1 d\omega_2}{2\pi} \gamma_{r_2}^{-1} D_{s_2 s_2 s_2}^{+\mu_3 \mu_4 \mu_2}(\omega_1, \omega_2, \omega_2 + \Omega) \Sigma_{r,s}^{\mu_3-}(\omega_1) \Sigma_{r_2 s_2}^{\mu_2 \mu_4}(\omega_2) \\
& \left. + \sum_{\mu_2, \mu_3, \mu_4} \sum_{s_2} \int \frac{d\omega_1 d\omega_2}{2\pi} (\gamma_{r_2}^*)^{-1} D_{s_2 s_2 s_2}^{+\mu_3 \mu_2 \mu_4}(\omega_1, \omega_2 - \Omega, \omega_2) \Sigma_{r,s}^{\mu_3-}(\omega_1) \Sigma_{r_2 s_2}^{\mu_4 \mu_2}(\omega_2) \right]. \tag{3.19}
\end{aligned}$$

Here we define the Fourier component of the two-particle GF as

$$\begin{aligned}
& D_{s_1 s_1 s_2 s_2}^{\mu_1 \mu_2 \mu_3 \mu_4}(t_1, t_2, t_3, t_4) \\
& = D_{s_1 s_1 s_2 s_2}^{\mu_1 \mu_2 \mu_3 \mu_4}(0, t_2 - t_1, t_3 - t_1, t_4 - t_1) \\
& = \int \frac{d\omega_1 d\omega_2 d\omega_3}{(2\pi)^3} D_{s_1 s_1 s_2 s_2}^{\mu_1 \mu_2 \mu_3 \mu_4}(\omega_1, \omega_2, \omega_3) e^{i\omega_1(t_2-t_1)} e^{-i\omega_2(t_3-t_1)} e^{i\omega_3(t_4-t_1)}. \tag{3.20}
\end{aligned}$$

Considering the Ω -linear term of the dynamic conductance, we obtain the Berry curvature

$$\begin{aligned}
A_{r,r_2} = & -2e \sum_s \text{Im} \left[\sum_{\mu} \int \frac{d\omega}{2\pi} \gamma_r^{-1} G_s^{+\mu}(\omega) \frac{\partial}{\partial \omega} \Sigma_{r,s}^{\mu-}(\omega) \delta_{r,r_2} \right. \\
& - \sum_{\mu_2, \mu_3, \mu_4} \sum_{s_2} \int \frac{d\omega_1 d\omega_2}{2\pi} \gamma_{r_2}^{-1} \frac{\partial}{\partial \omega_3} D_{s_2 s_2 s_2}^{+\mu_3 \mu_4 \mu_2}(\omega_1, \omega_2, \omega_3 = \omega_2) \Sigma_{r,s}^{\mu_3-}(\omega_1) \Sigma_{r_2 s_2}^{\mu_2 \mu_4}(\omega_2) \\
& \left. + \sum_{\mu_2, \mu_3, \mu_4} \sum_{s_2} \int \frac{d\omega_1 d\omega_2}{2\pi} (\gamma_{r_2}^*)^{-1} \frac{\partial}{\partial \omega_3} D_{s_2 s_2 s_2}^{+\mu_3 \mu_2 \mu_4}(\omega_1, \omega_3 = \omega_2, \omega_2) \Sigma_{r,s}^{\mu_3-}(\omega_1) \Sigma_{r_2 s_2}^{\mu_4 \mu_2}(\omega_2) \right]. \tag{3.21}
\end{aligned}$$

Throughout this derivation, we do not make any assumption on the strength of the Coulomb interaction and the dot-reservoir coupling, so this Berry connection is valid for the interacting quantum dot system. We note that this formula cannot be derived by the scattering theory.

In our formula, the effect of the Coulomb interaction is expressed in terms of the one- and two-particle GFs, as shown in Eq. (3.21). Since the one- and two-particle GFs can be calculated by several methods such as diagrammatic methods, numerical simulations, and the Fermi liquid theory, the present formalism is suitable to theoretical study on adiabatic pumping. Actually, we will utilize this formula in Chapters 4 and 5.

Chapter 4

Almost topological pumping in non-interacting quantum dot system

In this chapter, we focus on the adiabatic charge pumping via a non-interacting single-level quantum dot with two electron reservoirs [22]. The situation we consider is as follows (see Fig. 4.1): The energy level of the quantum dot is located above the Fermi level. The temperature and chemical potential are set to be equal for both reservoirs. The strengths of tunnel coupling between the reservoirs and the quantum dot are driven separately.

We show that the amount of pumped charge in one cycle is almost quantized to $e/2$ when the density of states of the reservoir is constant. We also show that the amount of pumped charge changes depending on the energy dependence of the density of states in the reservoirs. We clarify the relation between the quantized value and the reservoir band structure, and discovered that the quantized value can be characterized by one parameter λ , which is the ratio of the Lamb shift to the linewidth.

4.1 Model Hamiltonian

To discuss the adiabatic charge pumping induced by the time-dependent tunnel couplings via the single-level quantum dot without the Coulomb interaction, we consider the Hamiltonian as follows:

$$H = H_d + \sum_{r=L,R} (H_r + H_{T,r}), \quad (4.1)$$

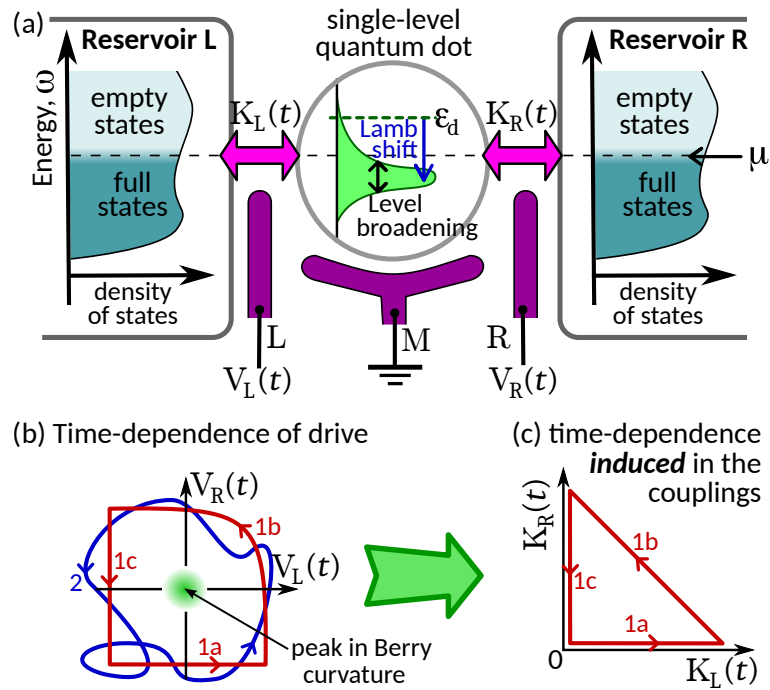


Fig. 4.1 (a) A quantum dot with tunnel-couplings $K_L(t)$ and $K_R(t)$ to the reservoirs, controlled by gates-voltages, $V_L(t)$ and $V_R(t)$. These are slowly varied around the cycle in (b), with gate M ensuring the dot-level is fixed at energy ϵ_d . Any contour enclosing the Berry curvature peak in (b) without touching it (e.g. contours 1 and 2) pumps the same fraction of an electron per cycle, up to exponentially small corrections. The couplings induce a level-broadening and a Lamb shift on the dot. Since $K_L(t)$ and $K_R(t)$ depend exponentially on $V_{L,R}(t)$, contour 1 in (b) maps to contour 1 in (c).

where

$$H_d = \varepsilon_d d^\dagger d, \quad (4.2)$$

$$H_r = \sum_k \varepsilon_k c_{rk}^\dagger c_{rk}, \quad (4.3)$$

$$H_{T,r} = \sum_k \gamma_r(t) (d^\dagger c_{rk} + c_{rk}^\dagger d). \quad (4.4)$$

This model is often called the Fano-Anderson model [51, 52]. Here, d^\dagger and d are creation and annihilation operators of electrons in the dot with energy ε_d , while c_{rk}^\dagger and c_{rk} are those of electrons in the reservoir $r = L, R$ with wavenumber k and energy ε_k . The tunnel-coupling between the system and the wavenumber k in reservoir r is $\gamma_r(t)$, which is taken to vary slowly with time. This model neglects electron-electron interactions in the quantum dot; the simplest experimental implementation is discussed in Sec. 4.2.4. Since this model only includes quadratic terms with respect to the creation and annihilation operators, it is exactly soluble. Therefore, we can study adiabatic pumping without making any approximations except the adiabatic approximation (in particular, it is not necessary to assume weak dot-reservoir coupling).

We take the reservoirs to have a continuum of states, and assume both of them have the same density of states $\rho(\omega)$. In general, this density of states may have energy (ω) dependence, band-gaps, etc. The couplings between the system and each reservoir is described in terms of the time-dependent function

$$\Gamma_r(\omega, t) = K_r(t) \rho(\omega) \quad (4.5)$$

where $K_r(t) = |\gamma_r(t)|^2$ is the coupling parameter. A second crucial quantity for the physics of this model is

$$\Lambda_r(\omega, t) = K_r(t) \text{P} \int d\varepsilon \frac{\rho(\varepsilon)}{\omega - \varepsilon}, \quad (4.6)$$

where the integral is the principal value. For compactness, we also define

$$\Gamma(\omega, t) = \Gamma_L(\omega, t) + \Gamma_R(\omega, t) \quad (4.7)$$

$$\Lambda(\omega, t) = \Lambda_L(\omega, t) + \Lambda_R(\omega, t) \quad (4.8)$$

We refer to $\Gamma_r(\omega, t)$ as *level-broadening*, and to $\Lambda_r(\omega, t)$ as a *Lamb shift*. This is a slight abuse of terminology, but it is justified by the dot's local density of states [51, 52] being $\Gamma(\omega) / [(\omega - \varepsilon_d - \Lambda(\omega))^2 + \Gamma^2(\omega)]$. So if Γ and Λ are ω -independent, then they are the

level-broadening and the Lamb shift, respectively. We simply keep this terminology for cases where Γ and Λ have an ω -dependence.

In what follows, our results become simplest if K_r is written in terms of the dimensionless coupling X_r , which measures the level-broadening in units of the distance of the dot level from the Fermi level;

$$X_r = \frac{\rho(\mu) K_r}{2(\varepsilon_d - \mu)} \quad \text{for } r = L, R, \quad (4.9)$$

where $\rho(\mu)$ is the density of states at the Fermi level, and the factor of two is introduced to make formulas compact.

As shown in Fig. 4.1, we realize the time-dependent coupling $K_r(t)$ by driving the gate-voltages. Typically, the dot is coupled to reservoir r through tunnel-barriers of height $E_r(V_r)$ and width $L_r(V_r)$, which are controlled by the gate-voltages $V_r(t)$. The coupling strength is estimated by the tunneling probability of the barriers, such as,

$$K_r \sim \exp[-\kappa_r], \quad (4.10)$$

where

$$\kappa_r = \hbar^{-1} L_r(V_r) \sqrt{2mE_r(V_r)}. \quad (4.11)$$

By choosing the zero-point of the gate-voltage to coincide with $X_r = 1$ and linearizing the κ_r , one can assume the relation,

$$X_r = \exp[\alpha_r V_r], \quad (4.12)$$

where $\alpha_r = -(\text{d}\kappa/\text{d}V_r) > 0$. We mainly work with Eq. (4.12) for simplicity. This assumption does not lose any generality of our discussion, because the almost topological fractional pumping always holds for $X_r = \exp[f_r(V_r)]$ as far as $f_r(V_r)$ takes a sufficiently positive(negative) value in the limit of $V_r \rightarrow \infty$ ($V_r \rightarrow -\infty$).

4.2 Adiabatic almost-topological pumping of a fraction of an electron per cycle

In this section, we briefly overview our main results, though the detailed calculations postponed to Sec. 4.3. Firstly, for a dot coupled to reservoirs without a band-structure, there is a

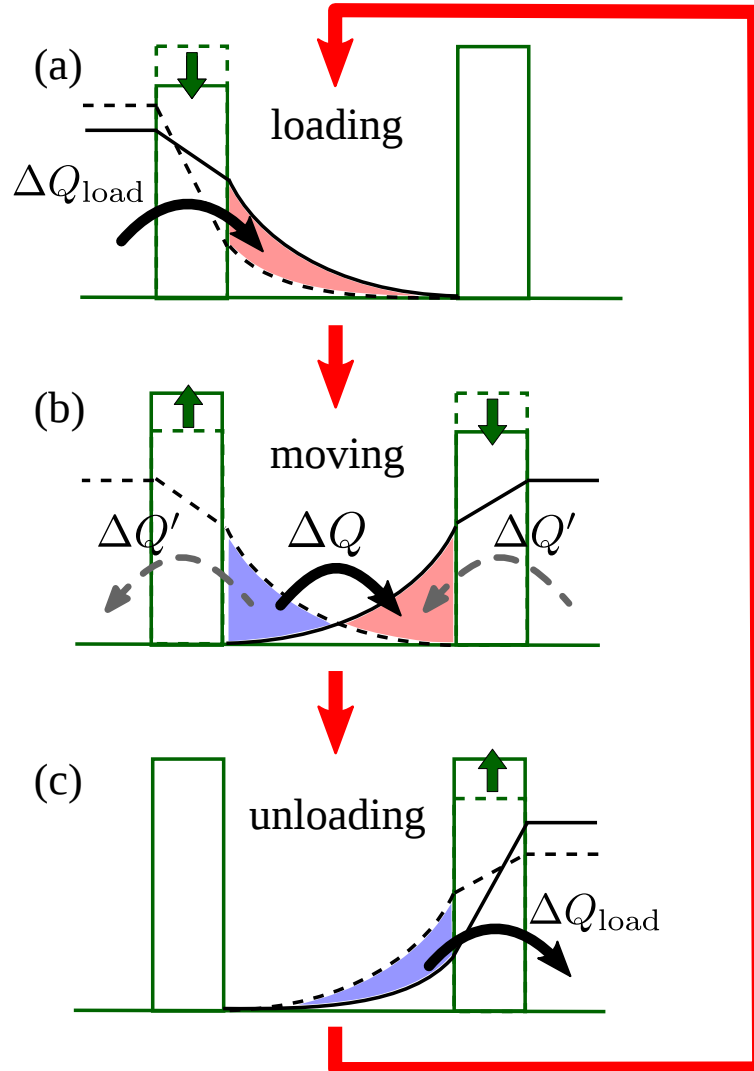


Fig. 4.2 Cartoon of the three steps correspond to the loading, the moving, and the unloading process, described in section 4.2.1, for a system without a Lamb shift ($\lambda = 0$). The central region represents the quantum dot, separated from the reservoirs by barriers, whose heights we can vary to change the tunnel-coupling between the dot and the reservoirs. Although the dot is a single site, it helps our intuition to show the dot's hybridization with reservoir L (R) due to the wavefunction penetrating the dot from the left (right). The pink region shows that the average occupation of the state increases with time, while the blue one shows that it decreases. The arrows indicate the average charge flow; the arrows in (b) indicate the charge ΔQ_{load} is split in two, with $\Delta Q' = \Delta Q_{\text{load}} - \Delta Q$ going back to L and a charge $\Delta Q'$ going from R. See section 4.4.

topological pumping at half an electron per cycle. Secondly, one can choose the reservoir band-structure to ensure the pumped charge is topologically quantized at an arbitrary fraction of an electron per cycle.

4.2.1 Half an electron per cycle

Here we consider a situation where the reservoir density of states is energy independent (ω -independent), which is known as the wide band limit, and so $\rho(\omega) = \rho$. Then the reservoir induces a level-broadening of the quantum dot's energy level, but induces no Lamb shift; $\Lambda(\omega; \mathbf{K}) = 0$ in Eq. (4.8). Our calculations show that this control of the level-broadening allows the pumping of half an electron per cycle in the low temperature limit.

The dot level is taken to be above the reservoir's Fermi level, $(\epsilon_d - \mu) > 0$, and the pumping cycle is taken to be the contour 1 in Fig. 4.1b,c, where neither ϵ_d nor μ changes during the pumping cycle. The basic physical process, sketched in Fig. 4.2 is the following:

- (a) Loading (segment 1a in Fig. 4.1c): The dot starts to be weakly coupled to the reservoirs (V_L and V_R very negative) so the dot's level-broadening is much less than $(\epsilon_d - \mu)$; as a result the dot's occupation is almost zero. The coupling to reservoir L is increased (V_L increased), then the reservoir wavefunctions spread into the dot (as in Fig. 4.2a), as the dot state hybridizes with reservoir states. The dot thus absorbs a charge of ΔQ_{load} . Once the level-broadening is much more than $(\epsilon_d - \mu)$, one reaches the limit where half the broadened level is below the reservoir's Fermi energy. In this limit, there is half an electron in the dot, $\Delta Q_{\text{load}} \rightarrow e/2$; in other words a 50% chance of finding the dot level occupied.
- (b) Moving (segment 1b in Fig. 4.1c): The coupling to reservoir L is slowly reduced to zero, while that to reservoir R is slowly increased to its maximum value (V_L reduced and V_R increased). During this process, the sum of the two couplings remains constant. Thus, the wavefunctions of reservoir R spread more into the dot, while those of reservoir L spread less into the dot. The occupation of the dot remains the same, but the hybridization of the dot state moves from reservoir L to reservoir R.
- (c) Unloading (segment 1c in Fig. 4.1c): The coupling to R is reduced (V_R reduced) so the level-broadening again becomes much less than $(\epsilon_d - \mu)$. As a result, the dot level empties into reservoir R, the reservoir wavefunctions spread into the dot become negligible, and one returns the dot to its initial state.

This cycle transfers a charge of ΔQ from reservoir L to reservoir R. Be sure that $\Delta Q \neq \Delta Q_{\text{load}}$. When the coupling is large enough that the level-broadening in step 1b is much more than $(\epsilon_d - \mu)$, then $\Delta Q \rightarrow \Delta Q_{\text{load}} \rightarrow e/2$.

4.2.2 Seeing the topology

The adiabatic charge pumped per cycle can be said to be topological when it is the same for all adiabatic pumping cycles of the gate voltages that have the same topology. We will show that one can pump the same amount of charge up to exponentially small corrections by arbitrary cycles of V_L and V_R under certain conditions, we call it “adiabatic almost-topological” pumping.

To see what this means, one must write the charge pumped into reservoir R as an integral over the surface in the V_L - V_R plane enclosed by the pumping cycle C ,

$$\Delta Q_R = e \int_C dV_L dV_R \Pi_R [V_L, V_R]. \quad (4.13)$$

Then one calculates $\Pi_R [V_L, V_R]$, which is referred to as the Berry curvature, for the pumping. If one finds that this Berry curvature is a Dirac δ -function, then the pumping is entirely topological; the adiabatically pumped charge only depends on how many times the pumping contour winds around the δ -function. Here, our central result, Eq. (4.28), indicates that the Berry curvature is not a δ -function, but it is strongly peaked with an exponential decay away from the peak, see Fig. 4.3. Then we call the pumping *almost topological*, because it depends only on the contours topology (how many times it winds around the peak) if the contour stays away from the peak, and if we neglect the exponentially small corrections coming from the tail of the peak. Thus contours 1 and 2 in Fig. 4.1b pump the same charge (up to exponentially small corrections) because they both have the same topology — each winds once around the peak.

Fig. 4.3b shows the peak for reservoirs with uniform density of states. The integral over this peak is $1/2$, so the contours in Fig. 4.3b will thus pump the charge

$$\Delta Q_{\text{quantized}} = e/2. \quad (4.14)$$

In the limit of thick tunnel barriers, $L \rightarrow \infty$, one sees that α_r in Eq. (4.12) also goes to infinity. Then the Berry curvature peak becomes a Dirac δ -function in the V_L - V_R plane. This means that the adiabatic pumping will become *entirely topological*. However, for $L \rightarrow \infty$, the tunnel coupling is exponentially small. In this case, by setting $(\epsilon_d - \mu)$ as small as the

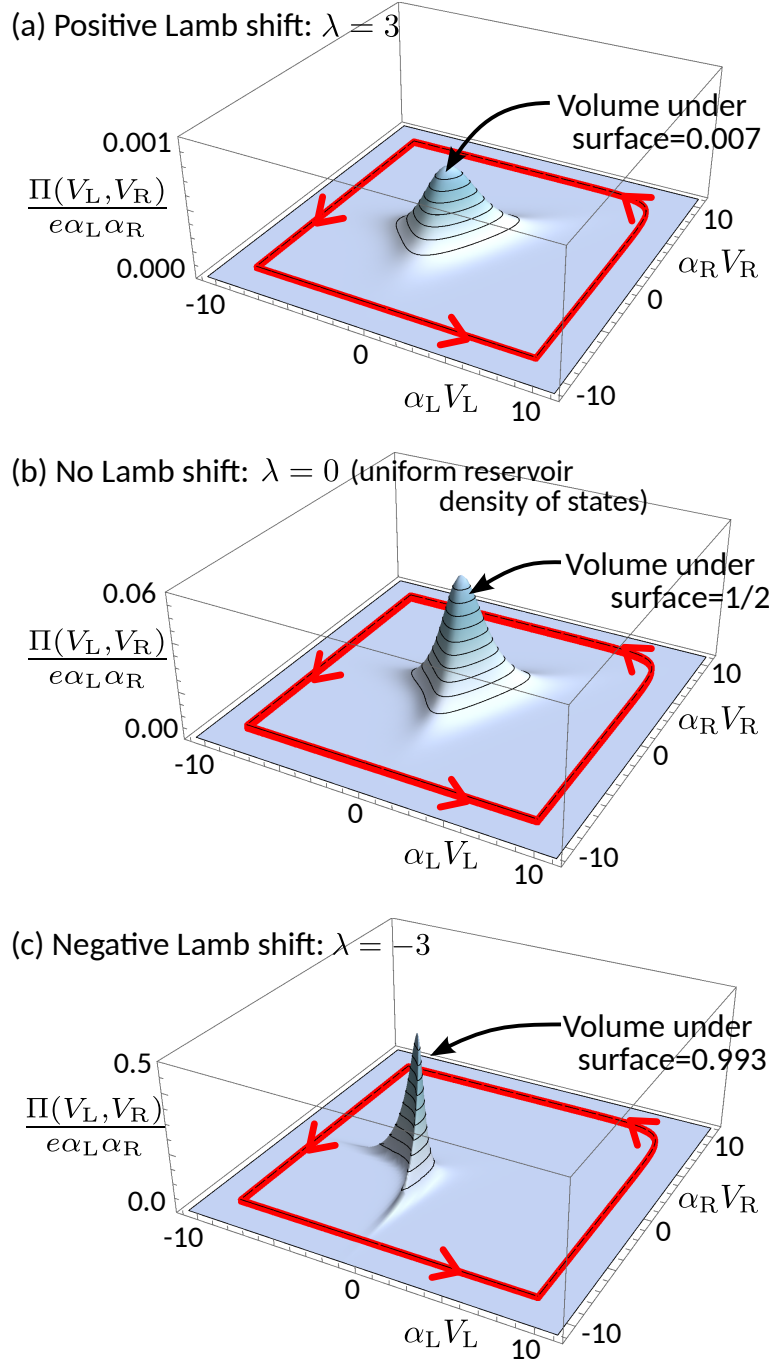


Fig. 4.3 Plots of the Berry curvature, $\Pi_R(V_L, V_R)$, for the dot-reservoir coupling in Eq. (4.12). This is given by Eq. (4.28). It is always a sharp peak, but the volume under the peak is highly λ -dependent, and given by Eq. (4.16). Contour 1 from Fig. 4.1b is also shown.

couplings, one can make X_L and X_R of order of one. Therefore the pumping contour can sufficiently enclose the δ -function peak.

4.2.3 Different fractions of an electron per cycle

Let us now consider reservoirs with a non-uniform density of states, where $\rho(\omega)$ depends on ω . In this case, the Lamb shift in Eq. (4.8) is non-zero; this means that the dot-reservoir coupling does not only broaden the dot-level into a resonance, it also causes the center of that resonance to be shifted in energy. Sec. 4.3 will use the Keldysh formalism to show that the adiabatic almost-topological pumping is quantized at a fraction of an electron (between 0 and 1), which is given by the ratio of the Lamb shift to the level-broadening. We define λ as the following dimensionless measure of this ratio at $\omega = \mu$,

$$\lambda = 2\Lambda(\mu, t)/\Gamma(\mu, t), \quad (4.15)$$

where the factor of 2 is introduced to make our results compact. It is surprising that the exact result for pumping at low-temperatures only depends on the ratio of the Lamb shift *at the Fermi level* to the level-broadening *at the Fermi level*, when many other observables depend on these quantities integrated over all energies (see e.g. $n(\mathbf{K})$ is Sec. 4.4). It is not easy to explain how this quantity emerges in the exact calculation, but we believe it is because we are at very low temperature and zero bias, so all charge flow between reservoirs happens at energies at (or extremely close to) the Fermi level. Hence the pumped charge also only depends on the physics of the Lamb shift and level-broadening at the Fermi level.

We will show that the almost topological charge pumped by the cycle described in Sec. 4.2.1 is

$$\Delta Q_{\text{quantized}} = \frac{e}{\pi} \left[\frac{\pi}{2} - \arctan(\lambda) - \frac{\lambda}{1 + \lambda^2} \right]. \quad (4.16)$$

Hence, for this pumping cycle, $\Delta Q_{\text{quantized}}$ is a monotonically decaying function of λ , and it takes values between e and 0. More precisely, $\Delta Q_{\text{quantized}}$ equals $[1 - 2/(3\pi\lambda^2)]e$ for $\lambda \ll -1$, equals $e/2$ at $\lambda = 0$, and equals $2e/(3\pi\lambda^2)$ for $\lambda \gg 1$.

Crucially, λ is entirely determined by the reservoir band-structure. From Eqs. (4.7), (4.8) and (4.15), λ can be described only by the density of states of reservoirs and the Fermi level, such as,

$$\lambda = \frac{2}{\rho(\mu)} \text{P} \int d\varepsilon \frac{\rho(\varepsilon)}{\mu - \varepsilon}, \quad (4.17)$$

so it is independent of K_L , K_R and t . By choosing a suitable reservoir band-structure and the Fermi level, one can choose arbitrary fraction between e and 0.

4.2.4 Requirements for experimental observation

There are four requirements for observing this quantized pumping of a fraction of an electron per cycle.

The first requirement is a quantum dot which mimics the Hamiltonian in Eqs. (4.1)-(4.4) which neglects electron-electron interactions on the dot. The simplest experimental implementation of Eqs. (4.1)-(4.4) is an interacting quantum dot (described by an Anderson impurity Hamiltonian) in a large enough magnetic field that the dot's spin-state with higher energy is always empty, which makes the on-dot interaction term negligible.

The second requirement is that $k_B T$ is much smaller than $(\epsilon_d - \mu)$, larger temperatures will destroy the quantization. At the same time $(\epsilon_d - \mu)$ should be small enough that we can make the dot-reservoir coupling $K \gg (\epsilon_d - \mu)/\rho(\mu)$. Thus we require that $k_B T \ll K_{\max}\rho(\mu)$, which means the required value of T depends on how strongly the dot can be coupled to the reservoirs.

The third requirement is related to the fact that the charge pumping is probabilistic, with only the *average* charge being quantized. This probabilistic nature of the pumping is typical whenever there is part of the pumping cycle in which the dot is coupled to both reservoirs at the same time (segment 1b of the cycle). Thus in any given cycle $n = 0, \pm 1, \pm 2, \dots$ electrons might flow. The central limit theorem tells us that averaging over many cycles will give an answer that will converge to the quantized fraction that we predict.

The fourth requirement is due to our assumption that ϵ_d is time-independent during the pumping cycle. Unfortunately, in practice, the electrostatic gates that vary K_L and K_R , will also have a capacitive coupling to the dot-level, causing ϵ_d to vary. Gate M in Fig. 4.1a will minimize this capacitive coupling, by partially screening the dot from gates L and R. Any remaining capacitive coupling to gates L and R will act much like the Lamb shift. However, this coupling grows linearly in V_L and V_R , while the level-broadening and Lamb shift (if present) grow exponentially, as can be seen in Eq. (4.12). Therefore, any effect of the capacitive coupling on ϵ_d will become negligible compared to the broadening at large $\alpha_r V_r$.

4.3 Detailed results

For the Hamiltonian in Eqs. (4.1)-(4.4), we find that the Berry connection contains two terms,

$$\mathbf{A}_r(\mathbf{K}) = \mathbf{A}_r^{\text{broad}}(\mathbf{K}) + \mathbf{A}_r^{\text{shift}}(\mathbf{K}), \quad (4.18)$$

because $\mathbf{A}_r(\mathbf{K})$ involves a derivative with respect to \mathbf{K} , and that derivative can act on the level-broadening (giving $\mathbf{A}^{\text{broad}}$) or the Lamb shift (giving $\mathbf{A}^{\text{shift}}$). If there is no Lamb shift then $\mathbf{A}_r^{\text{shift}}(\mathbf{K}) = 0$, while if the Lamb shift is much greater than the level-broadening, then Eq. (4.18) is dominated by $\mathbf{A}_r^{\text{shift}}(\mathbf{K})$. The Keldysh calculations outlined in Chapter 3 give

$$\left[\mathbf{A}_r^{\text{broad}}(\mathbf{K}) \right]_{r'} = \int \frac{d\omega}{2\pi} \left[\left(\mathcal{B}^2 - \frac{1}{4} \mathcal{A}^2 \right) f \Lambda_r - \frac{1}{2} \mathcal{A} \mathcal{B} f \Gamma_r - \delta_{r,r'} \mathcal{B}' f \right] \frac{\partial \Gamma}{\partial K_{r'}}, \quad (4.19)$$

$$\left[\mathbf{A}_r^{\text{shift}}(\mathbf{K}) \right]_{r'} = \int \frac{d\omega}{2\pi} \left[2 \mathcal{B} \mathcal{A} f \Lambda_r + \frac{1}{4} \mathcal{A}^2 (f' \Gamma_r - f \Gamma_r') + \mathcal{B}^2 (f \Gamma_r)' - \delta_{r,r'} (\mathcal{A} f)' \right] \frac{\partial \Lambda}{\partial K_{r'}}, \quad (4.20)$$

where r and r' are L or R, and $f = [1 + e^{(\omega - \mu)/T}]^{-1}$ is the Fermi function. The prime denotes the partial derivative with respect to ω . The quantities Λ_r and Γ_r are given in Eqs. (4.5-4.8), while $\mathcal{A} = 2\text{Im}[G^A(\omega)]$ and $\mathcal{B} = \text{Re}[G^A(\omega)]$. Here $G^A(\omega)$ is the advanced GF for a non-interacting quantum dot defined as

$$G^A(\omega) = \frac{1}{\omega - \varepsilon_d - \Lambda(\omega; \mathbf{K}) - i\Gamma(\omega; \mathbf{K})/2}. \quad (4.21)$$

Turning to the Berry curvature, we see it contains two derivatives (with respect to $K_{r'}$), because $[\mathbf{A}_r(\mathbf{K})]_{r'}$ contained one derivative. Hence $\Pi_r(\mathbf{K})$ contains three terms; a ‘‘broad-broad’’ term due to both derivatives acting on the broadening, a ‘‘shift-shift’’ term due to both derivatives acting the Lamb shift, and a ‘‘shift-broad’’ term with one derivative on each of them. The ‘‘shift-shift’’ term turns out to be zero, showing that the Lamb shift alone is not enough to do pumping. Intuitively, this can be understood as the Lamb shift only moving the dot level, which is not enough to do pumping. Hence

$$\Pi_R(\mathbf{K}) = \Pi_R^{\text{broad-broad}}(\mathbf{K}) + \Pi_R^{\text{shift-broad}}(\mathbf{K}), \quad (4.22)$$

and $\Pi_L(\mathbf{K}) = -\Pi_R(\mathbf{K})$, with

$$\Pi_R^{\text{broad-broad}}(\mathbf{K}) = \int \frac{d\omega}{4\pi} f' \mathcal{A} \mathcal{B} \frac{\Gamma^2(\omega, \mathbf{K})}{K^2}, \quad (4.23)$$

$$\Pi_R^{\text{shift-broad}}(\mathbf{K}) = \int \frac{d\omega}{4\pi} f' \mathcal{A}^2 \frac{\Gamma(\omega, \mathbf{K})\Lambda(\omega, \mathbf{K})}{K^2}. \quad (4.24)$$

where we have used the fact that Λ and Γ are proportional to $K = K_L + K_R$. A bit more algebra gives

$$\begin{aligned} & \Pi_R(\mathbf{K}) \\ &= \frac{e}{2} \int \frac{d\omega}{2\pi} \frac{(\omega - \varepsilon_d) \rho^2(\omega) \Gamma(\omega; \mathbf{K}) (\partial f / \partial \omega)}{\left[[\omega - \varepsilon_d - \Lambda(\omega; \mathbf{K})]^2 + \left[\frac{1}{2} \Gamma(\omega; \mathbf{K}) \right]^2 \right]^2}. \end{aligned} \quad (4.25)$$

This depends on the sum of the couplings, $K = (K_L + K_R)$, but not on the difference ($K_L - K_R$).

4.3.1 Low temperature pumping

In the limit of low temperature, we can make the approximation $(\partial f / \partial \omega) = -\delta(\omega - \mu)$ in Eq. (4.25). To justify this approximation one needs the other terms in the integrand of Eq. (4.25) to vary little over the window of ω given by $\mu \pm k_B T$. Then, the Berry curvature is

$$\Pi_R(\mathbf{K}) = \frac{e}{4\pi} \frac{(\varepsilon_d - \mu) \rho^2(\mu) \Gamma(\mu; \mathbf{K})}{\left[[\mu - \varepsilon_d - \Lambda(\mu; \mathbf{K})]^2 + \left[\frac{1}{2} \Gamma(\mu; \mathbf{K}) \right]^2 \right]^2}. \quad (4.26)$$

Writing this in terms of λ in Eq. (4.15), the low-temperature result for pumped charge per cycle (in units of e) is given by the dimensionless integral

$$\frac{\Delta Q_R}{e} = \frac{2}{\pi} \int_C dX_L dX_R \frac{X}{\left[(1 + \lambda X)^2 + X^2 \right]^2} \quad (4.27)$$

where X_r defined in Eq. (4.9) with ρ being $\rho(\mu)$, and $X = X_L + X_R$. Here C is a driving contour in the (X_L, X_R) -plane.

As explained in Sec. 4.1, we control gate-voltages V_r , in experiments. By substituting Eq. (4.12) into Eq. (4.27), we find the Berry curvature in the (V_L, V_R) -plane

$$\frac{\Pi_R(V_L, V_R)}{e} = \frac{2}{\pi} \frac{\alpha_L \alpha_R X e^{\alpha_L V_L} e^{\alpha_R V_R}}{\left[(1 + \lambda X)^2 + X^2 \right]^2} \Bigg|_{X=e^{\alpha_L V_L} + e^{\alpha_R V_R}}, \quad (4.28)$$

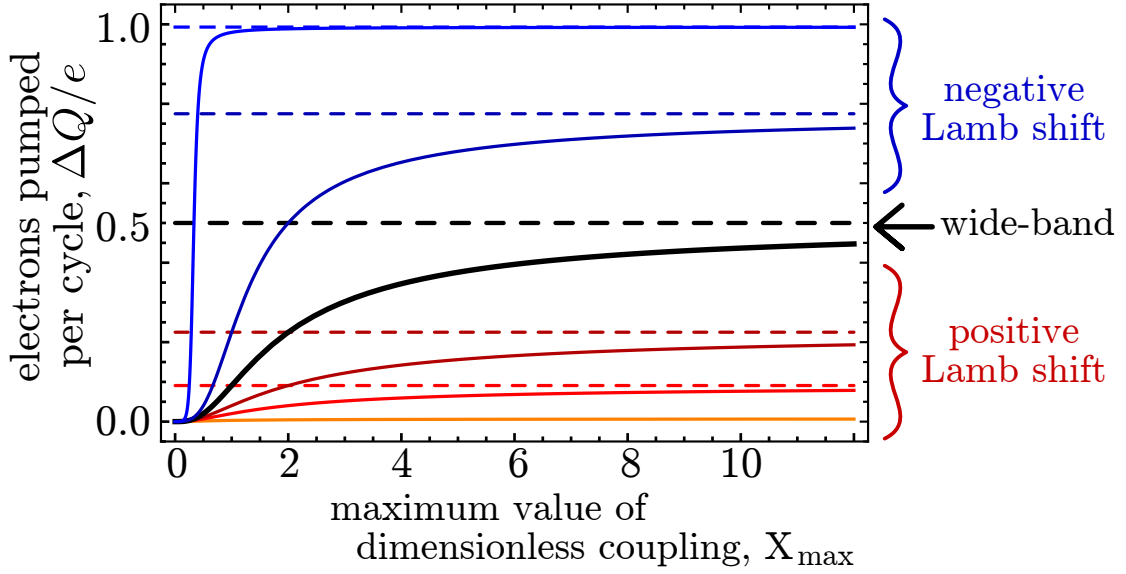


Fig. 4.4 The solid curves are the charge pumped per cycle on the triangular pumping cycle, given by Eq. (4.30). From top to bottom we have $\lambda = -3, -0.5, 0, 0.5, 1, 3$. The horizontal dashed lines show the large X_{\max} limit given by Eq. (4.16).

shown in Fig. 4.3. This is our *central result*, because both the fractional and topological nature of the adiabatic pumping follow from it, as we now show.

Eq. (4.28) has a peak at small $|\alpha_r V_r|$, and decays exponentially as $|V_r|$ grows. Hence, any pumping contour that encloses the peak without encroaching on it will give the same pumped charge per cycle (up to exponentially small corrections), ensuring quantized pumping.

To calculate the charge pumped by such a cycle, we return to Eq. (4.27) and consider a triangular contour C explained in Fig. 4.1c. The contour is the triangle defined by (X_L, X_R) going from $(0, 0) \rightarrow (X_{\max}, 0) \rightarrow (0, X_{\max}) \rightarrow (0, 0)$, where $X_{\max} = \rho K_{\max} / [2(\epsilon_d - \mu)]$. We write

$$\int_C dX_L dX_R, (\dots) = \frac{1}{2} \int_0^{X_{\max}} dX \int_{-X}^X dY (\dots), \quad (4.29)$$

where $Y = X_L - X_R$. Eq. (4.12) means that for large X_{\max} this triangular contour corresponds to contour 1 in Fig. 4.1b, that encloses the peak in $\Pi_R(V_L, V_R)$. We transform the integration variables to X and Y as in Eq. (4.29), then

$$\frac{\Delta Q_R}{e} = \frac{1}{\pi} \left[\frac{\pi}{2} - \arctan \left(\frac{1 + \lambda X_{\max}}{X_{\max}} \right) - \frac{X_{\max}(1 + \lambda X_{\max})}{1 + X_{\max}^2 + \lambda X_{\max}(2 + \lambda X_{\max})} \right], \quad (4.30)$$

see Fig. 4.4. We take $X_{\max} \rightarrow \infty$ to get the pumping for a contour that corresponds to one enclosing the peak of Eq. (4.28); this gives Eq. (4.16).

This gives our main results; the adiabatic pumping is almost topological, and pumps a fraction of an electron (between 0 and e) given by the value of λ , which is determined by the reservoir's band-structure and the Fermi level.

To see a gate-voltage dependence defined in Eq. (4.12), we substitute it into Eq. (4.27). Then Eq. (4.28) changes, but it still remains strongly peaked with exponentially small tails. This ensures that there is still adiabatic almost-topological pumping. Furthermore, the fraction pumped per cycle is the same for any voltage dependence, since it was calculated directly from Eq. (4.27).

4.4 Comparison with dot occupation

One might naively guess that the pump is simply due to filling the dot state from L in the “loading” part of the cycle, and then emptying it into R in the “unloading” part of the cycle. Then the charge transferred from L to R would equal the charge loaded into the dot, ΔQ_{load} . We show here that this is not the case; there is no simple relation between the pumped charge and ΔQ_{load} .

We are considering the adiabatically slow pumping, so electrons are continuously tunnelling in and out of the dot from L and R (and tunnelling through the dot from L to R) during the “moving” part of the cycle. They have too little energy to remain in the dot, but the uncertainty principle means they can be there for a time of order $\hbar/(\epsilon_d - \mu)$. Therefore, there is no reason to assume the pumped charge is related to the dot occupation. Indeed, the occupation of the dot at low temperatures, see e.g. Ref. [53], is

$$n(\mathbf{K}) = \int_{-\infty}^{\mu} \frac{d\omega}{2\pi} \frac{\Gamma(\omega; \mathbf{K})}{[\omega - \epsilon_d - \Lambda(\omega; \mathbf{K})]^2 + [\frac{1}{2}\Gamma(\omega; \mathbf{K})]^2}.$$

For a uniform density of states $\Lambda(\omega) = 0$, the integrand is a Lorentzian, and so $n(\mathbf{K}) = \arctan[X]/\pi$. Then

$$\Delta Q_{\text{load}} = e[n(\mathbf{K}_{\max}) - n(0)] = \frac{e \arctan[X_{\max}]}{\pi}. \quad (4.31)$$

From Eq. (4.30) with $\lambda = 0$, we see the pumped charge is smaller than ΔQ_{load} by a factor of $\Delta Q' = eX_{\max}/[\pi(1 + X_{\max}^2)]$, which vanishes when $X_{\max} \rightarrow \infty$. This means that the “moving” part of the pumping cycle in section 4.2.1 involves a small flow, $\Delta Q'$, from the R to L through the dot (the dashed arrows in the Fig. 4.2b).

For a non-uniform density of states, ΔQ_{load} depends on the ω -dependence of $\Gamma(\omega; \mathbf{K})$ and $\Lambda(\omega; \mathbf{K})$ for all $\omega \leq \mu$. In contrast, the pumped charge in Eq. (4.16) depends *only* on their values at $\omega = \mu$. Thus in general ΔQ and ΔQ_{load} will not be related in any way, although both will be between 0 and e . Either can be larger, so $\Delta Q'$ can be of either sign. Indeed, two different set-ups can have the same ΔQ and different ΔQ_{load} , or vice-versa.

4.5 Short summary

In this chapter, we discussed the quantization of the pumped charge in one cycle in a non-interacting quantum dot system, when the dot-reservoir couplings are driven adiabatically. We clarified the relation between the pumped charge and the density of states of the reservoirs in detail. By utilizing the general formula for the adiabatic charge pumping derived in Chapter 3, we calculated the pumped charge in one cycle. As a result, we found that the pumped charge is quantized to a fraction of an electron (between 0 and e) up to exponentially small corrections when the driving contour sufficiently encloses the peak of the Berry curvature in the driving parameter space. We refer to this quantized adiabatic pumping as the almost-topological pumping.

We also pointed out that the fractional value of the pumped charge is determined by only one parameter λ (Eq. (4.16)), which is defined as the ratio of the Lamb shift to the level-broadening at the Fermi level. This parameter depends on both the Fermi level and the density of states of the reservoirs. For positive (negative) λ , which indicates the Lamb shift is positive (negative), the quantized value of the pumped charge approaches to 0 (e) as $|\lambda|$ increases. For $\lambda = 0$, where the density of states of the reservoirs has no energy-dependence, the pumped charge is quantized to a half of the electron charge.

Chapter 5

Charge pumping in interacting quantum dot system

In this chapter, we discuss an adiabatic pumping via a quantum dot with the Coulomb interaction. We formulate adiabatic charge pumping induced by driving of the reservoir parameters such as electro-chemical potentials and temperatures. To describe time-dependent temperatures of the reservoirs, we introduce an artificial field called the thermomechanical field. We also clarify the effect of the Coulomb interaction, especially the Kondo effect, on adiabatic charge pumping within the renormalized perturbation theory (RPT).

5.1 Model

To clarify the effect of the Coulomb interaction on adiabatic charge pumping induced by time-dependent temperatures and electrochemical potentials of reservoirs, we consider the Anderson impurity model with the time-dependent reservoirs. The Hamiltonian is given by

$$H = H_d + \sum_{r=L,R} (H_r + H_{T,r}), \quad (5.1)$$

where H_d , H_r , and $H_{T,r}$ describe the quantum dot, the electron reservoir $r \in \{L, R\}$, and the dot-reservoir coupling, respectively:

$$H_d = \sum_s \varepsilon_d d_s^\dagger d_s + U d_\uparrow^\dagger d_\uparrow d_\downarrow^\dagger d_\downarrow, \quad (5.2)$$

$$H_r = \sum_{k,s} \varepsilon_k c_{rks}^\dagger c_{rks}, \quad (5.3)$$

$$H_{T,r} = \sum_{k,s} (\gamma_{rk}(t) c_{rks}^\dagger d_s + h.c.) \quad (5.4)$$

Here, d_s^\dagger (d_s) is the creation (annihilation) operator of an electron in the quantum dot with spin $s \in \{\uparrow, \downarrow\}$, and c_{rks}^\dagger (c_{rks}) is that of an electron in the reservoir r with spin s and wavenumber k . The electron energies in the quantum dot and the reservoirs are denoted by ε_d and ε_k , respectively. U is the strength of the Coulomb interaction in the quantum dot.

In order to describe time-dependent temperatures and electrochemical potentials, we introduce the time-dependent tunnel coupling constant defined as

$$\gamma_{rk}(t) = \gamma_r \sqrt{B_r(t)} \exp \left\{ -i \int_{-\infty}^t dt' [(B_r(t') - 1)\varepsilon_k + \mu_r(t')] \right\}, \quad (5.5)$$

where γ_r is a time-independent coupling constant. Here $B_r(t)$ and $\mu_r(t)$ are introduced to describe the time-dependent temperature and electrochemical potential of the reservoir r , respectively. We assume that they are periodic functions of t ,

$$B_r(t) = B_r(t + 2\pi\Omega^{-1}), \quad \mu_r(t) = \mu_r(t + 2\pi\Omega^{-1}), \quad (5.6)$$

where Ω is the pumping frequency. One might feel strange about the unfamiliar time-dependent field $B_r(t)$. This field, which is called the thermomechanical field, is introduced to describe the time-dependent temperature of reservoirs (for details, see Sec. 5.2.)

For simplicity, the Fermi levels of the reservoirs are set to zero in the absence of parameter driving ($B_r(t) = 1$, $\mu_r(t) = 0$). We also assume that, without parameter driving, the reservoirs are in thermal equilibrium with the reference temperature T . Throughout this section, we consider the wide-band limit,

$$\Gamma = \sum_{r=L,R} \Gamma_r, \quad (5.7)$$

$$\Gamma_r = 2\pi\rho |\gamma_r|^2, \quad (5.8)$$

where ρ is the density of states of reservoirs at the Fermi level.

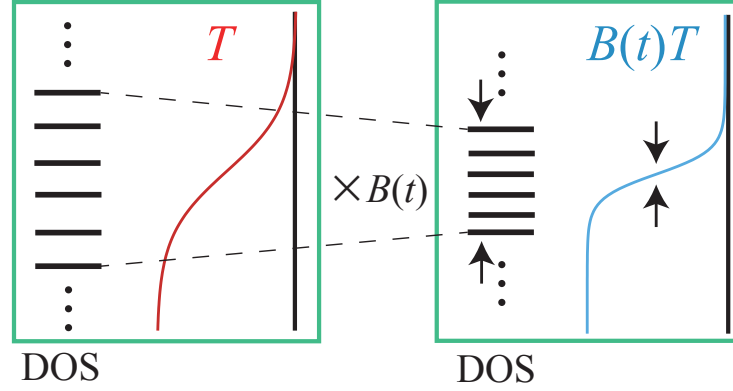


Fig. 5.1 Schematic of energy rescaling induced by the thermomechanical field. The left panel shows the reservoir energy levels and the Fermi distribution for the original setup [$B_r(t) = 1$], and the right panel shows those modified by a thermomechanical field for $B_r(t) < 1$. By this energy rescaling, the reservoir temperature effectively decreases.

5.2 Thermomechanical field method

The thermomechanical field method was first proposed by Luttinger [54] and has been employed in recent theoretical works [45, 55, 56]. In this section, we briefly explain how the thermomechanical field modifies the temperature of the reservoirs. For a detailed discussion, see Ref. [45, 56].

For simplicity, we consider the case of $\mu_r(t) = 0$. As shown in the Hamiltonian given by Eq. (5.3), the thermomechanical field rescales electron energies in the reservoirs as $\varepsilon_k \rightarrow B(t)\varepsilon_k$. Figure 5.1 is a schematic of how this energy rescaling modifies the temperature of the reservoir. First, before the energy scaling ($B_r(t) = 1$), the electron reservoirs are both in thermal equilibrium with the reference temperature T and their Fermi distribution function is denoted by $f_r(\varepsilon) = f(\varepsilon, T, 0)$, where $f(\varepsilon, T, \mu) = [e^{(\varepsilon - \mu)/T} + 1]^{-1}$. Then, after the energy scaling ($B_r(t) \neq 1$), the Fermi distribution functions of the reservoirs are rescaled into $\tilde{f}_r(\varepsilon)$ as

$$\tilde{f}_r(B_r(t)\varepsilon) = f_r(\varepsilon), \quad (5.9)$$

and this energy rescaling can be substituted into the temperature directly as

$$\tilde{f}_r(\varepsilon) = f_r(\varepsilon/B_r(t)) = f(\varepsilon, B_r(t)T, 0). \quad (5.10)$$

As a result, the temperature of the reservoir is rescaled by the thermomechanical field as

$$T_r(t) = B_r(t)T. \quad (5.11)$$

To keep the temperature positive, the thermomechanical field $B_r(t)$ should be positive.

Let's see how this mechanism works in practical calculation. For simplicity, we consider time-independent case, $B_r(t) = B_r, \mu_r(t) = \mu_r$. The lesser component of 1PI self-energy induced by the tunnel coupling with the thermomechanical field is calculated as

$$\begin{aligned} \Sigma_{r,s}^<(t_1, t_2) &= \sum_k \gamma_{rk}(t_1) g_{rks}^<(t_1, t_2) \gamma_{rk}^*(t_2) \\ &= i\Gamma_r B_r \int \frac{d\omega}{2\pi} \int d\varepsilon f(\varepsilon, T, 0) \delta(\omega - \varepsilon) e^{-i\omega(t_1-t_2)} e^{-i[(B_r-1)\varepsilon + \mu_r](t_1-t_2)} \\ &= i\Gamma_r B_r \int \frac{d\omega}{2\pi} f(\omega, T, 0) e^{-i(B_r\omega + \mu_r)(t_1-t_2)} \\ &= i\Gamma_r \int \frac{d\omega}{2\pi} f(B_r^{-1}(\omega - \mu_r), T, 0) e^{-i\omega(t_1-t_2)} \\ &= i\Gamma_r \int \frac{d\omega}{2\pi} f(\omega, T_r, \mu_r) e^{-i\omega(t_1-t_2)}. \end{aligned} \quad (5.12)$$

In the fourth line in Eq. (5.12), we use a variable conversion, $(B_r\omega + \mu_r) \rightarrow \omega$. As shown in the equation, this calculation result is equivalent to the result calculated by the reservoir with temperature T_r and electrochemical potential μ_r . This indicates that one can emulate the electron reservoir with arbitrary temperature by introducing the thermomechanical field.

We should note that the thermomechanical field describes only the rescaling effect of the Fermi distribution function. Therefore, the thermomechanical field is applicable only to the system under a time-independent temperature bias or a quasi-static driving of temperature. Non-adiabatic effect, which strongly disturbs the Fermi distribution function, cannot be discussed by this method.

5.3 Berry connection for the interacting quantum dot

In this section, we present the Berry connection and curvature for the present model. To simplify the equations, we use a parameter vector $\mathbf{X}(t)$ defined by

$$\mathbf{X}(t) = \left(X_\mu(t) \right) = \left(T_L(t), T_R(t), \mu_L(t), \mu_R(t) \right)^T. \quad (5.13)$$

We can utilize the result in Sec. 3.1 for derivation of the Berry connection. The different point is the driving parameter: What we want to derive is the Berry curvature for

time-dependent thermomechanical field and electrochemical potential, while the result in Sec. 3.1 discusses tunnel coupling constant driving. However, as shown in Eq. (5.5), the thermomechanical field and the electrochemical potential are introduced as a time-dependent tunnel coupling constant, so we can obtain the result by making a minor modification to Eq. (3.21).

To see what change should we make, let's compare the functional derivative with respect to the thermomechanical field and the electrochemical potential with the functional derivative with respect to tunnel coupling. The functional derivative with respect to $B_r(t)$ which acts on the action is calculated as

$$\begin{aligned} \frac{\delta S}{\delta T_r(\tau_1)} &= \frac{1}{T} \frac{\delta S}{\delta B_r(\tau_1)} = \frac{1}{T} \int d\tau \frac{\delta H(\tau)}{\delta B_r(\tau_1)} \\ &= \int d\tau \sum_{k,s} \gamma_{rk}(\tau) c_{rks}^\dagger(\tau) d_s(\tau) \left[\frac{1}{2T_r(\tau)} \delta(\tau - \tau_1) - i \frac{\epsilon_k}{T} \Theta(\tau - \tau_1) \right] \\ &\quad + \int d\tau \sum_{k,s} \gamma_{rk}^*(\tau) d_s^\dagger(\tau) c_{rks}(\tau) \left[\frac{1}{2T_r(\tau)} \delta(\tau - \tau_1) + i \frac{\epsilon_k}{T} \Theta(\tau - \tau_1) \right]. \end{aligned} \quad (5.14)$$

Here S denotes the action of the present model. In the same way,

$$\begin{aligned} \frac{\delta S}{\delta \mu_r(\tau_1)} &= -i \int d\tau \sum_{k,s} \gamma_{rk}(\tau) c_{rks}^\dagger(\tau) d_s(\tau) \Theta(\tau - \tau_1) \\ &\quad + i \int d\tau \sum_{k,s} \gamma_{rk}^*(\tau) d_s^\dagger(\tau) c_{rks}(\tau) \Theta(\tau - \tau_1). \end{aligned} \quad (5.15)$$

As a result, we obtain relations between the functional derivative with respect to $B_r(t)$ and $\mu_r(t)$ and that with respect to $\gamma_{rk}(t)$ and $\gamma_{rk}^*(t)$:

$$\frac{\delta}{\delta T_r(\tau_1)} = \int d\tau \sum_{k,s} \left[\frac{1}{2T_r(\tau)} \delta(\tau - \tau_1) - i \frac{\epsilon_k}{T} \Theta(\tau - \tau_1) \right] \gamma_{rk}(\tau) \frac{\delta}{\delta \gamma_{rk}(\tau)} + (\text{c.c.}), \quad (5.16)$$

$$\frac{\delta}{\delta \mu_r(\tau_1)} = -i \int d\tau \sum_{k,s} \Theta(\tau - \tau_1) \gamma_{rk}(\tau) \frac{\delta}{\delta \gamma_{rk}(\tau)} + (\text{c.c.}). \quad (5.17)$$

This relation holds as long as the functional derivative acts on the action.

Next, let's derive the Berry connection. As we discussed in Sec. 3.1, we consider infinitesimally small driving:

$$T_r(t) = T_{r,0} + \delta T_r e^{-i\Omega t} = T B_{r,0} + T \delta B_r e^{-i\Omega t}, \quad (5.18)$$

$$\mu_r(t) = \mu_{r,0} + \delta \mu_r e^{-i\Omega t}. \quad (5.19)$$

One can derive the dynamic conductance for B_r and μ_r driving by combining Eq. (5.17) and Eq. (3.19),

$$\begin{aligned}
& \mathcal{G}_{r,T_{r_1}}(\Omega) \\
&= 2e \sum_s \text{Re} \left\{ \sum_{\mu_1} \int \frac{d\omega}{2\pi} G_s^{+\mu_1}(\omega + \Omega) \Sigma_{r,s}^{\mu_1-}(\omega) \left[\frac{1}{2T_{r,0}} + \frac{\omega - \mu_{r,0}}{T_{r,0}\Omega} \right] \delta_{r,r_1} \right. \\
&+ \sum_{\mu_2, \mu_3, \mu_4} \sum_{s_1} \int \frac{d\omega_1 d\omega_2}{(2\pi)^2} D_{sss_1 s_1}^{+\mu_3 \mu_4 \mu_2}(\omega_1, \omega_2, \omega_2 + \Omega) \Sigma_{r,s}^{\mu_3-}(\omega_1) \Sigma_{r_1 s_1}^{\mu_2 \mu_4}(\omega_2) \left[\frac{1}{2T_{r,0}} + \frac{\omega_2 - \mu_{r_1,0}}{T_{r_1,0}\Omega} \right] \\
&+ \left. \sum_{\mu_2, \mu_3, \mu_4} \sum_{s_1} \int \frac{d\omega_1 d\omega_2}{(2\pi)^2} D_{sss_1 s_1}^{+\mu_3 \mu_2 \mu_4}(\omega_1, \omega_2 - \Omega, \omega_2) \Sigma_{r,s}^{\mu_3-}(\omega_1) \Sigma_{r_1 s_1}^{\mu_4 \mu_2}(\omega_2) \left[\frac{1}{2T_{r,0}} - \frac{\omega_2 - \mu_{r_1,0}}{T_{r_1,0}\Omega} \right] \right\}, \tag{5.20}
\end{aligned}$$

and

$$\begin{aligned}
& \mathcal{G}_{r,\mu_{r_1}}(\Omega) = 2e \sum_s \text{Re} \left\{ \sum_{\mu_1} \int \frac{d\omega}{2\pi} G_s^{+\mu_1}(\omega + \Omega) \Sigma_{r,s}^{\mu_1-}(\omega) \frac{1}{\Omega} \delta_{r,r_1} \right. \\
&+ \sum_{\mu_2, \mu_3, \mu_4} \sum_{s_1} \int \frac{d\omega_1 d\omega_2}{(2\pi)^2} D_{sss_1 s_1}^{+\mu_3 \mu_4 \mu_2}(\omega_1, \omega_2, \omega_2 + \Omega) \Sigma_{r,s}^{\mu_3-}(\omega_1) \Sigma_{r_1 s_1}^{\mu_2 \mu_4}(\omega_2) \frac{1}{\Omega} \\
&- \left. \sum_{\mu_2, \mu_3, \mu_4} \sum_{s_1} \int \frac{d\omega_1 d\omega_2}{(2\pi)^2} D_{sss_1 s_1}^{+\mu_3 \mu_2 \mu_4}(\omega_1, \omega_2 - \Omega, \omega_2) \Sigma_{r,s}^{\mu_3-}(\omega_1) \Sigma_{r_1 s_1}^{\mu_4 \mu_2}(\omega_2) \frac{1}{\Omega} \right\}. \tag{5.21}
\end{aligned}$$

Be sure that the Ω^{-1} factor appears in the temperature and electrochemical potential driving case and it leads the second order ω -derivative in the Berry connection. Considering Ω -linear term, the Berry connection is calculated as

$$\begin{aligned}
& A_{r,T_{r_1}} \\
&= e \sum_s \text{Im} \left\{ \sum_{\mu_1} \int \frac{d\omega}{2\pi} \frac{\partial}{\partial \omega} \left[G_s^{+\mu_1}(\omega) \right] \frac{\omega - \mu_{r,0}}{T_{r,0}} \frac{\partial}{\partial \omega} \left[\Sigma_{r,s}^{\mu_1-}(\omega) \right] \delta_{r,r_1} \right. \\
&+ \sum_{\mu_2, \mu_3, \mu_4} \sum_{s_1} \int \frac{d\omega_1 d\omega_2}{(2\pi)^2} \frac{\partial}{\partial \omega_3} \left[D_{sss_1 s_1}^{+\mu_3 \mu_4 \mu_2}(\omega_1, \omega_2, \omega_3) \right]_{\omega_3=\omega_2} \Sigma_{r,s}^{\mu_3-}(\omega_1) \frac{\omega_2 - \mu_{r_1,0}}{T_{r_1,0}} \frac{\partial}{\partial \omega_2} \left[\Sigma_{r_1 s_1}^{\mu_2 \mu_4}(\omega_2) \right] \\
&- \left. \sum_{\mu_2, \mu_3, \mu_4} \sum_{s_1} \int \frac{d\omega_1 d\omega_2}{(2\pi)^2} \frac{\partial}{\partial \omega_2} \left[D_{sss_1 s_1}^{+\mu_3 \mu_2 \mu_4}(\omega_1, \omega_2, \omega_3) \right]_{\omega_3=\omega_2} \Sigma_{r,s}^{\mu_3-}(\omega_1) \frac{\omega_2 - \mu_{r_1,0}}{T_{r_1,0}} \frac{\partial}{\partial \omega_2} \left[\Sigma_{r_1 s_1}^{\mu_4 \mu_2}(\omega_2) \right] \right\}, \tag{5.22}
\end{aligned}$$

and

$$\begin{aligned}
A_{r,\mu_{r_1}} &= e \sum_s \text{Im} \left\{ \sum_{\mu_1} \int \frac{d\omega}{2\pi} \frac{\partial}{\partial \omega} [G_s^{+\mu_1}(\omega)] \frac{\partial}{\partial \omega} [\Sigma_{r,s}^{\mu_1-}(\omega)] \delta_{r,r_1} \right. \\
&+ \sum_{\mu_2,\mu_3,\mu_4} \sum_{s_1} \int \frac{d\omega_1 d\omega_2}{(2\pi)^2} \frac{\partial}{\partial \omega_3} [D_{s s s_1 s_1}^{+\mu_3 \mu_4 \mu_2}(\omega_1, \omega_2, \omega_3)]_{\omega_3=\omega_2} \Sigma_{r,s}^{\mu_3-}(\omega_1) \frac{\partial}{\partial \omega_2} [\Sigma_{r_1 s_1}^{\mu_2 \mu_4}(\omega_2)] \\
&\left. - \sum_{\mu_2,\mu_3,\mu_4} \sum_{s_1} \int \frac{d\omega_1 d\omega_2}{(2\pi)^2} \frac{\partial}{\partial \omega_2} [D_{s s s_1 s_1}^{+\mu_3 \mu_2 \mu_4}(\omega_1, \omega_2, \omega_3)]_{\omega_3=\omega_2} \Sigma_{r,s}^{\mu_3-}(\omega_1) \frac{\partial}{\partial \omega_2} [\Sigma_{r_1 s_1}^{\mu_4 \mu_2}(\omega_2)] \right\}. \tag{5.23}
\end{aligned}$$

Using the following relations:

$$\frac{\omega - \mu_r}{T_r} \frac{\partial}{\partial \omega} \Sigma_{r,s}^{\mu_1 \mu_2}(\omega) = -\frac{\partial}{\partial T_r} \Sigma_{r,s}^{\mu_1 \mu_2}(\omega), \quad \frac{\partial}{\partial \omega} \Sigma_{r,s}^{\mu_1 \mu_2}(\omega) = -\frac{\partial}{\partial \mu_r} \Sigma_{r,s}^{\mu_1 \mu_2}(\omega), \tag{5.24}$$

one finally obtains

$$\begin{aligned}
A_{r,X_\mu} &= -e \sum_s \text{Im} \left\{ \sum_{\mu_1} \int \frac{d\omega}{2\pi} \frac{\partial}{\partial \omega} [G_s^{+\mu_1}(\omega)] \frac{\partial}{\partial X_\mu} [\Sigma_{r,s}^{\mu_1-}(\omega)] \right. \\
&+ \sum_{\mu_2,\mu_3,\mu_4} \sum_{s_1,r_1} \int \frac{d\omega_1 d\omega_2}{(2\pi)^2} \left[\frac{\partial}{\partial \omega_3} - \frac{\partial}{\partial \omega_2} \right] [D_{s s s_1 s_1}^{+\mu_3 \mu_4 \mu_2}(\omega_1, \omega_2, \omega_3)]_{\omega_3=\omega_2} \\
&\left. \times \Sigma_{r,s}^{\mu_3-}(\omega_1) \frac{\partial}{\partial X_\mu} [\Sigma_{r_1 s_1}^{\mu_2 \mu_4}(\omega_2)] \right\}. \tag{5.25}
\end{aligned}$$

This is the Berry connection which describes the adiabatic charge pumping induced by the time-dependent temperatures and electrochemical potentials of the reservoirs. As mentioned in Chapter 3, this formula is applicable to an arbitrary strength of the Coulomb interaction and the dot-reservoir coupling. All the effects of the Coulomb interaction are expressed by the one- and two-particle GFs.

5.4 Pumping Mechanism

In this section, we discuss the mechanism of the adiabatic charge pumping induced by the reservoir parameter driving. First, we show that the charge can be pumped by temperature and electrochemical potential driving only when the interaction exists, $U \neq 0$, in Sec. 5.4.1. Next, we present that the present charge pumping can be understood in terms of the delayed

response of the quantum dot to the time-dependent reservoir parameters in Sec. 5.4.2. Finally, we show that this delay in the response of the quantum dot can also be described in terms of the dynamic conductance in Sec. 5.4.3 and 5.4.4.

5.4.1 $U = 0$ case

For $U = 0$, the two-particle GF becomes a product of two one-particle GFs

$$D_{ss_1s_1}^{+\mu_3\mu_4\mu_2}(\omega_1, \omega_2, \omega_3) = G_{0,s}^{+\mu_2}(\omega_1)G_{0,s}^{\mu_4\mu_3}(\omega_3)2\pi\delta(\omega_1 - \omega_2)\delta_{s,s_1}, \quad (5.26)$$

so the Berry connection (Eq. (5.25)) becomes

$$A_{r,X_\mu} = -e \sum_s \text{Im} \left\{ \int \frac{d\omega}{2\pi} \frac{\partial}{\partial\omega} [G_{0,s}^R(\omega)] \frac{\partial}{\partial X_\mu} [\Sigma_{r,s}^<(\omega)] \right. \\ \left. + \sum_{r_1} \int \frac{d\omega}{2\pi} \left[\frac{\partial}{\partial\omega_1} - \frac{\partial}{\partial\omega_2} \right] G_{0,s}^R(\omega_1)G_{0,s}^A(\omega_2)\Sigma_{r,s}^A(\omega_2) \frac{\partial}{\partial X_\mu} [\Sigma_{r_1,s}^<(\omega)] \Big|_{\omega_1=\omega_2=\omega} \right\}. \quad (5.27)$$

Here, to calculate the summation of the Keldysh indices, we use the following relations:

$$\frac{\partial}{\partial X_\mu} \Sigma_{r,s}^{++}(\omega) = \frac{\partial}{\partial X_\mu} \Sigma_{r,s}^<(\omega), \quad (5.28)$$

$$\frac{\partial}{\partial X_\mu} \Sigma_{r,s}^{>}(\omega) = -\frac{\partial}{\partial X_\mu} \Sigma_{r,s}^<(\omega), \quad (5.29)$$

$$\frac{\partial}{\partial X_\mu} \Sigma_{r,s}^{--}(\omega) = \frac{\partial}{\partial X_\mu} \Sigma_{r,s}^<(\omega), \quad (5.30)$$

and

$$\frac{\partial}{\partial X_\mu} \Sigma_{r,s}^R(\omega) = \frac{\partial}{\partial X_\mu} \Sigma_{r,s}^A(\omega) = 0. \quad (5.31)$$

Because $G_{0,s}^A(\omega)$, $G_{0,s}^R(\omega)$, and $\Sigma_{0,s}^A(\omega)$ in Eq. (5.27) have no dependence on the temperature and the electrochemical potential of the reservoirs, the Berry connection with $U = 0$ can be described as a derivative of a function,

$$A_{r,X_\mu} = \frac{\partial}{\partial X_\mu} F(\mathbf{X}). \quad (5.32)$$

This leads to the fact that the Berry curvature is always zero, because

$$\frac{\partial A_{r,X_\mu}}{\partial X_\nu} - \frac{\partial A_{r,X_\nu}}{\partial X_\mu} = 0. \quad (5.33)$$

This indicates that charges are transferred between the reservoirs throughout the pumping cycle; however, the total charge transferred from the reservoir to the other is cancelled out in one cycle for the noninteracting system.

This situation is completely different from that we discussed in Sec. 4.2. While the finite amount of charge is pumped by tunnel coupling driving without interaction, the interaction effect is essential for adiabatic charge pumping induced by the reservoir parameter driving. To understand the mechanisms of pumping in the present case, we should find another scenario different from what we present in Sec. 4.2.

5.4.2 Delayed response

The most plausible scenario is that the quantum dot state, such as the occupation number, responds to the change of the temperature and the electrochemical potential of the reservoirs with a delay time, and charges are rectified by this delayed response. To understand the charge pumping in this framework, let us consider the steady-state charge current for arbitrary reservoir parameters $\mathbf{X}(t)$ *delayed* with a small time $\delta t (> 0)$:

$$\begin{aligned} I_r^{\text{delay}}(t) &= I_r^{\text{st.}}(\mathbf{X}(t - \delta t)) \\ &\simeq I_r^{\text{st.}}(\mathbf{X}(t)) - \sum_{\mu} \partial^{\mu} I_r^{\text{st.}}(\mathbf{X}(t)) \dot{X}_{\mu}(t) \delta t. \end{aligned} \quad (5.34)$$

It is easy to show that if we take the delay time as

$$\delta t = - \frac{\sum_{\mu} A_{r,X_{\mu}}(\mathbf{X}(t)) \dot{X}_{\mu}(t)}{\sum_{\mu} \partial^{\mu} J_r^{\text{st.}}(\mathbf{X}(t)) \dot{X}_{\mu}(t)}, \quad (5.35)$$

the correction of the steady-state current due to the time delay δt coincides with the adiabatic correction of the current:

$$I_r^{\text{delay}}(t) = I_r^{\text{st.}}(\mathbf{X}(t)) + \sum_{\mu} A_{r,\mu}(\mathbf{X}(t)) \dot{X}_{\mu}(t) + O(\ddot{X}_{\mu}(t), \dot{X}_{\mu}^2(t)) \quad (5.36)$$

We note that the definition of the delay time given in Eq. (5.35) holds for arbitrary strengths of U and Γ . This indicates that the transient effect in the adiabatic process is always represented only by the delay time δt . In our previous work [56], we discussed this delayed response

effect on the charge pumping within the first-order perturbation with respect to the Coulomb interaction U .

One might suspect that the definition of delay time δt is something artificial. To support our definition, we next consider low-frequency AC transport and an equivalent circuit of the present adiabatic pumping. In the low-frequency AC transport, it is known that the quantum dot is effectively equivalent to the RC -circuit. Equivalent circuit elements (a resistance and a capacitance) are estimated by considering the dynamic conductance in the low-frequency limit [4, 57, 58]. Using the equivalence to the RC -circuit, one can see that δt coincides with the relaxation time of the interacting quantum dot.

5.4.3 AC response: the single-reservoir case

Before we discuss the dynamic conductance in the present system, we consider the single-reservoir case, for which the low-frequency AC transport has been studied well [4, 57, 58]. We show that the time-dependent current under parameter driving can be understood in terms of the delay time, which can be related directly to circuit elements called a dynamic capacitance and a dynamic resistance.

We consider a quantum dot coupled to one reservoir, whose temperature and electrochemical potential are modulated as

$$T(t) = T_0 + \delta T e^{-i\Omega t}, \quad \mu(t) = \mu_0 + \delta \mu e^{-i\Omega t}, \quad (5.37)$$

where T_0 and μ_0 are the temperature and the electrochemical potential of the reservoir in equilibrium, respectively. δT and $\delta \mu$ are the amplitudes of AC driving for the reservoir parameter with a frequency Ω . For convenience of description, we define the parameter vector

$$\mathbf{X}(t) = (X_1, X_2) = (T(t), \mu(t)) \quad (5.38)$$

and rewrite Eq. (5.37) as

$$X_\mu(t) = X_{\mu,0} + \delta X_\mu e^{-i\Omega t}, \quad (\mu = 1, 2). \quad (5.39)$$

Here, we assume that the amplitude δX_μ is small and consider the current flowing into the quantum dot up to the linear order of δX_μ :

$$I(t) = \sum_{\mu} \mathcal{G}^{\mu}(\Omega) \delta X_{\mu} e^{-i\Omega t} + O((\delta X_{\mu})^2), \quad (5.40)$$

where $G^\mu(\Omega; \mathbf{X}_0)$ is the dynamic conductance. We note that the leading term of the charge current is proportional to $O(\delta X_\mu)$ because the system is in thermal equilibrium for $\delta X_\mu = 0$. In the low-frequency limit, the dynamic conductance can be expanded with respect to frequency Ω as

$$\mathcal{G}^\mu(\Omega; \mathbf{X}_0) = -i\Omega\mathcal{G}_1^\mu - \Omega^2\mathcal{G}_2^\mu + O(\Omega^3). \quad (5.41)$$

These coefficients, \mathcal{G}_1^μ and \mathcal{G}_2^μ , are described by circuit elements as follows:

$$\mathcal{G}_1^\mu = C_\mu, \quad \mathcal{G}_2^\mu = -C_\mu^2 R_\mu, \quad (5.42)$$

where C_μ and R_μ are the dynamic capacitance and dynamic resistance for electrochemical-potential modulation ($\mu = 1$) or temperature modulation ($\mu = 2$), respectively [4, 58]. Substituting Eqs. (5.41) and (5.42) into Eq. (5.40), we obtain

$$I(t) = -i\Omega \sum_{\mu} (\mathcal{G}_1^\mu - i\Omega\mathcal{G}_2^\mu) \delta X_\mu e^{-i\Omega t} + O((\delta X_\mu)^2, \Omega^3). \quad (5.43)$$

This current response can be represented by only one parameter, i.e., the delay time δt as

$$I(t) = I_0(t - \delta t), \quad (5.44)$$

$$I_0(t) = -i\Omega \sum_{\mu} \mathcal{G}_1^\mu \delta X_\mu e^{-i\Omega t}, \quad (5.45)$$

where $I_0(t)$ is the capacitive current component due to the instant response of the charge in the quantum dot to the external parameter driving. By comparing Eqs. (5.44) and (5.45) with Eq. (5.43), the time delay should be taken as

$$\delta t = -\frac{\sum_{\mu} \mathcal{G}_2^\mu \delta X_\mu}{\sum_{\mu} \mathcal{G}_1^\mu \delta X_\mu} = \frac{\sum_{\mu} C_\mu^2 R_\mu \delta X_\mu}{\sum_{\mu} C_\mu \delta X_\mu}. \quad (5.46)$$

One can see that δt is just an average of the relaxation time $R_\mu C_\mu$ of a quantum RC-circuit weighted by $C_\mu \delta X_\mu$. This relation shows that the time delay δt is closely related to the transport coefficients in the dynamic AC response of the quantum dot.

5.4.4 AC response: the two-reservoir case

For the present system, i.e., the quantum dot coupled to the two reservoirs, the simple interpretation by circuit elements described in the previous section is not applicable because

a steady-state current generally exists. However, we show that there is still a relation between the dynamic AC response and the delay time.

We first define the parameter vector by Eq. (5.13) and consider the time-dependent parameter modulation give by

$$X_\mu(t) = X_{\mu,0} + \delta X_\mu(t) e^{-i\Omega t}. \quad (5.47)$$

The time-dependent current induced by this parameter modulation is described by

$$I_r(t) = I_r^{\text{st.}}(\mathbf{X}_0) + \sum_{\mu} \mathcal{G}_r^\mu(\Omega) \delta X_\mu e^{-i\Omega t} + O((\delta X_\mu)^2), \quad (5.48)$$

where $I_r^{\text{st.}}(t)$ is the steady-state current for a fixed parameter $\mathbf{X} = \mathbf{X}_0$ and $\mathcal{G}_r^\mu(\Omega)$ is the dynamic conductance at $\mathbf{X} = \mathbf{X}_0$. We expand $\mathcal{G}_r^\mu(\Omega)$ with respect to Ω as

$$\mathcal{G}_r^\mu(\Omega; \mathbf{X}_0) = \mathcal{G}_{r,0}^\mu - i\Omega \mathcal{G}_{r,1}^\mu + O(\Omega^2). \quad (5.49)$$

Here, we can prove that the coefficients $\mathcal{G}_{r,0}^\mu(\mathbf{X}_0)$ and $\mathcal{G}_{r,1}^\mu(\mathbf{X}_0)$ are related to the stationary current and the Berry connection as

$$\mathcal{G}_{r,0}^\mu = \partial^\mu I_r^{\text{st.}}(\mathbf{X}_0), \quad (5.50)$$

$$\mathcal{G}_{r,1}^\mu = A_{r,X_\mu}(\mathbf{X}_0), \quad (5.51)$$

respectively (see Eq. (3.4), for example). This correspondence between the dynamic conductance and the Berry connection is reasonable because the dynamics of the system under low-frequency modulation is indeed an adiabatic process.

From this correspondence, we can introduce the delay time of the current under the parameter modulation and can relate it to the low-frequency response coefficients. Using Eqs. (5.48)-(5.51), we obtain

$$I_r(t) \simeq I_r^{\text{st.}}(\mathbf{X}_0) + \delta I_r(t - \delta t), \quad (5.52)$$

$$\delta I_r(t) = \sum_{\mu} \mathcal{G}_{r,0}^\mu \delta X_\mu e^{-i\Omega t}, \quad (5.53)$$

where $\delta I_r(t)$ is a time-dependent current component, which instantly responds to the parameter modulation, and the time delay δt is determined by

$$\delta t = - \frac{\sum_{\mu} \mathcal{G}_{r,1}^\mu \delta X_\mu}{\sum_{\mu} \mathcal{G}_{r,0}^\mu \delta X_\mu}. \quad (5.54)$$

This expression for the delay time, which coincides with the one defined in Eq. (5.35), indicates that the physical picture of the delay time for the charge pumping discussed in Sec. 5.4.2 is reasonable, because it is written in terms of the linear AC response to small and slow parameter modulation.

5.5 Evaluation of the Pumped Charge

In this section, we evaluate the adiabatic charge pumping with RPT discussed in Sec. 2.4.3. We consider the first-order perturbation with respect to the renormalized Coulomb interaction in the framework of RPT as an approximation. First, we present the interaction dependences of the renormalized parameters. Next, we calculate the pumped charge as a function of U and ε_d under the time-dependent electrochemical potentials of the reservoirs (Sec. 5.5.2) and the time-dependent temperatures of the reservoirs (Sec. 5.5.3). For simplicity, we assume the symmetric coupling, $\Gamma_L = \Gamma_R = \Gamma/2$, and consider a symmetrized adiabatic pumped charge δQ defined as

$$\begin{aligned}\delta Q &= \frac{1}{2}(\delta Q_L - \delta Q_R) \\ &= \frac{1}{2} \sum_{\mu} \int_C dX_{\mu} (A_{L,X_{\mu}} - A_{R,X_{\mu}}).\end{aligned}\quad (5.55)$$

5.5.1 Renormalized parameters

Figure 5.2 shows the renormalized parameters determined from the Bethe ansatz solution [50] for several values of $u \equiv U/\Gamma$. The effective linewidth $\tilde{\Gamma}$ indicates the peak width of the renormalized spectrum function of the quantum dot and gives the characteristic energy scale of the system, i.e., the Kondo temperature. In the presence of the Coulomb interaction, $\tilde{\Gamma}$ is strongly suppressed (the Kondo resonance). Actually, as seen in Fig. 5.2(a), the renormalized linewidth $\tilde{\Gamma}$ is reduced in the presence of the Coulomb interaction around the particle-hole symmetric point, $\varepsilon_d = U/2$. The renormalized Coulomb interaction \tilde{U} is also shown in Fig. 5.2(b); the ratio $\tilde{U}/\tilde{\Gamma}$ first increases as u increases, and shows a tendency of saturation for $u \gtrsim 3$. The renormalized quantum dot energy level $\tilde{\varepsilon}_d$ is shown in Fig. 5.2(c); it becomes flat near the particle-hole symmetric point due to the pinning effect because the occupation number of the electron in the quantum dot is fixed almost at one for the strong Coulomb interaction.

In the following calculation, we consider first-order perturbation theory with respect to the renormalized Coulomb interaction. In Ref. [56], we calculated the pumped charge up to

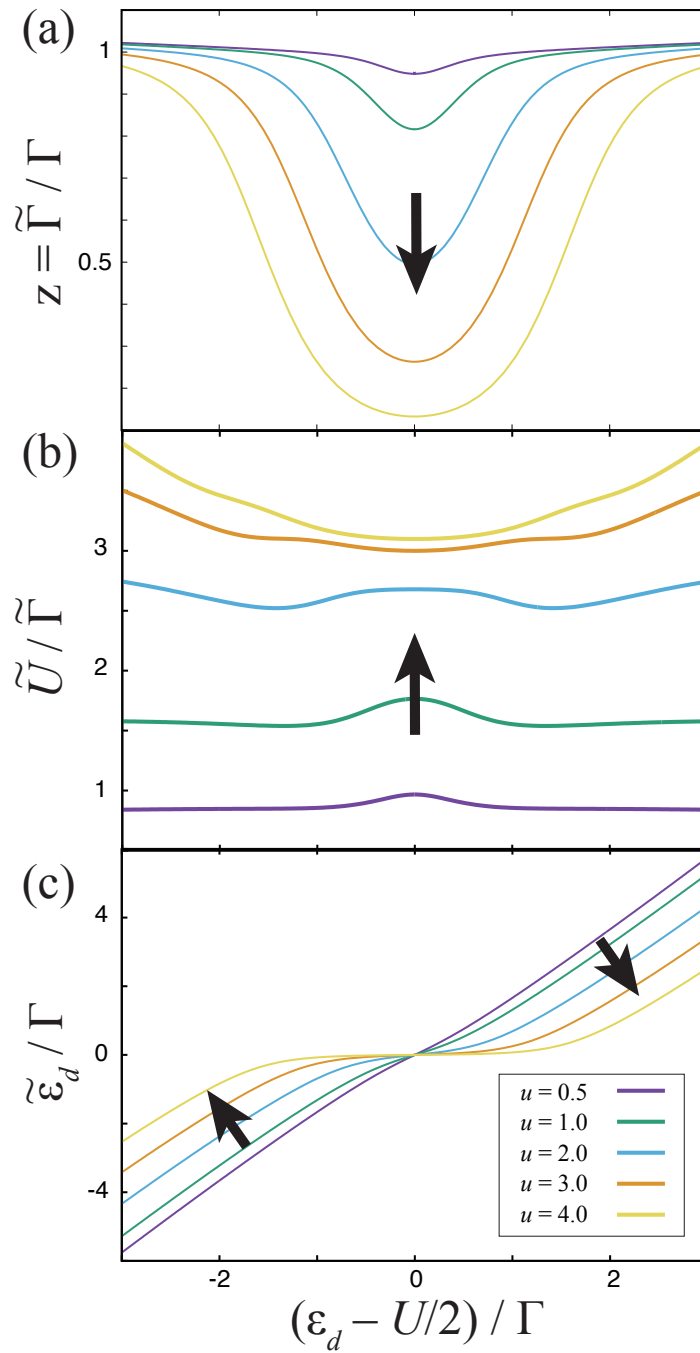


Fig. 5.2 Renormalized parameters are plotted as a function of $(\epsilon_d - U/2)/\Gamma$ for $u = U/\Gamma = 0.5, 1.0, 2.0, 3.0, 4.0$. (a) The renormalized linewidth $\tilde{\Gamma}$, (b) ratio between the renormalized Coulomb interaction \tilde{U} and the renormalized line width $\tilde{\Gamma}$, and (c) renormalized quantum dot energy level $\tilde{\epsilon}_d$.

the first-order perturbation for the bare model parameters. The present result is obtained by replacing the model parameters in Ref. [56] with the renormalized ones¹.

We give some remarks on the limitation of the first-order perturbation based on RPT: (i) Because the RPT is based on the local Fermi liquid theory, it is applicable when the temperature and the electrochemical potential are sufficiently small compared with the renormalized linewidth $\tilde{\Gamma}$. (ii) Although the first-order perturbation with the renormalized parameters still reflects more physics than that with the bare parameters, the higher order effects of the interaction are ignored. In this chapter, however, we focus on the qualitative tendency of how the parameter renormalization by the Coulomb interaction modifies the pumped charge. For this purpose, the first-order perturbation is sufficient, because its major effect of parameter renormalization is described in the present approximation.

5.5.2 Electrochemical-potential-driven pumping

First, we consider the time-dependent electrochemical potentials. We set the temperatures of the reservoirs as zero and consider only the time-dependent electrochemical potential in the near-equilibrium region,

$$\mu_r(t) = \varepsilon_F + \delta\mu_r(t), \quad (5.56)$$

where ε_F is the Fermi level (set as zero throughout this chapter), and $\delta\mu_r(t)$ is the time-dependent part of the electrochemical potential of the reservoir r . We assume that the amplitude of the time-dependent part is small:

$$\delta\mu \ll \tilde{\Gamma} < \Gamma, \quad (5.57)$$

where $\delta\mu = \max|\mu(t)|$. By Stokes' theorem, the symmetrized adiabatic pumped charge given in Eq. (5.55) is rewritten as

$$\delta Q = \frac{1}{2} \int_A d\mu_L d\mu_R \left[\frac{\partial(A_{L,\mu_R} - A_{R,\mu_R})}{\partial\mu_L} - \frac{\partial(A_{L,\mu_L} - A_{R,\mu_L})}{\partial\mu_R} \right], \quad (5.58)$$

¹This approximation does not violate the charge conservation, while the second-order perturbation may violate the charge conservation.

where A indicates the integral surface on the μ_L - μ_R plane whose boundary is C . For the small-amplitude driving of electrochemical potentials, $\delta\mu \ll \tilde{\Gamma}$, δQ can be approximated as

$$\delta Q = \Pi_{0,\text{volt.}} V(A) + O((\delta\mu/\tilde{\Gamma})^3), \quad (5.59)$$

$$V(A) = \tilde{\Gamma}^{-2} \int_A d\mu_L d\mu_R, \quad (5.60)$$

where $V(A)$ is a dimensionless quantity proportional to the area inside the contour C in the μ_L - μ_R plane. The kernel $\Pi_{0,\text{volt.}}$, which indicates the strength of the pumping, is calculated at zero temperature as

$$\begin{aligned} \Pi_{0,\text{volt.}} = e\Gamma^2 \sum_{s,s_2} \text{Im} \left\{ \sum_{\mu_2,\mu_3,\mu_4} \int \frac{d\omega_1 d\omega_2}{(2\pi)^2} \left[\frac{\partial}{\partial\omega_2} - \frac{\partial}{\partial\omega_3} \right] \left[D_{ss_2s_2}^{+\mu_3\mu_4\mu_2}(\omega_1, \omega_2, \omega_3) \right]_{\omega_3=\omega_2} \right. \\ \left. \times \left[\frac{\partial}{\partial\mu_L} \Sigma_{L,s}^{\mu_3-}(\omega_1) \frac{\partial}{\partial\mu_R} \Sigma_{R,s_2}^{\mu_2\mu_4}(\omega_2) + \frac{\partial}{\partial\mu_R} \Sigma_{R,s}^{\mu_3-}(\omega_1) \frac{\partial}{\partial\mu_L} \Sigma_{L,s_2}^{\mu_2\mu_4}(\omega_2) \right] \right\}. \end{aligned} \quad (5.61)$$

Now, we apply the first-order perturbation in the framework of the RPT to Eq. (5.61). The two-particle GF is written in terms of the renormalized GFs as

$$D_{ss_2s_2}^{+\mu_3\mu_4\mu_2}(\omega_1, \omega_2, \omega_3) = -iz^2 \tilde{U} \sum_{\mu_1} \tilde{G}_{s,0}^{+\mu_1}(\omega_1) \tilde{G}_{s,0}^{\mu_1\mu_3}(\omega_1 - \omega_2 + \omega_3) \tilde{G}_{s',0}^{\mu_4\mu_1}(\omega_2) \tilde{G}_{s',0}^{\mu_1\mu_2}(\omega_3), \quad (5.62)$$

where $\tilde{G}_{s,0}^{\mu_1\mu_2}(\omega)$ is the GF with the renormalized parameters. The retarded and advanced one-particle GFs with renormalized parameters, $\tilde{G}_{s,0}^R(\omega)$ and $\tilde{G}_{s,0}^A(\omega)$, are defined respectively as

$$\tilde{G}_{s,0}^R(\omega) = \frac{1}{\omega - \tilde{\epsilon}_d + i\tilde{\Gamma}/2}, \quad (5.63)$$

$$\tilde{G}_{s,0}^A(\omega) = \frac{1}{\omega - \tilde{\epsilon}_d - i\tilde{\Gamma}/2}. \quad (5.64)$$

As a result, $\Pi_{0,\text{volt.}}$ is written as

$$\Pi_{0,\text{volt.}} = -\frac{e}{8\pi^2} \frac{z^2 \tilde{U} \tilde{\epsilon}_d \tilde{\Gamma}^6}{(\tilde{\epsilon}_d^2 + \tilde{\Gamma}^2/4)^4} + O((\tilde{U}/\tilde{\Gamma})^2). \quad (5.65)$$

In Fig. 5.3, we plot $\Pi_{0,\text{volt.}}$ as a function of ϵ_d for several values of U . As seen from the figure, $\Pi_{0,\text{volt.}}$ is an odd function with respect to $\epsilon_d - U/2$, which is the deviation from the

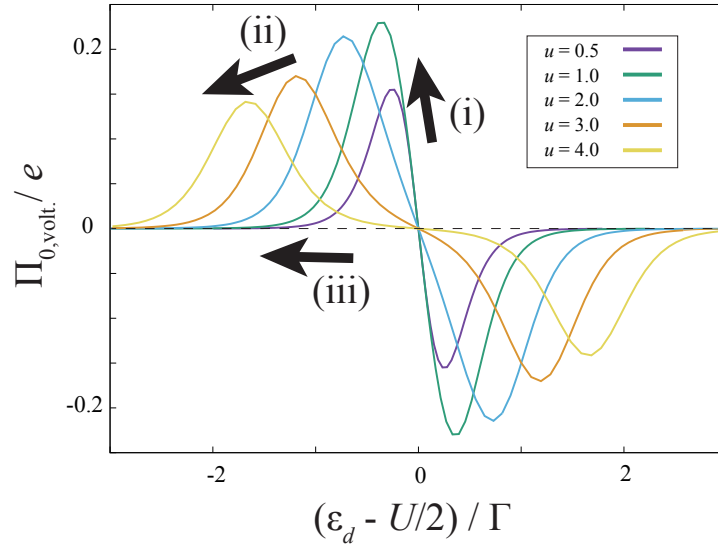


Fig. 5.3 Quantum dot energy level dependence of $\Pi_{0,\text{volt.}}$ for different values of the Coulomb interaction. Five results are plotted for $u = U/\Gamma = 0.5, 1.0, 2.0, 3.0, 4.0$. As the Coulomb interaction becomes stronger, the amplitude is enhanced for $u \lesssim 1.0$ and suppressed for $u \gtrsim 1.0$. The shape becomes increasingly broadened and the peak and dip positions are shifted to larger values.

particle-hole symmetric point, and changes its sign at $\varepsilon_d = U/2$. This feature reflects the energy derivative of the spectrum function of the quantum dot, $\Pi_{0,\text{volt.}} \sim A(\varepsilon_F)A'(\varepsilon_F)$. The qualitative change in $\Pi_{0,\text{volt.}}$ due to the increase of the Coulomb interaction is summarized as follows: (i) the amplitude of its peak is first enhanced for $U \lesssim \Gamma$ due to the increase in $\tilde{U}/\tilde{\Gamma}$, (ii) it is suppressed when the Coulomb interaction U exceeds Γ because the suppression of the wavefunction renormalization factor z becomes relevant, and (iii) the peak position moves away from the particle-hole symmetric point because of the pinning effect for the renormalized quantum dot energy level $\tilde{\varepsilon}_d$. Thus, the whole features of the pumped charge can be captured qualitatively by the quasi-particle renormalization, which reflects the Kondo physics.

5.5.3 Temperature-driven pumping

Next, let us consider temperature-driven pumping. We set the electrochemical potentials to the Fermi energy (set as zero throughout this paper) and consider only the temperature

driving in the near-equilibrium region,

$$T_r(t) = T_0 + \delta T_r(t), \quad (5.66)$$

where T_0 is the average temperature and $\delta T_r(t)$ is the time-dependent part of the temperature of reservoir r . We assume that the amplitude of the time-dependent part is small:

$$\delta T, T_0 \ll \tilde{\Gamma} < \Gamma, \quad (5.67)$$

where $\delta T = \max|\delta T_r(t)|$.

In the same manner as for electrochemical potential driving, the symmetrized adiabatic pumped charge is written as

$$\delta Q = \Pi_{0,\text{temp.}} V(A) + O((\delta T/\tilde{\Gamma})^3, (T_0/\tilde{\Gamma})^3), \quad (5.68)$$

$$V(A) = \tilde{\Gamma}^{-2} \int_A dT_L dT_R \frac{T_L T_R}{T_0^2}. \quad (5.69)$$

where $V(A)$ is a dimensionless quantity proportional to the area inside the contour C in the T_L - T_R plane. As we present in Sec. 5.5.2, the kernel $\Pi_{0,\text{temp.}}$, which indicates the strength of the temperature pumping, is calculated within the first-order perturbation as

$$\Pi_{0,\text{temp.}} = -\frac{e\pi^2 z^2 T_0^2 \tilde{U} \tilde{\Gamma}^8 \tilde{\epsilon}_d (\tilde{\Gamma}^2/4 - 3\tilde{\epsilon}_d^2)}{18\tilde{\Gamma}^2 (\tilde{\epsilon}_d^2 + \tilde{\Gamma}^2/4)^6}. \quad (5.70)$$

In Fig. 5.4, we plot $\Pi_{0,\text{temp.}}$ as a function of ϵ_d for several values of U . As seen from the figure, $\Pi_{0,\text{temp.}}$ is also an odd function with respect to $\epsilon_d - U/2$ and changes its sign three times, at $\epsilon_d = U/2$, and two other values of ϵ_d . This feature reflects the higher energy derivatives of the spectrum function of the quantum dot, $\Pi_{0,\text{temp.}} \sim A'(\epsilon_F)A''(\epsilon_F)$. The qualitative change in $\Pi_{0,\text{temp.}}$ for increasing the Coulomb interaction is summarized as follows: (i) the amplitude of its peak continues to increase due to the increase in $\tilde{U}/\tilde{\Gamma}$, (ii) its peak growth saturates due to the saturation of $\tilde{U}/\tilde{\Gamma}$ for $u \gtrsim 3$, and (iii) the peak position moves away from the particle-hole symmetric point because of the pinning effect for the renormalized quantum dot energy level $\tilde{\epsilon}_d$. The behavior (ii) is different from that in the case of electrochemical potential driving. This is because $\Pi_{0,\text{temp.}}$ contains temperature-dependent factor, $(T_0/\tilde{\Gamma})^2$, which counters the wavefunction renormalization factor dependence.

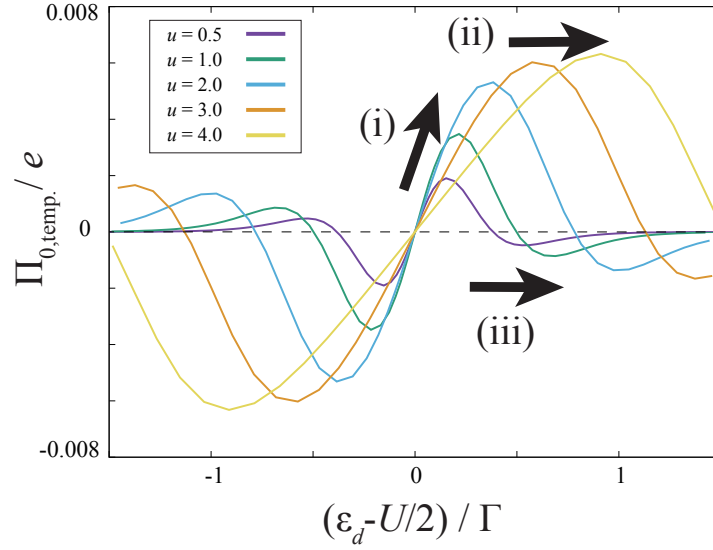


Fig. 5.4 Quantum dot energy-level dependence of $\Pi_{0,temp.}$ for different values of the Coulomb interaction. Five results are plotted for $u = U/\Gamma = 0.5, 1.0, 2.0, 3.0, 4.0$. We set the average temperature as $T_0 = 0.01\Gamma$. As the Coulomb interaction becomes stronger, the amplitude is enhanced for $u \lesssim 1.0$ and suppressed for $u \gtrsim 1.0$. The shape becomes increasingly broadened and the peak and dip positions are shifted to larger value.

5.6 Short summary

In this chapter, we discussed the adiabatic charge pumping via the quantum dot induced by the time-dependent temperatures and electrochemical potentials of reservoirs and clarified the effect of the Coulomb interaction on the pumped charge. We considered the single-level quantum dot with the Coulomb interaction coupled to two electron reservoirs with time-dependent temperatures and chemical potentials. Using the general formula derived in Chapter 3, we derived the Berry connection for the present adiabatic charge pumping. To describe the time-dependence of temperatures, we employed the thermomechanical field. Our result is applicable to an arbitrary strength of the Coulomb interaction and the dot-reservoir tunnel couplings.

We also clarified that the present pumping is caused by the rectification effect. When the temperatures and electrochemical potentials of reservoirs are modified, the electronic state in the quantum dot also changes with a delay time. This delayed response rectifies the charge current and transfers net charge from one reservoir to the other. This delay time can be estimated as a relaxation time by considering the equivalent RC -circuit of the quantum dot.

To discuss the effect of the Coulomb interaction on the pumped charge, we employed the renormalized perturbation theory and considered the first-order perturbation with respect to the renormalized Coulomb interaction for both the temperature driving case and the electrochemical potential driving case (Figs. 5.3 and 5.4). We calculated the pumped charge in a unit driving area as a function of the dot level for several values of the Coulomb interaction. We found that the peak position of the pumped charge is shifted far from the particle-hole symmetric point. This indicates that the Coulomb blockade effect strongly suppresses the charge pumping.

Chapter 6

Summary and Perspectives

6.1 Summary and Future problems

In this thesis, we have studied adiabatic charge pumping via a quantum dot. We mainly discussed two themes: (i) Almost topological feature of adiabatic charge pumping via a non-interacting quantum dot system and (ii) the effect of the Coulomb interaction on adiabatic charge pumping via a quantum dot system.

In Chapter 3, we introduced a general formula in the Keldysh formalism which describes the adiabatic charge pumping via the quantum dot systems. This formalism, which describes adiabatic charge pumping in terms of the one- and two-particle GFs, is applicable to the interacting quantum dot with drivings of arbitrary parameters. This result is one of the fundamental results in our thesis and utilized in Chapters 4 and 5.

In Chapter 4, we discussed the “almost” topological feature of adiabatic charge pumping in the single-level quantum dot system without the Coulomb interaction. Here “almost topological” means that the pumped charge in one cycle is insensitive to any change of the driving contour as long as the driving contour surrounds the whole of the peak of the Berry curvature. We figured out that the number of pumped electrons in one cycle is quantized into a fractional value, between zero and one. This fractional value depends on the band structure of the electron reservoirs. We showed that the fractional value can be characterized by one parameter, λ , defined by the ratio of the Lamb shift to the level-broadening at the Fermi level. It is an important future problem to clarify how our classification is modified in the quantum dot with the Coulomb interaction.

In Chapter 5, we discussed the adiabatic charge pumping via a single-level quantum dot with the Coulomb interaction. Time-dependent temperatures and electrochemical potentials of reservoirs were considered. We derived an analytical formula of the Berry connection applicable to an arbitrary strength of the Coulomb interaction and the tunnel coupling. We

also figured out the mechanism of the adiabatic charge pumping induced by temperature and electrochemical potential driving. The quantum dot responds to the change of temperatures and electrochemical potentials of the reservoirs with the delayed time and this delayed response rectifies the charge current. By considering the equivalent RC -circuit, the delay time is estimated as the relaxation time of the quantum dot. Using RPT, we gave some numerical results (Figs. 5.3 and 5.4) which show the interaction dependence on adiabatic charge pumping beyond the Hartree approximation. We figured out that the renormalization effects of the Coulomb interaction are observed in the pumped charge: the peak position of the pumped charge is shifted far from the particle-hole symmetric point. This indicates that the charge pumping is strongly suppressed by the Coulomb blockade effect. The present formalism states that the adiabatic charge pumping can be evaluated by the two-particle Green's function of the electrons in the quantum dot, which can be in principle calculated by numerical methods, such as the numerical renormalization group and the continuous-time quantum Monte Carlo method. It is an important future problem to compute the pumped charge accurately in the strong Coulomb interaction region.

In Chapters 4 and 5, we discussed the averaged value of the pumped charge in one cycle. One can observe our results by repeating the pumping cycle and averaging the amount of charge transfer. In order to distinguish the charge transfer by the pumping from that by the steady charge current, one can consider pumping frequency-dependence: The amount of the pumped charge in unit time is proportional to the pumping frequency, while the steady charge current is independent of the pumping frequency. Observing the time-dependence of the occupation number of the quantum dot through the pumping is another option to distinguish the adiabatic charge pumping from the steady charge current. Especially, it is possible to observe the difference between the pumping current and the steady current by discussing the time-correlation of the occupation number. Because the time-correlation of the occupation number cannot be discussed in our formalism, it is an interesting future problem in the adiabatic pumping.

6.2 Perspective: Towards steady state thermodynamics

Our results provide a clear description of the physical mechanism of adiabatic charge pumping in the quantum dot system where the hybridization between the dot and the reservoirs strongly affects the transport. By generalizing our result to heat transport, we will be able to study the thermodynamic property of quantum heat engines in nanoscale. For example, understanding how the strong hybridization effect between the system and the reservoirs affects the entropy

for a non-equilibrium steady state (NESS) is an important problem, which has been recently discussed in steady state thermodynamics (SST).

SST [59–63] is a phenomenological proposal to generalize a concept of thermodynamics toward NESS. When one discusses the thermodynamic property of NESSs, steady flows of heat and particles under an external bias between the reservoirs are an inevitable problem. One way to overcome this problem is to introduce a concept of an *excess* heat, which is defined as a heat transfer after subtracting the contribution of the steady flow (see Appendix E for more detail). The excess heat is a key idea to construct the framework of SST for NESSs based on an operational approach. In SST, one expects that the non-equilibrium entropy production can be related to the excess heat by the modified Clausius relation. In the weakly biased case, this extended Clausius relation was proved for classical systems [64, 65] and quantum systems [66]. In the strongly biased case, it was reported that the excess heat is related not with the entropy but with the entropy production [15, 16].

In the theoretical frameworks of SST mentioned above, it is assumed that the coupling between the system and the reservoirs is negligibly small, so the definition of the entropy for quantum systems with the strong hybridization between the system and reservoirs has been a mystery. Recently, a new theoretical framework of operational thermodynamics and the new definition of the entropy for NESS were proposed for single-level quantum dots [67] and coupled harmonic oscillators [68]. In these framework, the strong hybridization effect between the system and the reservoirs is taken into account. However, the frameworks are valid for specific models and it is still unknown they are valid for general quantum systems.

Since adiabatic pumping can be regarded as a quasi-static and cyclic operation, it can be used as a fundamental operation in construction of SST. Therefore, we will be able to study strong hybridization effect on the entropy of NESS by generalizing our formalism of the adiabatic charge pumping to the adiabatic heat pumping.

References

1. D. J. Thouless, *Phys. Rev. B* **27**, 6083–6087, ISSN: 2469-9969 (May 1983).
2. H. Pothier, P. Lafarge, C. Urbina, D. Esteve, M. H. Devoret, *EPL* **17**, 249 (1992).
3. L. P. Kouwenhoven, A. T. Johnson, N. C. van der Vaart, C. J. P. M. Harmans, C. T. Foxon, *Phys. Rev. Lett.* **67**, 1626–1629 (12 Sept. 1991).
4. M. Büttiker, A. Prêtre, H. Thomas, *Phys. Rev. Lett.* **70**, 4114–4117 (26 June 1993).
5. I. L. Aleiner, A. V. Andreev, *Phys. Rev. Lett.* **81**, 1286–1289 (6 Aug. 1998).
6. P. W. Brouwer, *Phys. Rev. B* **58**, R10135–R10138, ISSN: 2469-9969 (Oct. 1998).
7. M. Moskalets, M. Büttiker, *Phys. Rev. B* **66**, 205320 (20 Nov. 2002).
8. L. Arrachea, M. Moskalets, *Phys. Rev. B* **74**, 245322 (24 Dec. 2006).
9. M. Moskalets, M. Büttiker, *Phys. Rev. B* **78**, 035301, ISSN: 2469-9969 (July 2008).
10. S. Camalet, J. Lehmann, S. Kohler, P. Hänggi, *Phys. Rev. Lett.* **90**, 210602 (21 May 2003).
11. T. J. Suzuki, T. Kato, *Phys. Rev. B* **91**, 165302 (16 Apr. 2015).
12. A. Ronzani *et al.*, *Nature Physics* **14**, 991–995 (July 2018).
13. J. Ren, P. Hänggi, B. Li, *Phys. Rev. Lett.* **104**, 170601 (17 Apr. 2010).
14. S. Juergens, F. Haupt, M. Moskalets, J. Splettstoesser, *Phys. Rev. B* **87**, 245423 (June 2013).
15. T. Yuge, T. Sagawa, A. Sugita, H. Hayakawa, *Journal of Statistical Physics* **153**, 412–441, ISSN: 1572-9613 (Nov. 2013).
16. S. Nakajima, Y. Tokura, *Journal of Statistical Physics* **169**, 902–928, ISSN: 1572-9613 (Dec. 2017).
17. D. V. Averin, K. K. Likharev, *Journal of Low Temperature Physics* **62**, 345–373, ISSN: 1573-7357 (Feb. 1986).
18. J. König, J. Schmid, H. Schoeller, G. Schön, *Phys. Rev. B* **54**, 16820–16837 (23 Dec. 1996).
19. F. Reckermann, J. Splettstoesser, M. R. Wegewijs, *Phys. Rev. Lett.* **104**, 226803 (22 June 2010).
20. H. L. Calvo, L. Classen, J. Splettstoesser, M. R. Wegewijs, *Phys. Rev. B* **86**, 245308, ISSN: 2469-9969 (Dec. 2012).
21. O. Entin-Wohlman, A. Aharony, Y. Levinson, *Phys. Rev. B* **65**, 195411 (19 Apr. 2002).
22. M. Hasegawa, É. Jussiau, R. S. Whitney, *Phys. Rev. B* **100**, 125420 (12 Sept. 2019).

23. J. Kondo, *Progress of Theoretical Physics* **32**, 37–49, ISSN: 0033-068X (July 1964).
24. K. G. Wilson, *Rev. Mod. Phys.* **47**, 773–840 (4 Oct. 1975).
25. P. Nozières, *Journal of Low Temperature Physics* **17**, 31–42, ISSN: 1573-7357 (Oct. 1974).
26. P. Nozières, A. Blandin, *Journal de Physique* **41**, 193–211 (Oct. 1980).
27. A. C. Hewson, *Phys. Rev. Lett.* **70**, 4007–4010 (25 June 1993).
28. A. C. Hewson, *Journal of Physics: Condensed Matter* **13**, 10011–10029 (Oct. 2001).
29. D. Goldhaber-Gordon *et al.*, *Nature* **391**, 156–159 (1998).
30. S. M. Cronenwett, T. H. Oosterkamp, L. P. Kouwenhoven, *Science* **281**, 540–544, ISSN: 0036-8075 (1998).
31. W. G. van der Wiel *et al.*, *Science* **289**, 2105–2108, ISSN: 0036-8075 (2000).
32. W. Izumida, O. Sakai, Y. Shimizu, *Journal of the Physical Society of Japan* **67**, 2444–2454 (1998).
33. A. Oguri, *Phys. Rev. B* **64**, 153305 (15 Sept. 2001).
34. A. Oguri, *Journal of the Physical Society of Japan* **74**, 110–117 (2005).
35. A. O. Gogolin, A. Komnik, *Phys. Rev. Lett.* **97**, 016602 (1 July 2006).
36. O. Zarchin, M. Zaffalon, M. Heiblum, D. Mahalu, V. Umansky, *Phys. Rev. B* **77**, 241303 (24 June 2008).
37. Y. Yamauchi *et al.*, *Phys. Rev. Lett.* **106**, 176601 (17 Apr. 2011).
38. M. Ferrier *et al.*, *Nature Physics* **12**, 230 (3 Mar. 2016).
39. E. Sela, Y. Oreg, F. von Oppen, J. Koch, *Phys. Rev. Lett.* **97**, 086601 (8 Aug. 2006).
40. C. Mora, X. Leyronas, N. Regnault, *Phys. Rev. Lett.* **100**, 036604 (3 Jan. 2008).
41. R. Sakano, T. Fujii, A. Oguri, *Phys. Rev. B* **83**, 075440 (7 Feb. 2011).
42. B. Wang, J. Wang, *Phys. Rev. B* **65**, 233315 (23 June 2002).
43. T. Aono, *Phys. Rev. Lett.* **93**, 116601 (11 Sept. 2004).
44. J. Splettstoesser, M. Governale, J. König, R. Fazio, *Phys. Rev. Lett.* **95**, 246803, ISSN: 1079-7114 (Dec. 2005).
45. M. Hasegawa, T. Kato, *J. Phys. Soc. Jpn.* **87**, 044709 (2018).
46. Y. Meir, N. S. Wingreen, *Phys. Rev. Lett.* **68**, 2512–2515 (16 Apr. 1992).
47. M. Büttiker, H. Thomas, A. Prêtre, *Physics Letters A* **180**, 364–369, ISSN: 0375-9601 (1993).
48. M. Büttiker, H. Thomas, A. Prêtre, *Zeitschrift für Physik B Condensed Matter* **94**, 133–137, ISSN: 1431-584X (Mar. 1994).
49. A.-P. Jauho, N. S. Wingreen, Y. Meir, *Phys. Rev. B* **50**, 5528–5544 (8 Aug. 1994).
50. N. Kawakami, A. Okiji, *Journal of the Physical Society of Japan* **52**, 1119–1121 (1983).
51. U. Fano, *Phys. Rev.* **124**, 1866 (1961).
52. P. W. Anderson, *Phys. Rev.* **124**, 41 (1961).

53. É. Jussiau, M. Hasegawa, R. S. Whitney, *Phys. Rev. B* **100**, 115411 (11 Sept. 2019).
54. J. M. Luttinger, *Phys. Rev.* **135**, A1505–A1514 (6A Sept. 1964).
55. G. Tatara, *Phys. Rev. Lett.* **114**, 196601 (19 May 2015).
56. M. Hasegawa, T. Kato, *J. Phys. Soc. Jpn.* **86**, 024710 (2017).
57. S. E. Nigg, R. López, M. Büttiker, *Phys. Rev. Lett.* **97**, 206804 (20 Nov. 2006).
58. J. S. Lim, R. López, D. Sánchez, *Phys. Rev. B* **88**, 201304 (20 Nov. 2013).
59. Y. Oono, M. Paniconi, *Progress of Theoretical Physics Supplement* **130**, 29–44, ISSN: 0375-9687 (Jan. 1998).
60. T. Hatano, S.-i. Sasa, *Phys. Rev. Lett.* **86**, 3463–3466 (16 Apr. 2001).
61. S.-i. Sasa, H. Tasaki, *Journal of Statistical Physics* **125**, 125–224, ISSN: 1572-9613 (Oct. 2006).
62. T. S. Komatsu, N. Nakagawa, S.-i. Sasa, H. Tasaki, *Phys. Rev. Lett.* **100**, 230602 (23 June 2008).
63. G. Benenti, G. Casati, K. Saito, R. S. Whitney, *Phys. Rep.* **694**, 1–124 (2017).
64. T. S. Komatsu, N. Nakagawa, S.-i. Sasa, H. Tasaki, *Journal of Statistical Physics* **142**, 127–153, ISSN: 1572-9613 (Jan. 2011).
65. T. S. Komatsu, N. Nakagawa, S.-i. Sasa, H. Tasaki, *Journal of Statistical Physics* **159**, 1237–1285, ISSN: 1572-9613 (June 2015).
66. K. Saito, H. Tasaki, *Journal of Statistical Physics* **145**, 1275–1290, ISSN: 1572-9613 (Dec. 2011).
67. M. Esposito, M. A. Ochoa, M. Galperin, *Phys. Rev. Lett.* **114**, 080602 (8 Feb. 2015).
68. M. A. Ochoa, N. Zimbovskaya, A. Nitzan, *Phys. Rev. B* **97**, 085434 (8 Feb. 2018).

Appendix A

Keldysh Green's functions

In this appendix, we summarize the definition and analytical formulas of one-particle GFs for the Anderson impurity model.

The one-particle GF of electrons in the quantum dot is defined using the Keldysh time as

$$G_s(\tau_1, \tau_2) = (-i) \left\langle \mathcal{T}_K \left\{ d_s(\tau_1) d_s^\dagger(\tau_2) \right\} \right\rangle. \quad (\text{A.1})$$

Each Keldysh component of the one-particle GF is written as

$$G_s^{++}(t_1, t_2) = (-i) \left\langle \mathcal{T} \left\{ d_s(t_1) d_s^\dagger(t_2) \right\} \right\rangle, \quad (\text{A.2})$$

$$G_s^<(t_1, t_2) = i \left\langle d_s^\dagger(t_2) d_s(t_1) \right\rangle, \quad (\text{A.3})$$

$$G_s^>(t_1, t_2) = (-i) \left\langle d_s(t_1) d_s^\dagger(t_2) \right\rangle, \quad (\text{A.4})$$

$$G_s^{--}(t_1, t_2) = (-i) \left\langle \bar{\mathcal{T}} \left\{ d_s(t_1) d_s^\dagger(t_2) \right\} \right\rangle, \quad (\text{A.5})$$

$$G_s^A(t_1, t_2) = i\Theta(t_2 - t_1) \left\langle \left[d_s(t_2), d_s^\dagger(t_1) \right]_+ \right\rangle, \quad (\text{A.6})$$

$$G_s^R(t_1, t_2) = (-i)\Theta(t_1 - t_2) \left\langle \left[d_s(t_1), d_s^\dagger(t_2) \right]_+ \right\rangle, \quad (\text{A.7})$$

respectively.

For time-independent Hamiltonians, one can calculate the advanced and retarded GFs by solving the Dyson's equation as,

$$G^A(\omega) = \frac{1}{\omega - \varepsilon_d - \Sigma_{\gamma,s}^A(\omega) - \Sigma_{U,s}^A(\omega)} \quad (\text{A.8})$$

$$G^R(\omega) = \frac{1}{\omega - \varepsilon_d - \Sigma_{\gamma,s}^R(\omega) - \Sigma_{U,s}^R(\omega)}, \quad (\text{A.9})$$

where $\Sigma_{\gamma,s}$ and $\Sigma_{U,s}$ are 1PI self-energies induced by the dot-reservoir coupling and the Coulomb interaction, respectively. The self-energy $\Sigma_{\gamma,s}$ can be written as

$$\Sigma_{\gamma,s}^{A/R/<}(\omega) = \sum_r \Sigma_{r,s}^{A/R/<}(\omega), \quad (\text{A.10})$$

$$\Sigma_{r,s}^A(\omega) = \Lambda_r(\omega) + \frac{i}{2}\Gamma_r(\omega), \quad (\text{A.11})$$

$$\Sigma_{r,s}^R(\omega) = \Lambda_r(\omega) - \frac{i}{2}\Gamma_r(\omega), \quad (\text{A.12})$$

$$\Sigma_{r,s}^<(\omega) = i\Gamma_r(\omega)f_r(\omega), \quad (\text{A.13})$$

where

$$\Lambda_r(\omega) = |\gamma_r|^2 \int d\varepsilon \frac{\rho(\varepsilon)}{\omega - \varepsilon}, \quad (\text{A.14})$$

$$\Gamma_r(\omega) = 2\pi|\gamma_r|^2\rho(\omega). \quad (\text{A.15})$$

We note that the other self-energy $\Sigma_{U,s}$ cannot be written by a simple form in general.

For $U = 0$, one can describe one-particle GFs as

$$G_{0,s}^A(\omega) = \frac{1}{\omega - \varepsilon_d - \Lambda(\omega) - \frac{i}{2}\Gamma(\omega)} \quad (\text{A.16})$$

$$G_{0,s}^R(\omega) = \frac{1}{\omega - \varepsilon_d - \Lambda(\omega) + \frac{i}{2}\Gamma(\omega)} \quad (\text{A.17})$$

$$\begin{aligned} G_{0,s}^<(\omega) &= G_{0,s}^R(\omega)\Sigma_s^<(\omega)G_{0,s}^A(\omega) \\ &= i\frac{\sum_r \Gamma_r(\omega)f_r(\omega)}{(\omega - \varepsilon_d - \Lambda(\omega))^2 + \Gamma^2(\omega)/4}. \end{aligned} \quad (\text{A.18})$$

Appendix B

Bethe anzats

In this appendix, we briefly introduce the Bethe anzats method for the Anderson impurity model to calculate the renormalized parameters. Here we just summarize the results. For detailed derivation, see Ref. [50].

Using the Bethe anzats, one can calculate the occupation number n_d , spin susceptibility χ_s , and charge susceptibility χ_c for zero temperature system. The renormalized parameters can be defined by following simple relations:

$$n_d = \frac{1}{2} - \frac{1}{\pi} \arctan(2\tilde{\epsilon}_d/\tilde{\Gamma}), \quad (\text{B.1})$$

$$\chi_s = \frac{g\mu_b}{2} \tilde{\rho} (1 + \tilde{U} \tilde{\rho}), \quad (\text{B.2})$$

$$\chi_c = 2\tilde{\rho} (1 - \tilde{U} \tilde{\rho}), \quad (\text{B.3})$$

where

$$\tilde{\rho} = \frac{\tilde{\Gamma}/2\pi}{\tilde{\epsilon}_d^2 + \tilde{\Gamma}^2/4}. \quad (\text{B.4})$$

Here g and μ_b are the g-factor and the Bohr magneton, respectively.

The occupation number, spin susceptibility, and charge susceptibility are calculated by solving a set of integral equations as follows:

$$n_d = 1 - \int_{-\infty}^{\alpha} d\Lambda \sigma(\Lambda), \quad (\text{B.5})$$

$$\chi_s = \frac{\Gamma}{4} \frac{C(\alpha)D(\beta)\rho(\beta)t(\beta)^{-1} - C(\beta)D(\alpha)\sigma(\alpha)s(\alpha)^{-1}}{C(\alpha)D(\beta) - C(\beta)D(\alpha)}, \quad (\text{B.6})$$

$$\chi_c = \frac{\Gamma}{4} \frac{C(\alpha)D(\beta)\sigma(\alpha)s(\alpha)^{-1} - C(\beta)D(\alpha)\rho(\beta)t(\beta)^{-1}}{C(\alpha)D(\beta) - C(\beta)D(\alpha)}, \quad (\text{B.7})$$

where

$$C(\alpha) = s(\alpha)^{-1} \frac{\partial}{\partial \alpha} \left[\int_{-\infty}^{\alpha} d\Lambda s(\Lambda) \right], \quad (\text{B.8})$$

$$D(\beta) = t(\beta)^{-1} \frac{\partial}{\partial \beta} \left[\int_{-\infty}^{\beta} dk t(k) \right], \quad (\text{B.9})$$

and

$$\sigma(\Lambda) = \int_{-\infty}^{\alpha} d\Lambda' R(\Lambda - \Lambda') \sigma(\Lambda') - \int_{-\infty}^{\beta} dk Q(B(k) - \Lambda) \rho(k) + \rho^i(\Lambda), \quad (\text{B.10})$$

$$\rho(k) = -B'(k) \left[\int_{-\infty}^{\beta} dk' R(B(k) - B(k')) \rho(k') + \int_{-\infty}^{\alpha} d\Lambda Q(B(k) - \Lambda) \sigma(\Lambda) \right] + \rho^i(k), \quad (\text{B.11})$$

$$s(\Lambda) = \int_{-\infty}^{\alpha} d\Lambda' R(\Lambda - \Lambda') s(\Lambda') - \int_{-\infty}^{\beta} dk Q(B(k) - \Lambda) t(k) + \int_{-\infty}^{\infty} dk (2\pi)^{-1} Q(B(k) - \Lambda), \quad (\text{B.12})$$

$$t(k) = -B'(k) \left[\int_{-\infty}^{\beta} dk' R(B(k) - B(k')) t(k') + \int_{-\infty}^{\alpha} d\Lambda Q(B(k) - \Lambda) s(\Lambda) \right] + \frac{1}{2\pi} \left[1 + B'(k) \int_{-\infty}^{\infty} dk' R(B(k) - B(k')) \right], \quad (\text{B.13})$$

$$\sigma^i(\Lambda) = \int_{-\infty}^{\infty} \frac{dk}{2\pi} \frac{\Gamma}{(k - \varepsilon_d)^2 + \Gamma^2/4} Q(\Lambda - B(k)), \quad (\text{B.14})$$

$$\rho^i(k) = \frac{1}{2\pi} \frac{\Gamma}{(k - \varepsilon_d)^2 + \Gamma^2/4} + \frac{B'(k)}{2\pi} \int_{-\infty}^{\infty} dk' \frac{\Gamma}{(k' - \varepsilon_d)^2 + \Gamma^2/4} R(B(k) - B(k')). \quad (\text{B.15})$$

The functions $B(k)$, $R(\Lambda)$, and $Q(\Lambda)$ are defined as

$$B(k) = k(k - U - 2\varepsilon_d) \quad (\text{B.16})$$

$$R(\Lambda) = \frac{1}{2} \int_{-\infty}^{\infty} \frac{d\omega}{2\pi} \operatorname{sech}(U\Gamma\omega/2) e^{i\omega\Lambda}, \quad (\text{B.17})$$

$$Q(\Lambda) = \int_{-\infty}^{\infty} \frac{d\omega}{2\pi} \frac{1}{1 + \exp[U\Gamma|\omega|]} e^{i\omega\Lambda}. \quad (\text{B.18})$$

The parameters α and β are determined by the following condition:

$$\int_{-\infty}^{\alpha} d\Lambda s(\Lambda) = \frac{U + 2\varepsilon_d}{2\pi}, \quad (\text{B.19})$$

$$\int_{-\infty}^{\beta} dk t(k) = \frac{H}{2\pi}. \quad (\text{B.20})$$

Here H is a magnetic field. When one considers no magnetic field case, $H = 0$, the parameter $\beta = -\infty$.

Appendix C

Overcounting problem and counter term

In this appendix, we explain the overcounting problem in RPT and how to solve this problem by introducing the counter terms.

RPT is the perturbation theory based on a quasi-particle picture. In the framework of RPT, all the GFs are derived from the action of the quasi-particles

$$S_{\text{qp}} = \int_K d\tau \mathcal{L}_{\text{qp}}, \quad (\text{C.1})$$

where \mathcal{L}_{qp} is the Lagrangian of the quasi-particle defined as

$$\begin{aligned} \mathcal{L}_{\text{qp}} = & \sum_{r,k,s} \left[c_{rks}^\dagger(\tau) \left(i \frac{\partial}{\partial \tau} - \epsilon_k \right) c_{rks}(\tau) \right] + \sum_s \left[\tilde{d}_s^\dagger(\tau) \left(i \frac{\partial}{\partial \tau} - \tilde{\epsilon}_d \right) \tilde{d}_s(\tau) \right] \\ & + \tilde{U} \tilde{d}_\uparrow^\dagger(\tau) \tilde{d}_\uparrow^\dagger(\tau) \tilde{d}_\downarrow^\dagger(\tau) \tilde{d}_\downarrow(\tau) + \sum_{r,k,s} \left[\tilde{\gamma}_r \tilde{d}_s^\dagger(\tau) c_{rks}(\tau) + c_{rks}^\dagger(\tau) \tilde{d}_s(\tau) \right]. \quad (\text{C.2}) \end{aligned}$$

Here $\tilde{\epsilon}_d$ is the renormalized quantum-dot level, \tilde{U} is the renormalized Coulomb interaction, $\tilde{\gamma}_r = \sqrt{z} \gamma_r$ is the renormalized tunnel coupling strength, and \tilde{d}_s^\dagger and \tilde{d}_s are creation and annihilation operators of the quasi-particle with a spin s . Using this Lagrangian, the advanced GF of the quasi-particles, $\tilde{G}_s^A(\omega)$, is derived as

$$\tilde{G}_s^A(\omega) = \frac{1}{\omega - \tilde{\epsilon}_d - i\tilde{\Gamma}/2 - z\tilde{\Sigma}_{\tilde{U},s}^A(\omega)}, \quad (\text{C.3})$$

where $\tilde{\Sigma}_{\tilde{U},s}^A(\omega)$ is the advanced component of the renormalized 1PI self-energy induced. Except the overall factor z , this GF of quasi-particles should be consistent with the GF of

original electrons in Eq. (2.86),

$$z\tilde{G}_s^A(\omega) = \frac{z}{\omega - \tilde{\epsilon}_d - i\tilde{\Gamma}/2 - \Sigma_{U,s}^{\text{rem},A}(\omega)}. \quad (\text{C.4})$$

To satisfy this equation, $\tilde{\Sigma}_{\tilde{U},s}^A(\omega)$ should satisfy the conditions as follows:

$$\tilde{\Sigma}_{\tilde{U},s}^A(0) = z\Sigma_{U,s}^{\text{rem},A}(0) = 0, \quad (\text{C.5})$$

$$\frac{\partial}{\partial \omega} \tilde{\Sigma}_{\tilde{U},s}^A(\omega = 0) = z \frac{\partial}{\partial \omega} \Sigma_{U,s}^{\text{rem},A}(\omega = 0) = 0. \quad (\text{C.6})$$

These two conditions are known as the renormalized condition for the renormalized 1PI self-energy. In addition to these two conditions, one more condition is required for the renormalized 2PI four-point vertex function:

$$\tilde{I}_{ss\bar{s}\bar{s}}^{++++}(0,0,0,0) = \tilde{U}. \quad (\text{C.7})$$

Eqs. (C.5)-(C.7) cannot be satisfied only by considering the Lagrangian of the quasi-particle. This problem is called the overcounting problem. In order to solve this problem, one should add the Lagrangian of the counter terms, defined as

$$\mathcal{L}_{\text{CT}} = \sum_s \left[\tilde{d}_s^\dagger(\tau) \left(i\lambda_2 \frac{\partial}{\partial \tau} - \lambda_1 \right) \tilde{d}_s(\tau) \right] + \lambda_3 \tilde{d}_\uparrow^\dagger(\tau) \tilde{d}_\uparrow^\dagger(\tau) \tilde{d}_\downarrow^\dagger(\tau) \tilde{d}_\downarrow(\tau), \quad (\text{C.8})$$

where $\lambda_1, \lambda_2, \lambda_3$ are counter terms for $\tilde{\epsilon} = d, z, \tilde{U}$. Controlling these three degrees of freedom, one can satisfy the renormalized conditions, Eqs. (C.5)-(C.7).

Appendix D

Derivation of Eq. (3.8)

In this appendix, we give a detailed derivation of Eq. (3.8). As shown in Eq. (3.3), the dynamical conductance is defined as a linear response coefficient of δX_n

$$\mathcal{G}_{r,n}(\Omega)e^{-i\Omega t_1} = \left. \frac{\partial \langle I_r(t_1) \rangle}{\partial (\delta X_n)} \right|_{\delta X_n=0}. \quad (\text{D.1})$$

The right hand side of Eq. (D.1) is calculated by functional derivative in the Keldysh formalism, such as,

$$\left. \frac{\partial \langle I_r(t_1) \rangle}{\partial (\delta X_n)} \right|_{\delta X_n=0} = \int dt_2 F(t_1, t_2) e^{-i\Omega t_2}. \quad (\text{D.2})$$

where a function $F(t_1, t_2)$ is defined as

$$\begin{aligned} F(t_1, t_2) &= \left. \frac{\delta \langle I_r(t_1) \rangle}{\delta X_n(t_2)} \right|_{\delta X_n=0} \\ &= \left. \frac{\delta \langle I_r(t_1) \rangle}{\delta X_n(t_{2,+})} \right|_{\delta X_n=0} - \left. \frac{\delta \langle I_r(t_1) \rangle}{\delta X_n(t_{2,-})} \right|_{\delta X_n=0}. \end{aligned} \quad (\text{D.3})$$

Here $\frac{\delta}{\delta X_n(t_{2,+})}$ and $\frac{\delta}{\delta X_n(t_{2,-})}$ denote a functional derivative with respect to $X_n(t_2)$ on contour C_+ and C_- , respectively (see Fig. 2.4). As we consider the limit of $\delta X_n \rightarrow 0$, the function $F(t_1, t_2)$ depends only on the difference of time arguments $t_1 - t_2$ and its Fourier component can be defined as

$$F(t_1, t_2) = \int \frac{d\omega}{2\pi} F(\omega) e^{-i\omega(t_1-t_2)}. \quad (\text{D.4})$$

Substituting Eqs. (D.2) and (D.4) into Eq. (D.1), one obtains

$$\begin{aligned}
 \mathcal{G}_r(\Omega)e^{-i\Omega t_1} &= \int \frac{d\omega}{2\pi} F(\omega)e^{-i\omega t_1} \int dt_2 e^{-i(\Omega-\omega)t_2} \\
 &= \int \frac{d\omega}{2\pi} F(\omega)e^{-i\omega t_1} 2\pi\delta(\omega - \Omega) \\
 &= F(\Omega)e^{-i\Omega t_1}.
 \end{aligned} \tag{D.5}$$

Using the inverse Fourier transform, we finally conclude

$$\begin{aligned}
 \mathcal{G}_{r,n}(t_1, t_2) &= F(t_1, t_2) \\
 &= \frac{\delta \langle I_r(t_1) \rangle}{\delta X_n(t_2)} \Big|_{\delta X_n=0}.
 \end{aligned} \tag{D.6}$$

Appendix E

Brief review of excess heat and extended Clausius relation

In this appendix, we briefly introduce the extended Clausius relation [15, 16, 64–66] which describes the relation between the entropy production and the heat transfer in SST.

In equilibrium thermodynamics, the Clausius relation describes the inequality between the entropy production and the heat exchange due to a thermodynamic operation. In the quasi-static limit, the entropy production exactly equals to the amount of heat transfer due to the operation, such as

$$S_f - S_i = \beta Q_{\text{tot}}, \quad (\text{E.1})$$

where S_i and S_f are the entropy at the initial and the final state, respectively, Q_{tot} is a total heat flowing into a system, and β is an inverse temperature.

In SST, this equation does not hold, because the total heat, Q_{tot} , diverges in the quasi-static limit. In order to overcome this problem, *excess* heat is considered in SST. The excess heat, Q_{ex} , is defined as an extra heat transfer due to the operation (Fig. E.1). As the heat transfer due to the steady heat current is subtracted, the excess heat is a proper object in SST which does not diverge in the quasi-static limit.

To see how the excess heat relates with the entropy production of steady-states, we employ the Hamiltonian,

$$H = H_s + \sum_{r=1, \dots, N} H_r + \gamma H_c, \quad (\text{E.2})$$

where H_s is the Hamiltonian of the system, H_r is that of the reservoir r , and H_c is that of coupling between the system and the reservoirs. Here γ is a dimensionless parameter which

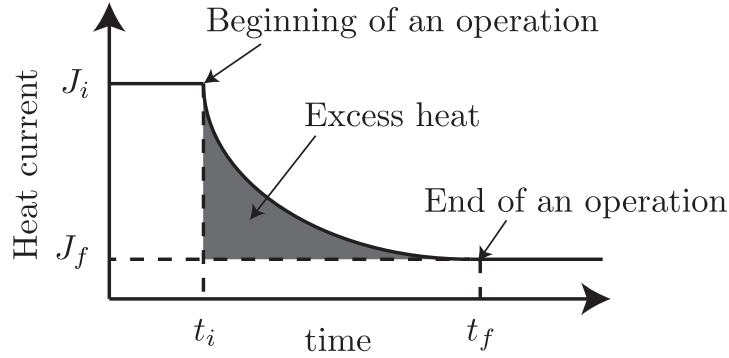


Fig. E.1 A schematic of the excess heat. An operation starts at a time t_i , and ends at a time t_f . During the operation, the heat current changes from J_i to J_f . The excess heat is defined as the heat obtained by subtracting the steady heat production due to heat current of the final steady state from the total heat (the grey area in the figure).

indicates the strength of coupling between the system and the reservoirs. We consider the situation as follows: The reservoir r are set in equilibrium with the inverse temperature $\beta_{r,i}$ and the system is prepared in the initial steady-state described by the density matrix for the initial steady state, $\rho_{SS,i}$. At the initial time $t = t_i$, the temperature of the reservoirs $\beta_{r,i}$ are changed to $\beta_{r,f}$. The system and the reservoirs evolves and finally relaxes to new steady-state described by the density matrix $\rho_{SS,f}$ at time $t = t_f$. Under this situation, the excess heat and the entropy production between the initial and the final steady-states satisfies the relation known as the extended Clausius relation:

$$S_{\text{sym}}(\rho_{SS,f}) - S_{\text{sym}}(\rho_{SS,i}) = \sum_r \beta_{r,f} Q_{\text{ex},r} + \{O(\varepsilon) + O(\gamma)\}^2 O(\delta) + O(\delta^2). \quad (\text{E.3})$$

Here $S_{\text{sym}}(\rho)$ is the symmetrized von Neumann entropy defined as

$$S_{\text{sym}}(\rho) = -\text{Tr}_S \left[\rho \frac{\ln(\rho) + \ln(\text{T}\rho\text{T})}{2} \right], \quad (\text{E.4})$$

where $\text{Tr}_S[\cdot]$ is a trace with respect to the degree of freedom of the system and T is the time-reversal operator. $Q_{\text{ex},r}$ is the excess heat flowing from the reservoir r . ε is a parameter of non-equilibriumness defined as

$$\varepsilon = \sum_{r=1 \dots N} \left[\frac{|\beta_{r,i} - \beta_i|}{\beta_i} - \frac{|\beta_{r,f} - \beta_f|}{\beta_f} \right], \quad (\text{E.5})$$

$$\beta_{i/f} = N^{-1} \sum_{r=1 \dots N} \beta_{r,i/f}, \quad (\text{E.6})$$

and δ is an parameter describing the amount of chage

$$\delta = \sum_{r=1, \dots, N} \frac{\beta_{r,f} - \beta_{r,i}}{\beta_{r,i}}. \quad (\text{E.7})$$

